DOT/FAA/CT-89/4

FAA Technical Center
Atlantic City International Airport
N.J. 08405

Aircraft Jet Engine Exhaust Blast Effects on Par-56 Runway Threshold Lamp Fixtures

Jacob K. Struck

U.S. Army, Armament Research,
Development and Engineering Center
Dover, New Jersey

Anthony J. Barile
FAA Technical Center

June 1989

Final Report

U.S. Department of Transportation
Federal Aviation Administration
Program Engineering Service

NOTICE

This document is disseminated under the sponsorship of the U. S. Department of Transportation in the interest of information exchange. The United States Government assumes no liability for the contents or use thereof.

The United States Government does not endorse products or manufacturers. Trade or manufacturers' names appear herein solely because they are considered essential to the objective of this report.

Technical Report Documentation Page

1. Report No.	2. Government Accession No.	3. Recipient's Catalog No.
DOT/FAA/CT-89/4		

4. Title and Subtitle	5. Report Date
AIRCRAFT JET ENGINE EXHAUST BLAST EFFECTS ON PAR-56 RUNWAY THRESHOLD LAMP FIXTURES	June 1989
	6. Performing Organization Code
7. Author(s) Jacob K. Struck (ARDEC) Anthony J. Barile (FAA Technical Center)	8. Performing Organization Report No. SMCAR-TSE-1L
9. Performing Organization Name and Address U.S. Army, Armament Research, Development and Engineering Center Dover, New Jersey 07801	10. Work Unit No. (TRAIS) DOT/FAA/CT-89/4
	11. Contract or Grant No. DTFA03-84-A-40020
12. Sponsoring Agency Name and Address U.S. Department of Transportation Federal Aviation Administration Program Engineering Service Washington, DC 20591	13. Type of Report and Period Covered Final Report
	14. Sponsoring Agency Code APS-400

15. Supplementary Notes

16. Abstract

The effects of jet engine exhaust blast on PAR-56 lamps located at the runway threshold were measured in this project. Sensors were placed on and near the lamp assemblies which measured blast velocity and temperature, bulb face temperature, lamp fixture acceleration and sound pressure level. These sensors were coupled to a computer-controlled instrumentation system housed in a van located near the threshold of runway 13 at La Guardia Airport. Data were acquired during the engine runup and takeoff roll of some 162 aircraft during the measurement phase. The data were recorded on digital magnetic tape and video tape to form a permanent record of the raw data. The data were later plotted and analyzed, both manually and using a computer in order to extract the worst case environmental parameters encountered during the measurement phase. A prediction algorithm was developed to allow prediction of key environmental effects on the PAR-56 lamps caused by new aircraft or aircraft not measured. The algorithm was developed by correlating the acquired data against the manufacturers' published jet exhaust blast velocity and temperature contours.

A protective shroud was devised and installed on one of the instrumented lamp assemblies during the last portion of data collection. The data suggest a beneficial reduction of the hostile jet blast effects measured on the shrouded lamp versus the unshrouded lamp.

17. Key Words	18. Distribution Statement
Jet Exhaust Blast PAR-56 Runway Threshold Lamp Protective Shroud	Document is available to the public through the National Technical Information Service, Springfield, Virginia 22161

19. Security Classif. (of this report)	20. Security Classif. (of this page)	21. No. of Pages	22. Price
Unclassified	Unclassified	78	

Form DOT F 1700.7 (8-72) Reproduction of completed page authorized

PREFACE

The Federal Aviation Administration (FAA) Technical Center, Atlantic City International Airport, New Jersey, initiated efforts to measure certain physical effects of jet blast (as caused by aircraft jet engines) on runway PAR-56 threshold lamp assemblies. The purpose was to determine necessary corrective actions to prevent costly premature threshold lamp failures. Mr. Anthony J. Barile was the FAA Contracting Officer's Technical Representative. He provided the management and direction necessary to achieve FAA goals and objectives.

The task was carried out through an Interagency Agreement with the U.S. Army Armament Research, Development and Engineering Center (ARDEC), Picatinny Arsenal, New Jersey, contract number DTAFA03-84-40020. Mr Jacob K. Struck was the Senior Project Leader. He provided project technical leadership, overall system design and specification. A Data Acquisition System was designed, specified and configured by Mr. Struck and Mr. Daniel Ramer.

Other ARDEC personnel who provided support were as follows: Mr. Jeffery Fornoff and Mr. Alfredo Alza developed the data acquisition computer program. The data reduction was performed by Mr. Henry Lee. Data review was performed by Mr. Struck, Mr. Anthony Barone, Mr. Lee, Mrs. Lydia Chang, and Mr. Altaf Khan. Final data reduction algorithms and plotting were performed by Mr. Lee. The data interpretation and extrapolation were performed by Mr. Struck. Mr. Raymond Kyle and Mr. George Khowong assisted in the field, erecting the system and acquiring the data.

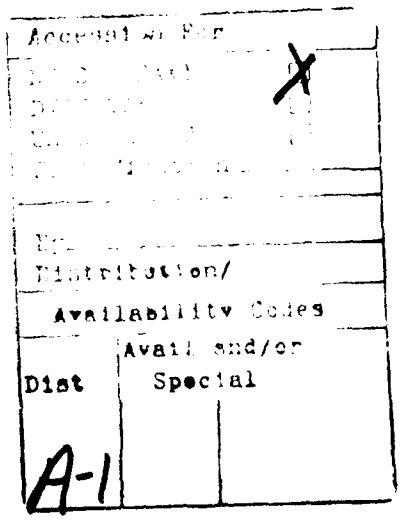

TABLE OF CONTENTS

LIST OF ILLUSTRATIONS

LIST OF TABLES

EXECUTIVE SUMMARY

The Federal Aviation Administration (FAA) Technical Center, Atlantic City International Airport, initiated an effort to measure the effects of jet engine exhaust blast on PAR-56 lamps located at the threshold of a runway during the takeoff of many different aircraft. The purpose of these measurements was to characterize the environment created by the blast so that corrective action might be taken to prevent premature lamp failure.

An interagency agreement between the FAA and the U.S. Army Armament Research, Development and Engineering Center (ARDEC), Picatinny Arsenal, New Jersey, was formed; and a test plan and an instrumentation system allowing automated data acquisition were designed and developed by ARDEC personnel.

The sensors and data acquisition system were located at the threshold of runway 13 at La Guardia Airport in New York City, and data from 162 aircraft takeoffs were acquired during this phase. The data were recorded on digital magnetic tape and video tape for archival purposes. The data contained on these tapes were conditioned, scaled and plotted for analysis. Specific data runs were selected for further analysis and for removal of spurious artifacts which occurred during data acquisition due to the extreme environment caused by the jet blast.

The processed data plots were analyzed and reviewed by a team of individuals and the worst case parameters were extracted and charted for each type of aircraft encountered. The worst case parameters for all aircraft encountered were also identified and listed.

The manufacturers' published jet exhaust velocity and temperature contours were reviewed for many different aircraft and entered into a computer. The data were then plotted and analyzed with the intent of determining whether the data from these contour plots, taken at takeoff thrust, could be used in an algorithm which would allow the prediction of worst-case environmental parameters for new types of aircraft. If the relationship could be made, then the effect of a new aircraft on the existing PAR-56 test specifications could be evaluated.

The algorithm was developed and it provides a reasonable estimate of the key environmental parameters caused by the jet exhaust of a new aircraft. The key parameters which affect the life of the PAR-56 lamp are the total acceleration, both peak and root-mean-square, and the maximum rate of change of bulb face temperature.

An FAA designed and built experimental lamp shroud was installed in a threshold light array. Full-scale tests showed a considerable reduction of the jet blast effects.

INTRODUCTION

PURPOSE

The purpose of this work is to investigate the aircraft jet engine exhaust blast effects on the PAR-56 lamp fixtures located at the runway threshold, and from the effects observed, specify the worst-case environment to which any equipment located at or near the runway threshold will be exposed. An extrapolation algorithm is presented which allows the environmental effects of new aircraft jet engine blast profiles to be predicted.

BACKGROUND

Excessive premature failure of the PAR-56 lamp housed in the runway threshold light assembly precipitated this project. A contract was initiated by the FAA to measure the various physical phenomena associated with blast plumes generated by jet aircraft engines and to measure their effect on the PAR-56 assembly. The instrumentation system comprised a sensor array, a multi-channel, computer-controlled data acquisition system, and a video imaging and recording system which was designed and configured specifically for this task.

All test data were obtained at La Guardia Airport, New York City, New York at the threshold of runway 13 during normal airport operations. An Army Armament Research, Development and Engineering Center (ARDEC) equipment van, fielded by the Instrumentation Section, was used to house the instrumentation, computer, video equipment and personnel. Installation, calibration and maintenance of the sensors located at the runway threshold was accomplished from midnight to 6 a.m. so as not to conflict with heavy air traffic.

Perfect weather conditions prevailed throughout the test periods, March 3 through March 22, 1986, which included rain, snow flurries, drizzle, cold, clear and bright.

TEST OBJECTIVES

In order to characterize the environment created by the aircraft jet engine blast plume, it was decided to measure the following physical phenomena: the velocity of the blast at each sensor array; the fluid temperature within the blast plume; and the sound pressure level at the sensor array. To characterize the effect of the blast plume on the PAR-56 lamp assembly, the following physical phenomena were measured: bulb surface temperatures at three points per bulb (at various illumination intensity steps); and the three-axis acceleration of each lamp housing.

A video camera was aimed at the runway threshold from within the instrumentation van to allow estimation of the distance between the aircraft and the sensor array. The recorded video signal was encoded with a time signal. Each data acquisition recorded on digital magnetic tape was also encoded with the time signal to allow time-synchronous evaluation of data and video image. The sound pressure level signal as well as the air traffic control communications channel were recorded on the video tape recorder with the video image.

It was decided to measure the effects of each of the major types of aircraft as many times as possible since so many variables seem to affect the measured blast intensity. This technique allowed a better analysis of each aircraft because with many measurements, the likelihood of encountering worst-case conditions is higher. Since the landing blast plume effects were noted to be negligible at the sensor locations used, it was decided not to record any landing traffic.

Although not originally requested by the program sponsor, another test objective added by the COTR was to evaluate the possible benefits of a metal shroud placed over the lamp assembly providing a "shielding" effect from the jet blast plume. Near the conclusion of the tests, a shroud was installed over one of the two instrumented lamp fixtures.

DISCUSSION

DESCRIPTION OF MEASUREMENTS

The decision as to what measurements were to be made was driven by the need to determine the jet exhaust plume characteristics in the immediate vicinity of the lamp housing, such as temperature, velocity, and sound pressure level, as well as the effect of the blast plume on the lamps themselves. Vibration induced by the blast plume was certainly an important parameter to be measured, but thermal stress induced by the blast plume on the glass envelope was also suspected as a cause of lamp failure.

Since vibration can be induced in a structure by buffeting caused by the turbulence of the impinging blast plume as well as by exposure to intense sound pressure waves, it was decided to attempt to measure the sound pressure level within the high-velocity, high-temprature blast environment using a calibrated probe microphone.

The documented lamp failures also seemed to be a function of atmospheric conditions. It was thus decided that the measurements would be made in late January and early February to acquire data during the foggy, freezing rain conditions during which most failures occur.

DESCRIPTION OF SENSOR SITING

Two adjacent PAR-56 lamp assemblies in the threshold bar were selected to be instrumented. Not all lamp assemblies were present in the threshold bar, so the best adjacent pair was selected. This pair was closest to the most likely offset from the center of the runway to be exposed to jet exhaust plume blast from most aircraft. A three-axis accelerometer was mounted on each lamp housing and three thermocouples were attached to the face of each lamp glass envelope. A pitot tube was placed near each assembly with a thermocouple placed in the vicinity of the lamp assemblies to measure the blast and temperature, as well as a calibrated microphone capable of reproducing high-intensity sound pressure mounted between the instrumented lamp assemblies.

Figure 1 depicts the plan view of the end of runway 13 at La Guardia Airport (LGA), showing the location of the sensor array, the location of the instrumentation van, and the field of view of the video camera which recorded a visual image of each data run. Figure 2 is a detailed drawing of the sensor array, showing where each sensor was located. Also included in Figure 2 are the definitions of the X, Y, and Z axes of the accelerometers, and the sign conventions used in plotting the data.

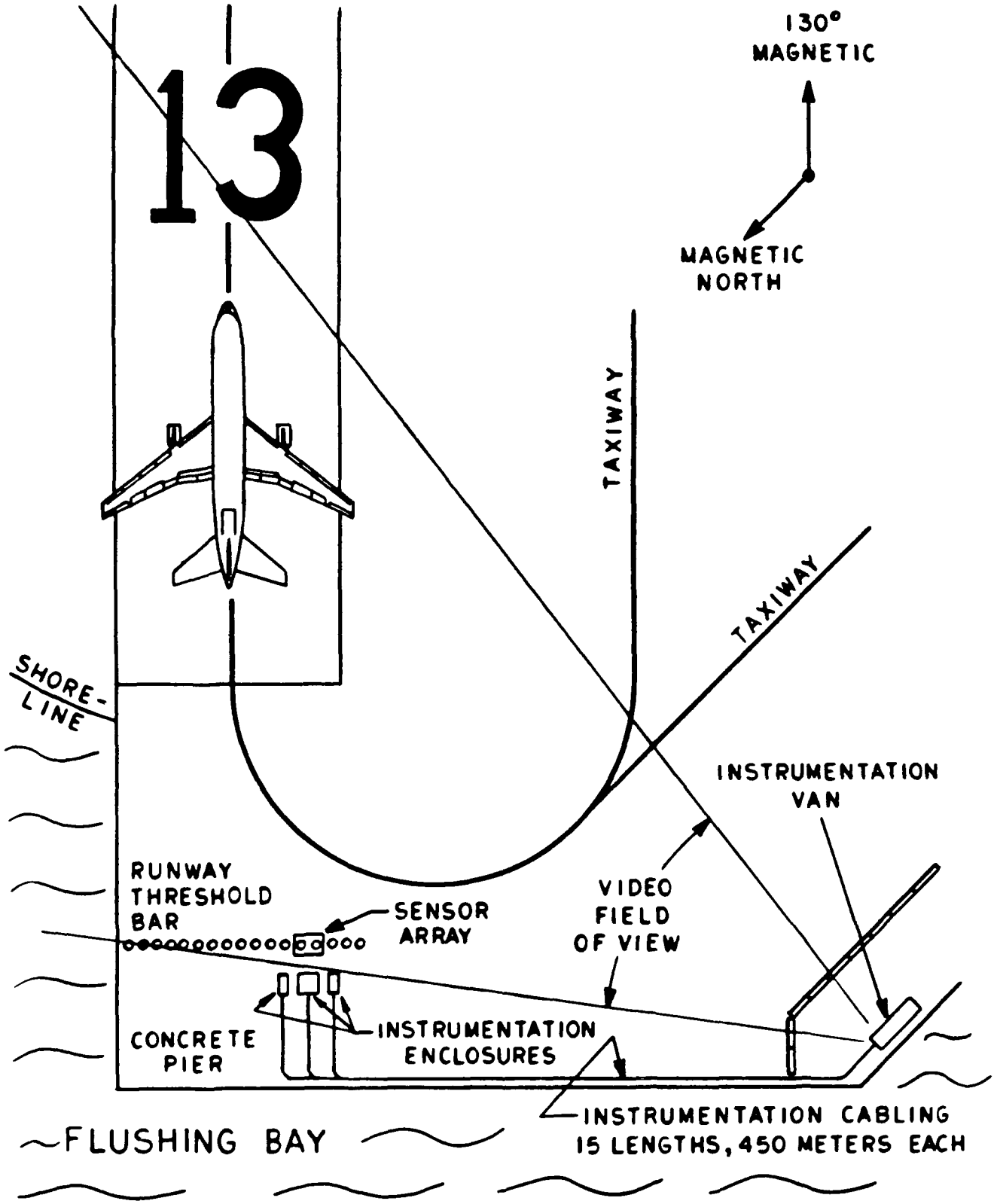

FIGURE 1. PLAN VIEW OF RUNWAY 13 THRESHOLD

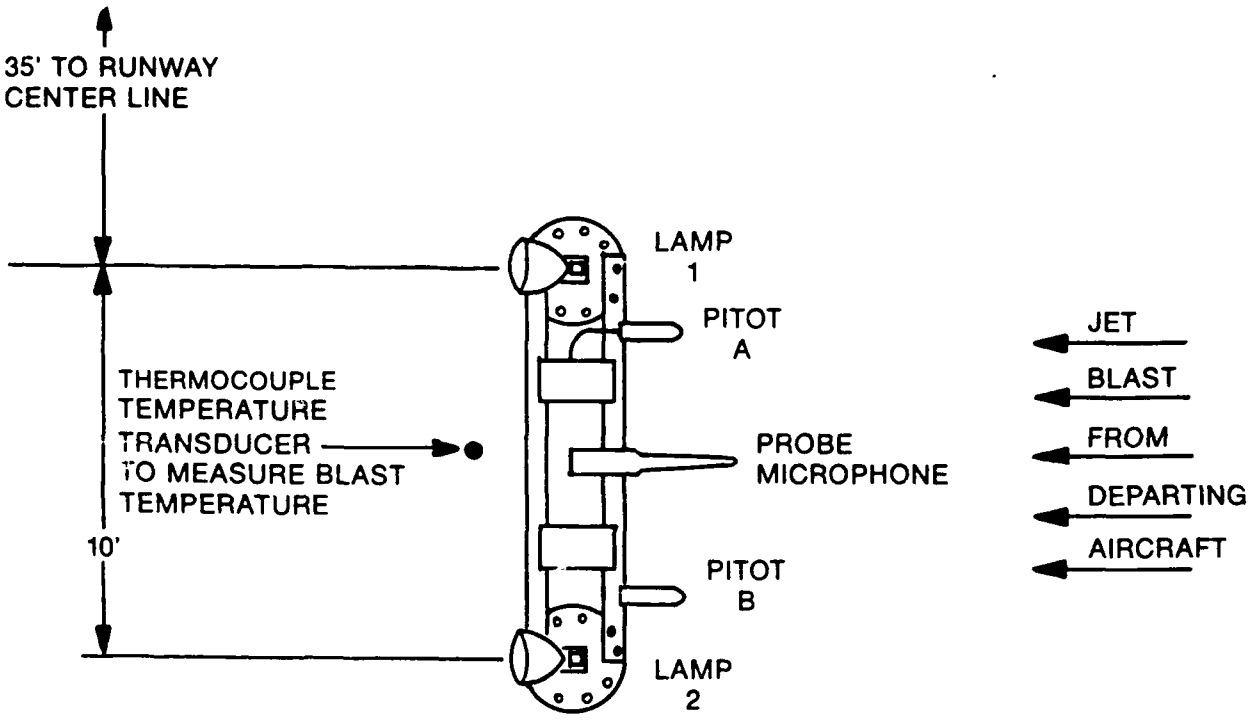

TOP VIEW OF SENSOR ARRAY

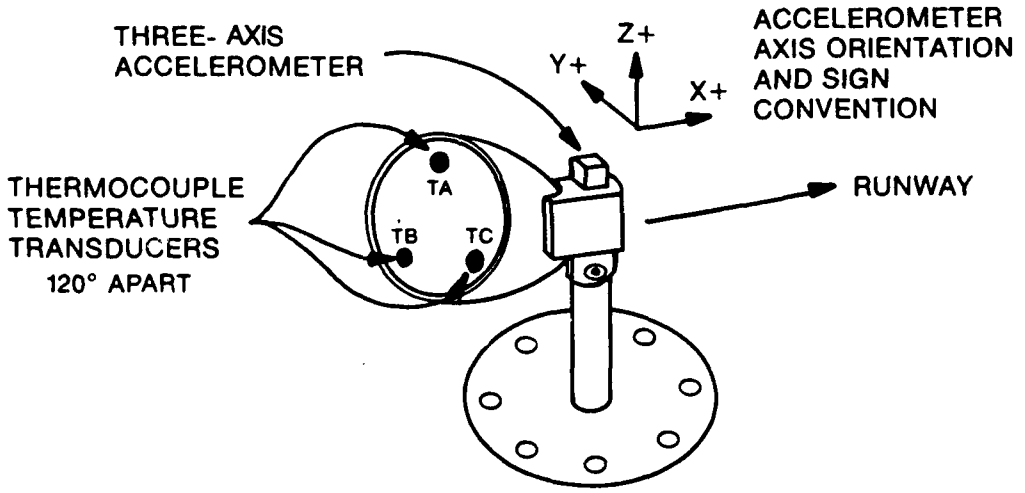

SENSOR LOCATION ON EACH PAR-56 LAMP FIXTURE

FIGURE 2. SENSOR LOCATION DETAILS

DESCRIPTION OF INSTRUMENTATION SYSTEM

A multi-channel, computer-controlled data acquisition system was used to acquire and record the outputs of each sensor. Figure 3 is a block diagram of the sensors used in the array. Figure 4 is a block diagram of the instrumentation system used for the test. The acquisition system employed 15 simultaneous channels of input which were scanned and digitized by a high-speed analog-to-digital (A/D) converter system. The digital output of the A/D converter was routed by the computer to a mass memory storage device which allowed temporary storage of up to 28 seconds of 15 channels of information. At the end of each run, the contents of the mass memory (all of the data associated with each data run) were recorded on a 9-track digital tape drive.

The multi-channel A/D converter was chosen since it readily interfaced with the existing computer and the mass memory storage device. It allowed the sequential scanning of 15 channels of analog data with a per channel sampling rate of 1195.848 samples per second. Thus, at this sampling rate, and with 15 channels being sampled sequentially, the A/D converter was actually sampling at a rate of 17,937.72 samples per second.

The electronic mass memory device has a total capacity of one megabyte, or one million 8-bit words of data. Since the A/D converter had an accuracy of 12 bits (one part in 4096, or 0.0244%), each sample occupies two bytes of mass memory. Thus, at the applied sample rate, the mass memory could hold approximately 28 seconds of data to be acquired. This data plus the preamble and the digital overhead completely filled the mass memory for each data run.

This 28-second duration proved to be more than adequate since, in practice, the takeoff runup and rollout time was in the range of 5 to 15 seconds. After 5 to 15 seconds, the sensors indicated no remaining effect from the blast. This comfortable margin of time allowed manual triggering by the computer operator of each data acquisition as soon as the pilot had been granted takeoff clearance by the air traffic controller. Even with the highly variable takeoff rolls and engine runups based on aircraft loading, weather conditions, and individual pilot's style's, it was very unlikely that any data would be lost due to the 28-second hardware limitation.

Table 1 lists the analog-to-digital converter channel allocation, and table 2 lists the data parameters recorded as the preamble to the data recording for each run.

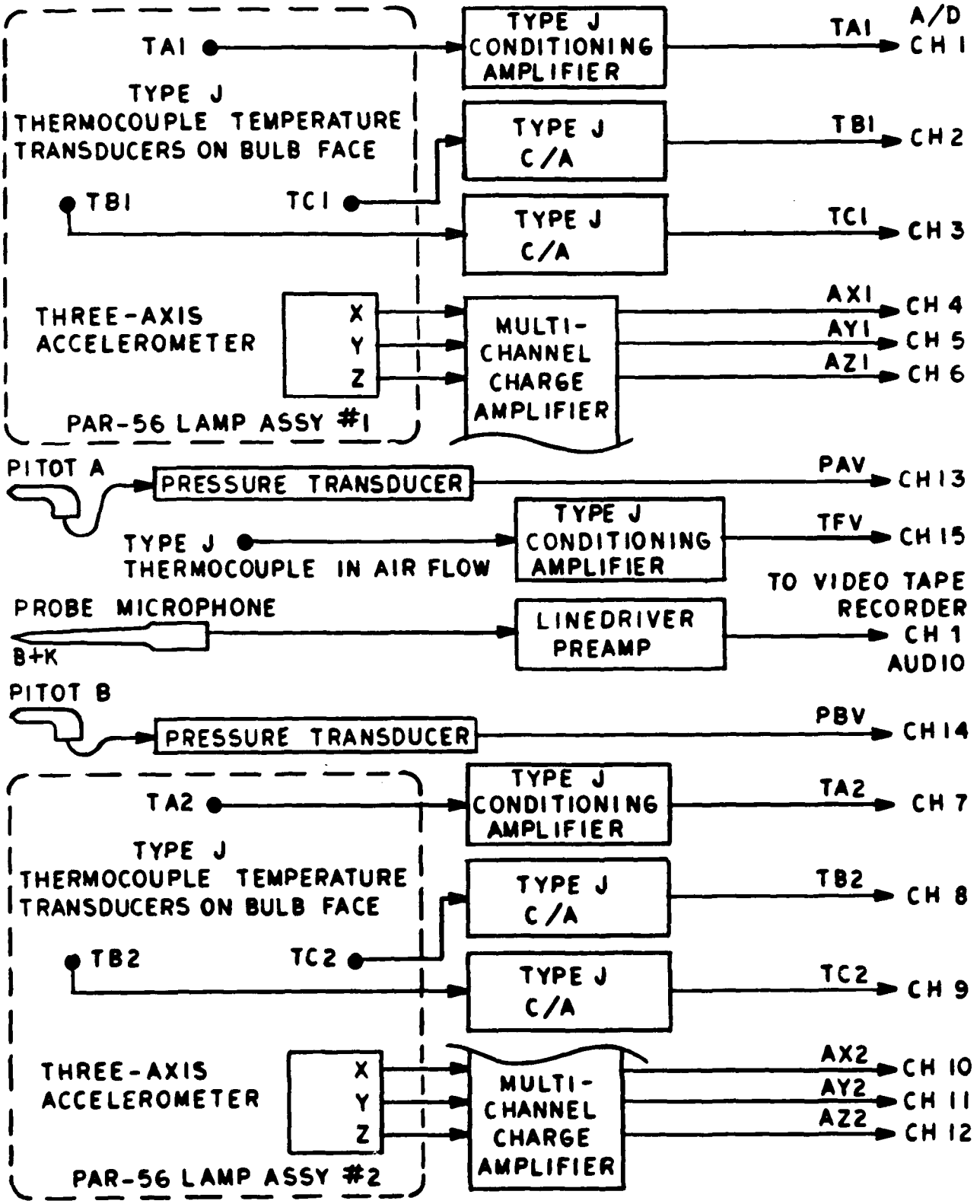

FIGURE 3. SENSOR ARRAY

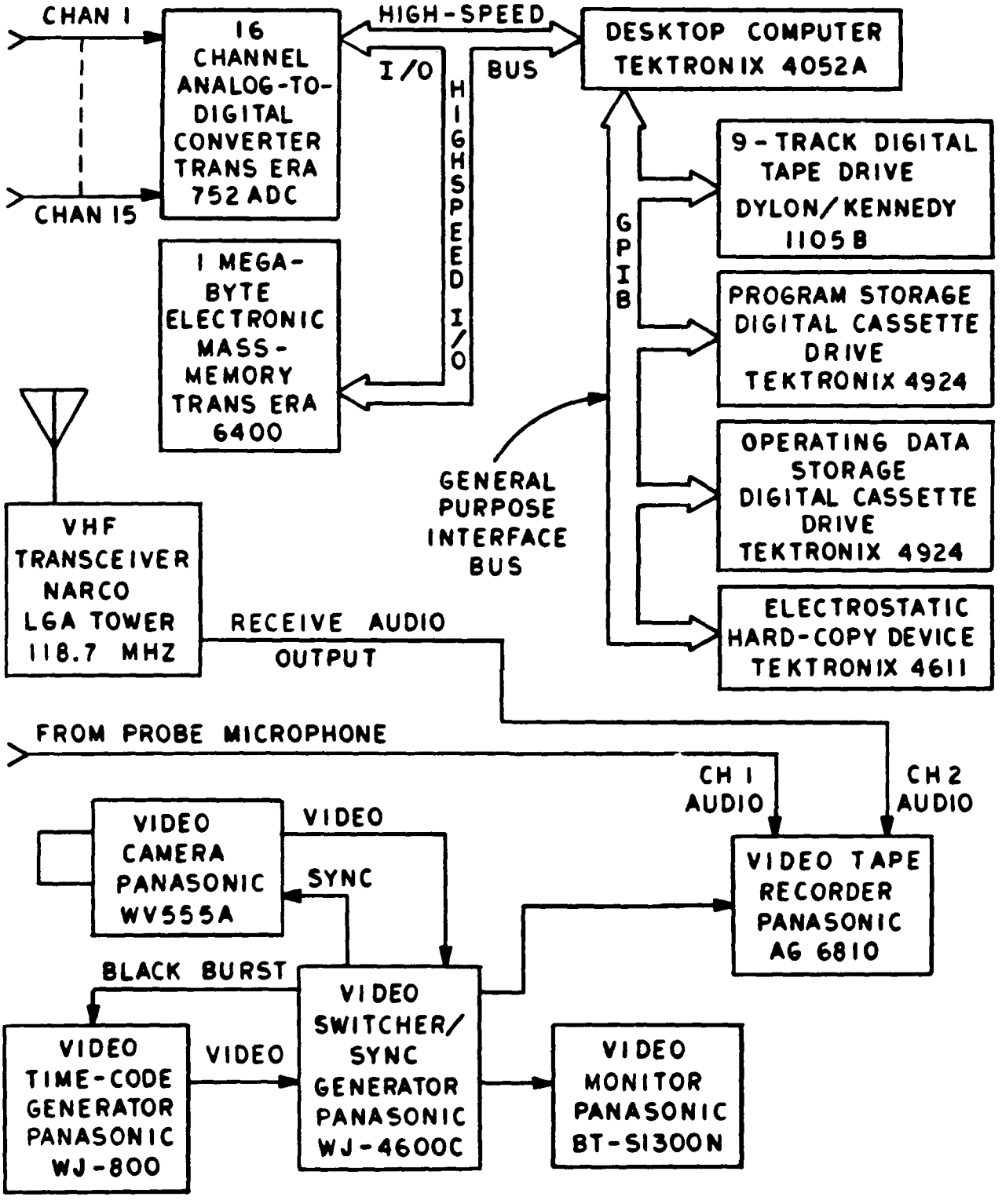

FIGURE 4. INSTRUMENTATION SYSTEM

TABLE 1. A/D CHANNEL ALLOCATION

CHAN	ID	SENSOR DESCRIPTION/LOCATION
1.	TA1	Lamp #1, Bulb Surface Temp., Top Center
2.	TB1	Lamp #1, Bulb Surface Temp., Left, 120 Deg. from top
3.	TC1	Lamp #1, Bulb Surface Temp., Right, 120 Deg. from top
4.	AX1	Lamp #1, Accelerometer: X-Axis
5.	AY1	Lamp #1, Accelerometer: Y-Axis
6.	AZ1	Lamp #1, Accelerometer: Z-Axis
7.	TA2	Lamp #2, Bulb Surface Temp., Top Center
8.	TB2	Lamp #2, Bulb Surface Temp., Left, 120 Deg. from top
9.	TC2	Lamp #2, Bulb Surface Temp., Right, 120 Deg. from top
10.	AX2	Lamp #2, Accelerometer: X-Axis
11.	AY2	Lamp #2, Accelerometer: Y-Axis
12.	AZ2	Lamp #2, Accelerometer: Z-Axis
13.	PAV	Velocity, Pressure, Pitot A
14.	PBV	Velocity, Pressure, Pitot B
15.	TFV	Velocity, Fluid Temp.

TABLE 2

DATA PARAMETERS RECORDED IN PREAMBLE

1. Data Run Nmber: Determined by computer.

2. Time and Date: From computer real-time clock which is synchronized with National Bureau of Standards Coordinated Universal Time and the video time generator.

3. Aircraft Type: Determined by observation. Entered by the operator from the keyboard.

4. Airline and Flight Number (or Tail Number if Business Jet): Determined from listening to air traffic control communications. Entered by the operator from the keyboard.

5. Ambient Temperature, Relative Humidity and Barometric Pressure: Entered from the keyboard whenever the Automatic Terminal Information System (ATIS) message changed, automatically recorded on each run.

6. Sensor location for each run: Only changes when sensors are moved. Entered by operator from keyboard, automatically recorded on each run.

7. Comments: Special meteorological conditions or anything unique to particular run were entered by operator from keyboard if applicable and recorded only for that run.

DATA PROCESSING AND ANALYSIS

The data acquired from each takeoff were recorded on a 9-track digital magnetic tape. Each reel of digital magnetic tape was capable of storing 22 million eight-bit words, or 22 megabytes of data. Since each takeoff contained about one megabyte of digital data, 22 takeoffs were stored on each tape. There were 162 takeoffs acquired during the test. This required seven reels of magnetic tape. Thus, the data processing required the handling of 162 megabytes of digital data.

At the end of the field data acquisition phase, the contents of the 7 digital magnetic tapes were loaded onto a hard disk drive of a Digital Equipment Corporation (DEC) VAX 11/750 computing system, located at ARDEC, where the data could be processed in an efficient, high-speed fashion. Each data run contained 15 channels of individual sensor data which was read from memory, scaled in proper engineering units by reading calibration coefficients stored in the preamble of each run, and then plotted together with the appropriate axes and labeling information.

The first task was to develop the plotting software and to plot all 15 sensor channels for all 162 data runs. It was assumed that the raw data would be adequate for the analysis phase. It became obvious after reviewing the raw data, however, that some of the the instrumentation used to condition the sensor signals (charge amplifiers, thermocouple preamplifiers, and line drivers) were affected by the rain and blast buffeting, despite being housed in an enclosure near the threshold bar.

The jet blast impinging on the conditioning electronics caused temperature changes in the circuitry and in some cases, resultant artifacts to appear in some sensor channels. Some of these artifacts were eliminated with additional digital signal processing of the data, but some artifacts contaminated the data irrecoverably. Also, moisture migrated into some of the circuitry due to the extreme environment and affected their electrical outputs. Again, some of these artifacts were easily removed with the judicious use of digital signal processing techniques, but some artifacts have irrecoverably destroyed the data. Fortunately, while at all times at least one channel of data was adversely affected by the above-mentioned data corruption mechanisms, with the use of signal processing, most of the data was recovered.

The accelerometer conditioning amplifiers were most prone to thermal drift during takeoff conditions. In some cases, the baseline drift was ten times the amplitude of the acceleration signal. The thermocouple temperature conditioning amplifiers generated high-level noise, and in some cases, all signals were contaminated with 60 Hertz line-related noise. In each instance, a digital signal processing algorithm was developed which allowed the reduction or removal of the contamination without affecting the essential information within the data.

The algorithm developed to remove the baseline drift in the accelerometer channels took advantage of the fact that the drift was a low frequency signal and the acceleration data had most of its energy at higher frequencies. Thus, a discrete signal process equivalent to a first-order high-pass filter was used. It effectively reduced the apparent baseline drift artifact to a level that was insignificant without affecting the integrity of the actual data. The equation describing the process used is as follows:

$$x'_n = x_n - \frac{1}{2k+1} \sum_{i=n-k}^{n+k} x_i \qquad (1)$$

Where x'_n is the new corrected value of the nth data point in question, x_n is the raw uncorrected value of the nth data point in question, and k is the index used to determine the number of data points in the averaging ensemble. The above equation describes a "sliding average" type of high-pass filter. In effect, it takes the average value of the data points extending k points ahead and k points before the data point in question and subtracts that average value from the point to be corrected. By carefully selecting the

value of k, the cutoff frequency of the resulting high-pass filter can be controlled. In practice, a cutoff frequency of 1 Hertz proved best for the nature of the data encountered in this project.

The above process is non-causal, meaning that its output is a result of data occurring before and data occurring after the data point to be corrected. This process cannot be done in real time as the event unfolds. It can only be done with a time delay (a pipeline delay) or during post-processing after the event. The advantage of this process is that the estimate of the correction factor used on the corrupted data is more realistic, since it includes information from data before and after the point occurs and therefore can "anticipate" future trends in the data.

Figure 5 shows the effect of imposing the above baseline correction algorithm to a particularly extreme case of baseline drift due to thermal imbalance caused by jet blast. The upper trace is raw, uncorrected data. The lower trace is the result of baseline correction using the algorithm. As can be seen, a dramatic reduction in baseline drift has been effected.

The temperature data were corrupted with high frequency noise caused by the conditioning amplifiers and the relatively long cables (upwards of 450 meters or 1500 feet) between the sensor array and the instrumentation van. The rate of change of temperature on the bulb faces was relatively slow, or stating it another way, the information bandwidth of the temperature signal was relatively low and occupied the low frequency end of the spectrum. Thus, the corrupting signal occupied the higher frequency end of the spectrum, and a simple data smoothing or averaging algorithm could be used.

The formula for the algorithm used is below:

$$x'_n = \frac{1}{k} \sum_{i=n}^{n+k} x_i \qquad (2)$$

Where x'_n is the new corrected value of the nth data point in question, and k is the number of data points used in the averaging ensemble. The value of k determines the cutoff frequency of the smoothing function and the resulting smoothed output can be thought of as having been low-pass filtered. The best results were obtained using a filter cutoff frequency of approximately 2 Hertz.

Some data runs had channels that were corrupted with 60 Hertz line-related components. Consideration was given to imposing a recursive all-pass function on the data to see if usable data could be recovered. The effect of a recursive all-pass filter is to insert a sharp notch filter at each harmonic of the 60 Hertz line interference. This would reject the interference while allowing all of the data information except for that which was coincident to the rejected line-related harmonics to appear at the output.

Theoretically, this approach is very attractive and has much merit. In

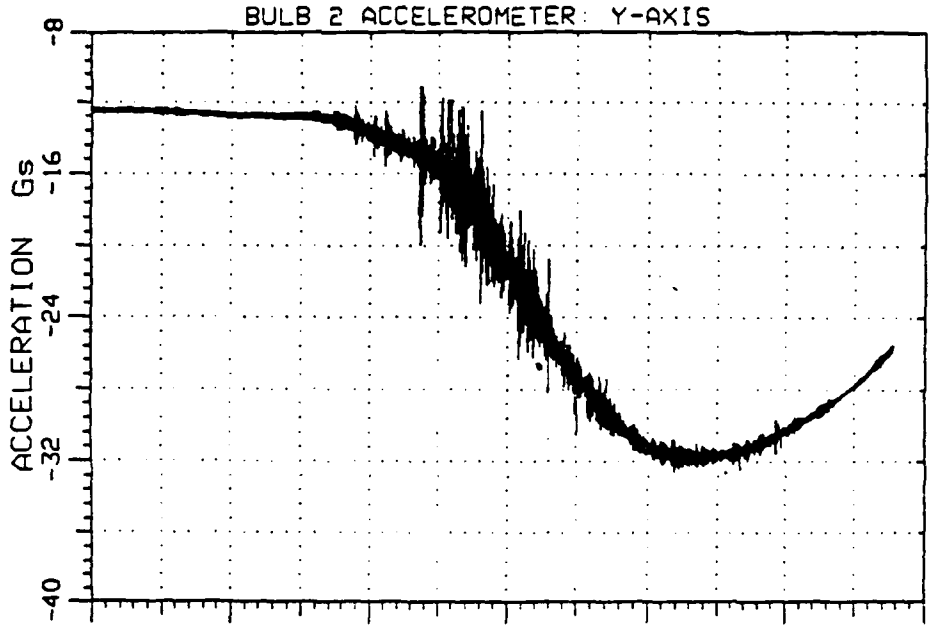

Figure 5A. Raw Acceleration Data showing excessive baseline drift artifact caused by instrumentation/blast interaction.

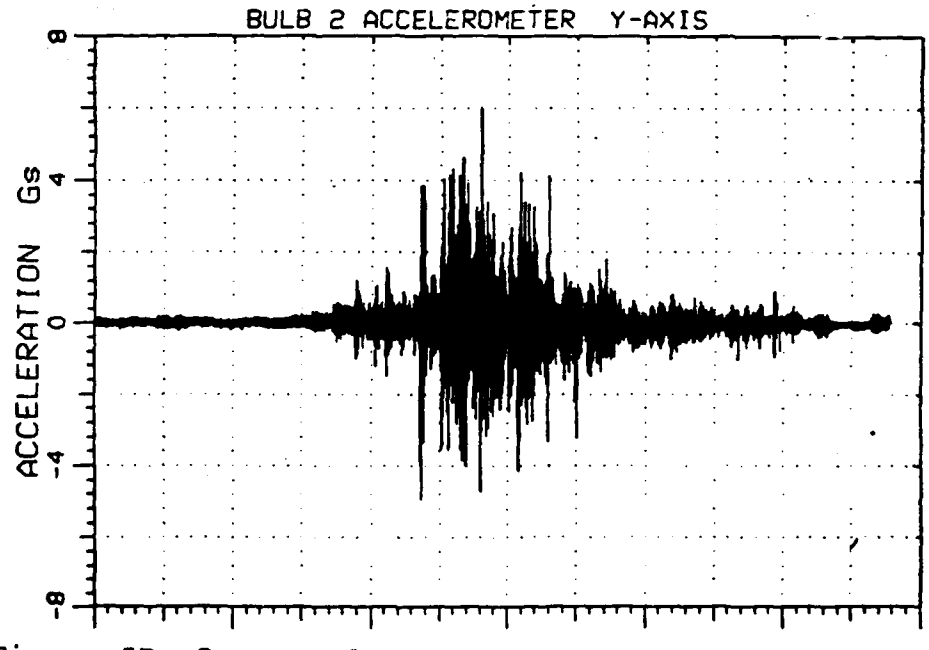

Figure 5B. Corrected Acceleration Plot. Note expanded Acceleration scale.

FIGURE 5. EFFECT OF BASELINE CORRECTION ALGORITHM

practice however, it only can be effective if the data sampling rate (the analog to digital converter sampling rate) is exactly at, or very close to an integer multiple of the 60 Hertz interference. The sampling rate allowed by the A/D converter used was 1195.848 samples per second. The closest integer multiple of 60 Hertz is 1200 Hertz. A crude estimate of a proposed filter's efficacy can be made by evaluating the ratio of the sampling rate to the closest harmonic, together with the number of bits of amplitude quantization.

With the imposition of the above ratio and quantization, the very best filter of moderate complexity, and with theoretically ideal conditions, could reduce the interference by 25 to 30 decibels. It was decided that this improvement would not yield usable data and the recursive all-pass approach was abandoned. Thus, at this point the data runs which have line-related interference cannot be sufficiently improved using simple all-pass filtering techniques. There are other, more complex all-pass algorithms which could yield a theoretical 40 to 50 decibel improvement but their complexity would require additional time and effort, not anticipated within or funded by the existing contract.

During the data acquisition phase at LaGuardia airport it was noted that some aircraft seemed to induce accelerations in the lamp fixtures that appeared to be primarily due to the strong coherent acoustic output of the jet engines. The L-1011 in particular, which has Rolls-Royce engines, produces a loud "moaning" sound during runup which appeared to be evident in the output of an accelerometer channel which was being monitored with an oscilloscope in the instrumentation van.

A Discrete Fast-Fourier Transform algorithm (FFT) was used to produce spectral plots of the accelerometer channels and of the sound pressure information of several data runs of the L-1011. This provides comparison of the frequency components in each to see if the vibration could be related to the acoustic output. This FFT transform was performed on the Tektronix 4052A computer.

The transform uses a 1024 point input ensemble, which represents approximately one second of data. The resulting output has 512 points of frequency resolution, an analysis bandwidth of 510.22 Hertz, and with each spectral line representing the energy contained in a 0.996 Hertz band. Conventional input windowing using a Hanning or raised-cosine weighting function was used. Since the amplitude quantization was 12 bits, a theoretical 72 decibels of amplitude accuracy was available at the output. The input signals had signal-to-noise ratios far worse than the available accuracy of the discrete FFT, so only data within 30 to 40 decibels of the maximum signal should be considered valid.

MEASUREMENT RESULTS

RAW DATA ACQUIRED

The "mass production" plotting of all the raw data acquired revealed many things. It became clear that the sheer volume of data acquired was much more than was necessary to fulfill the original goals of the project. To be sure that representative data extremes were encountered, many data runs were acquired, resulting in much redundant data. It also was found that some of the data was corrupted with various artifacts which needed to be eliminated or reduced to acceptable levels by additional signal processing. It also became evident that a selection or culling process should be done to reduce the volume of data needing further processing, without eliminating data runs of particular worth in fulfilling the project goals.

Some consideration was given to writing a program which could perform the culling process with a minimum of human interaction. This process proved to be highly complex. The end result was that the effort required to develop the code necessary to perform the task was equal to or greater than the effort to manually perform the task.

Thus, the data plots produced by the original "mass production" process, which were raw, uncorrected plots were manually reviewed by several skilled individuals with the following guidelines:

1. Select representative data runs for each of the major aircraft encountered during the data acquisition phase.

2. These runs should include one run which shows typical or "average" data values.

3. Two runs with maximum data values should be selected to represent an extreme case for each aircraft type.

4. The runs selected should have the maximum available useful data channels.

5. The data in each selected run should readily lend itself to the data correction algorithms to maximize useful information content in the corrected data.

6. The runs should be selected using the annotations made by the test leader in the data run log as a guide to identifying "typical" and "extreme" cases.

These criteria made data run selection very difficult and time-consuming. In some cases, several individuals had to pass judgment on a particular aircraft in order to select data runs which fulfilled all of the above requirements. Also, in some cases, a particularly promising data run had to be eliminated due to missing data channels considered to be essential to a

careful analysis of that run.

Some plots from several of the more representative data runs appear in Appendix A. The accelerometer plots have been baseline corrected using the correction algorithm discussed in the data processing section. The temperature plots have been smoothed using the algorithm presented in the discussion. These plots were selected to show representative high-value parameters to give the reader a feel for the nature and duration of the effects measured in this project. They are not representative of the worst-case environment encountered, but they show more the quality of the environment, rather than portraying the worst-case magnitude of any given parameter.

The bulb face temperature of one runway-mounted PAR-56 lamp assembly was measured under ambient conditions to establish normal operating levels as a baseline. Table 3 lists the results and the ambient weather conditions reported by LGA Tower at the time of measurement.

TABLE 3

PAR-56 BULB TEMPERATURE AS A FUNCTION OF ILLUMINATION STEP
Note: Only one SIDE temperature listed since both sides were virtually identical.

STEP LEVEL	TOP		SIDE	
	TEMP oC	TEMP oF	TEMP oC	TEMP oF
OFF	4	39	4	39
1	99	210	80	177
2	131	268	106	223
3	189	372	155	311
4	248	478	208	406
5	309	589	259	498

Reported Weather Conditions:

Temperature:	39 oF
Dew Point:	31 oF
Barometer:	30.14 inHg
Wind:	350-360o @ 8-9 Kt.

INTERPRETATION OF DATA

TIME ANALYSIS

The time analysis of the data was relatively straight-forward. The 15 plots from each selected aircraft run were manually reviewed by a skilled engineer and the pertinent parameters were noted. The parameters reviewed were acceleration versus time for three axes, bulb surface temperature versus time for two bulbs, each having three thermocouple temperature transducers epoxied in place, blast temperature versus time and two wind velocities versus time.

The volume of data made interpretation a difficult task. To facilitate interpretation, a data matrix was created which lists 23 different parameters for each aircraft selected. There were 12 major aircraft types, with a total of 30 data runs representing typical and extreme selections for each type of aircraft. The matrix was broken up into two parts for clarity of presentation.

Table 4 is the data matrix which lists accelerations encountered with each aircraft. Both peak and Root Mean Square (RMS) accelerations are listed for each axis. At the bottom of the matrix are also listed the maximum values for the selected aircraft and maximum values ever encountered.

Table 5 is the data matrix listing minimum and maximum bulb face temperatures, maximum rate of change of temperature, minimum and maximum blast temperature, maximum rate of change of blast temperature, and two maximum blast velocities. At the bottom of the matrix are also listed maximum values for listed data as well as for all data acquired in this project.

SPECTRAL ANALYSIS

Spectral analysis of the data was performed for two reasons. The first reason was to establish the power spectral density of the acceleration signals so that the mechanical designer would have peak and RMS acceleration values as well as the power spectral density of the acceleration at his disposal when new lamp fixture designs or specifications are formulated. Figure 6 shows a typical acceleration power spectral density signature, measured on a single axis of the tri-axial accelerometer. This plot is a good example of the spectrum encountered in most cases.

The plot presents the acceleration induced by an L1011. It is a one second capsule of the acceleration power spectral density taken 1.71 seconds into the takeoff roll. The amplitude scale is not absolute. The important fact displayed by the plot is that the acceleration signature is relatively broadband random noise with no part of the spectrum having significantly higher energy than another. No significant structural resonances appear in this plot, or in any other reviewed during the analysis of the data. Had any

TABLE 4

DATA MATRIX OF ACCELERATION VALUES

FAA DATA MATRIX ACCELERATION														
			PEAK ACCELERATION						RMS ACCELERATION					
AIRCRAFT TYPE	TYP OR EXTRM	RUN #	X1 G	Y1 G	Z1 G	X2 G	Y2 G	Z2 G	X1 G	Y1 G	Z1 G	X2 G	Y2 G	Z2 G
L1011	T	57	5.5	5.1	3.4	3.5	N/A	1.8	3.8	3.1	1	0.9	N/A	0.28
	E	20	6.2	6	1.5	7.5	N/A	2.5	1.7	2.2	0.2	2	N/A	0.4
	E	52	8	13	18	7.4	N/A	6.5	2.5	4.1	4.2	5.1	N/A	0.56
DC10	T	58	3.8	3.5	3	2	N/A	1.2	1.5	1.5	0.75	0.8	N/A	0.2
	E	117	4	4.9	N/A	4.1	N/A	2.3	0.85	0.38	N/A	1.7	N/A	2.3
	E	131	7.4	11	10.3	7.2	N/A	2.7	2.3	4.9	1.9	0.9	N/A	0.7
DC9/MD80	T	11	3.4	1.5	1.2	3	N/A	1.6	0.75	0.5	0.2	1.2	N/A	0.4
	E	89	3.7	1.5	N/A	0.6	N/A	0.2	0.15	1.2	N/A	0.3	N/A	0.1
	E	109	2.7	2.9	17	2.5	8	1.2	1.4	1.3	4.9	1.1	4.5	0.4
767	T	48	7	10	3	3.9	N/A	1.75	2	2	1	1.3	N/A	0.6
	E	107	6	9	4.2	6.5	N/A	2.4	2.2	5	2.1	3	N/A	0.7
	E	133	7.5	12	7	11	1.2	11	3.2	6	3	3.8	0.3	2.5
757	T	136	5.7	9.4	3.9	4.2	0.7	3.3	2.1	4.1	1.8	1.7	0.12	1.1
	E	78	5.5	7	3.8	5.5	N/A	2.2	2	3.2	1.2	1.8	N/A	0.6
	E	94	6.1	12	N/A	1.8	N/A	1.2	1.2	5.5	N/A	0.6	N/A	0.62
737	T	135	1.4	1.2	1.1	0.8	N/A	0.38	0.5	0.4	0.26	0.23	N/A	0.15
	E	90	1	2	N/A	0.3	N/A	0.2	0.2	0.7	N/A	>0.1	N/A	> 0.1
	E	104	2.4	4.9	2.1	0.62	N/A	N/A	0.65	1.7	0.8	0.21	N/A	N/A
737-300	T	37	1.4	2	0.6	1	N/A	0.3	0.5	0.3	0.1	0.1	N/A	>0.1
	E	5	7.1	1.7	1.4	0.8	N/A	0.65	0.2	0.2	0.6	0.2	N/A	>0.1
727	T	2	6.5	5.5	5.5	8.5	N/A	7	2.5	2.1	2	3.75	N/A	3
	E	60	10	5	3.2	5.5	N/A	3.5	4.2	2.1	1.3	3.2	N/A	1.35
	E	120	0.75	1.2	N/A	0.6	N/A	1	>0.1	>0.1	N/A	>0.1	N/A	0.2
A300 AIRBUS	T	115	2.7	4.2	2.05	2.2	N/A	1.1	0.9	1.8	1.1	0.61	N/A	0.65
	E	64	3.7	7.1	3.1	1.5	N/A	1.8	1.8	1.5	1	0.78	N/A	0.1
	E	41	3	3	1	1.8	N/A	0.75	1	0.75	0.2	0.4	N/A	0.15
FALCON	T	61	1.1	0.9	0.4	0.7	N/A	0.22	0.36	0.38	>0.1	0.22	N/A	>0.1
BUS JET	T	93	0.22	0.23	N/A	0.4	N/A	0.37	>0.1	>0.1	N/A	>0.1	N/A	0.2
HAWKER	T	124	0.3	0.7	N/A	N/A	N/A	N/A	>0.1	>0.1	N/A	N/A	N/A	N/A
BAC111	T	126	1.4	1.6	1.2	1.2	N/A	0.95	0.6	0.7	0.4	0.8	N/A	0.55
MAX. LISTED DATA			8	10	18	11	8	7	4.2	6	4.9	5.1	4.5	3
MAX EVER			20	20	20	20	20	20	8	8	8	8	8	8

TABLE 5

DATA MATRIX OF TEMPERATURE AND VELOCITY VALUES

FAA DATA MATRIX TEMPERATURE & VELOCITY														
			BULB #1 A, B, C			BULB #2 A, B, C			FLUID			VELOCITY	
AIRCRAFT TYPE	TYP OR EXTRM	RUN #	MIN C	MAX C	MAX dT/t C / SEC	MIN C	MAX C	MAX dT/t C / SEC	MIN C	MAX C	MAX dT/t C / SEC	MAX A M / SEC	MAX B M / SEC
L1011	T	57	10	18	0.16	4	6	-0.1	N/A	N/A	N/A		
	E	20	12	15	0.8	12	15	0.6	16	24	2.1		
	E	52	10	19	0.36	3	6	-2.5	N/A	N/A	N/A		
DC10	T	58	11	17	0.2	3	6	-0.1	N/A	N/A	N/A		
	E	117	74	105	-5.1	55	128	-2.5	20	27	2		
	E	131	92	145	-4.3	62	149	-4.6	24	32	2.3		
DC9/MD80	T	11	31	41	-0.1	19	19	0	20	21	0.1		
	E	89	100	156	-2.3	127	142	-1.3	19	23	0.8		
	E	109	94	152	-2.7	72	156	-4	15	17	0.67		
767	T	48	9	16	0.3	N/A	N/A	N/A	8	27	-5.3		
	E	107	62	98	-1.6	49	111	-1.6	16	27	1.9		
	E	133	91	161	-3.3	66	157	-5.7	20	33	4		
757	T	136	76	121	-4.7	54	129	-2.2	21	33	2.2		
	E	78	9	11	0.4	7	9	0.3	51	54	7.2		
	E	94	98	156	-6.4	120	141	-4	18	26	1.6		
737	T	135	89	145	-4.6	88	136	-3.2	20	29	1.5		
	E	90	93	156	-4.3	124	140	-2.9	18	23	2.6		
	E	104	88	137	-4	58	128	-1.6	17	21	-0.4		
737-300	T	37	36	64	-1.1	N/A	N/A	N/A	12	18	0.9		
	E	5	13	17	0.8	13	21	0.9	16	28	6		
727	T	2	30	52	-0.25	30	49	-0.3	8.7	9.6	0.3		
	E	60	46	77	1.6	58	86	3.2	8	54	5.3		
	E	120	133	193	-3.3	91	196	-6	17	20	0.8		
A300 AIRBUS	T	115	68	114	-2.1	51	123	-1.5	18	24	-1		
	E	64	58	91	-1.7	57	64	-1.3	2	6	1.6		
	E	41	13	15	0.4	11	13	0.18	16	23	1.3		
FALCON BUS JET	T	61	69	99	0.53	67	75	0.8	2.5	6.8	1.6		
	T	93	125	169	-0.67	143	157	-3.3	18	18	0		
HAWKER	T	124	96	156	-2.6	80	162	-3.3	17	18	0.6		
BAC111	T	126	129	170	-0.8	87	126	-2.3	19	20	>0.1		
MAX. LISTED DATA					6.4			5.7			7.2		
MAX EVER					10			10			15		

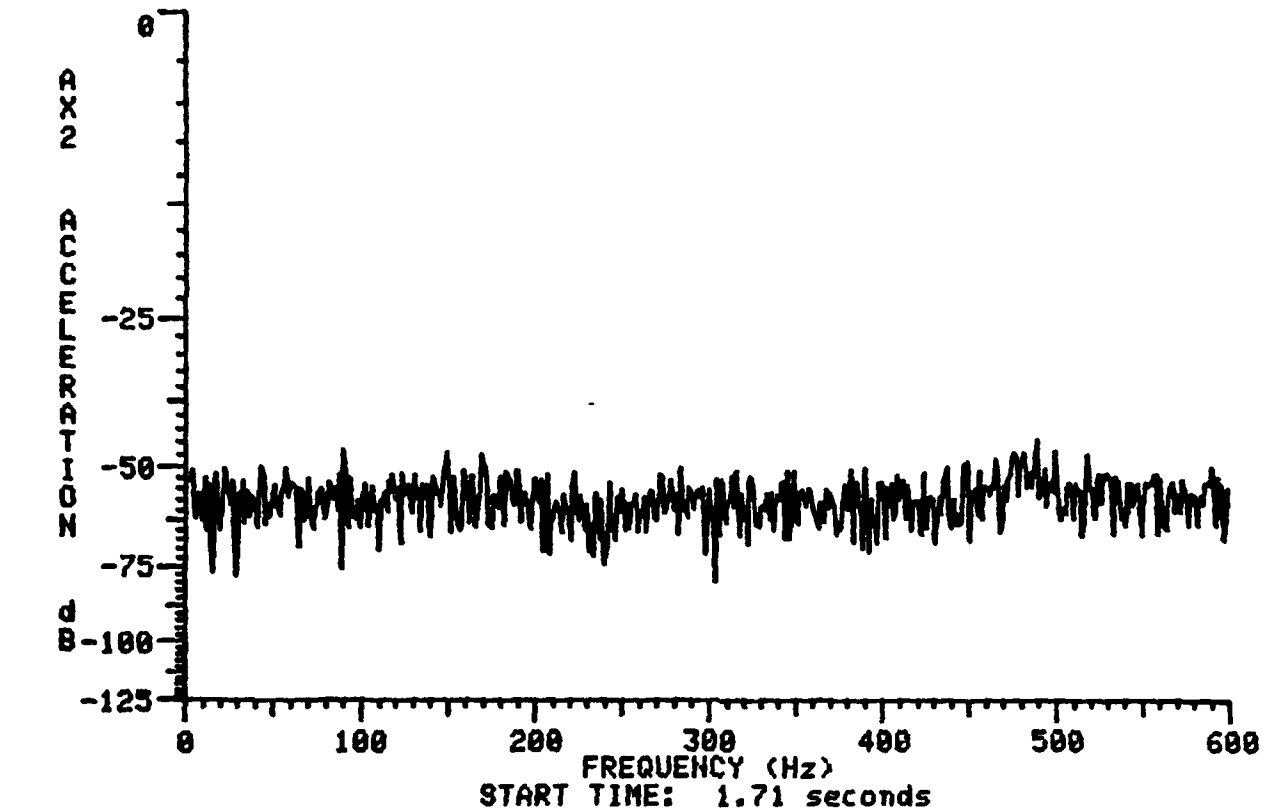

FIGURE 6. TYPICAL ACCELERATION POWER SPECTRAL DENSITY

part of the structure had a tendency towards a High-Q resonance, the type of broadband random excitation exhibited in this plot would certainly have induced the resonance and it would have appeared as a pronounced peak at a particular frequency.

The second reason was to establish whether there are accelerations induced by the acoustic output of an engine or if the main driving source of vibration is the buffeting caused by the impinging jet exhaust blast. If such accelerations are induced, their magnitudes with respect to the random excitation should be evaluated. In Figure 7, a direct correlation can be seen between the coherent spectral energy in the acoustic output of the Rolls-Royce engines in an L1011 and the coherent spectral energy in the acceleration measured on the lamp fixture. This coherent energy is the "moaning" sound heard in the beginning of the runup of the engine and is probably due to compressor stall.

Figure 7A is a plot of the power spectral density of the acoustic output of the engines of the L1011. The coherent components at 120 and 135 Hertz are circled. Notice that these components project 25 dB above the adjacent random noise. Notice also that there are three other coherent signals at 360, 450, and 520 Hertz. These components could be due to the whining of the blades within the turbines.

Figure 7B is a plot of the acceleration signature of the X-axis accelerometer mounted on one of the PAR-56 lamp assemblies. The two circled coherent components at 120 and 135 Hertz are very evident in the acceleration. They do not project as much above the adjacent random noise, but if the lamp assembly had a structural resonance at this part of the spectrum, the potential for structural damage would exist with a long enough exposure to this type of coherent excitation. Note that the higher frequency turbine components, which were evident in the acoustic signal, are not apparent at all in the acceleration signal.

Thus, if there were a new engine which had a strong, coherent acoustic output in the lower part of the frequency spectrum (less than 200 Hertz), where acoustic energy coupling to a mechanical structure is most likely, the engine's effect on the structure of any mechanical device in the vicinity of the threshold bar should be investigated. One way to predict if such coupling may be likely would be to request that spectral analyses of the acoustic output of a new jet engine be performed and reported with the exhaust velocity and temperature contours. These spectral plots would be evaluated for significant coherent outputs within the known frequency regions where coupling is likely.

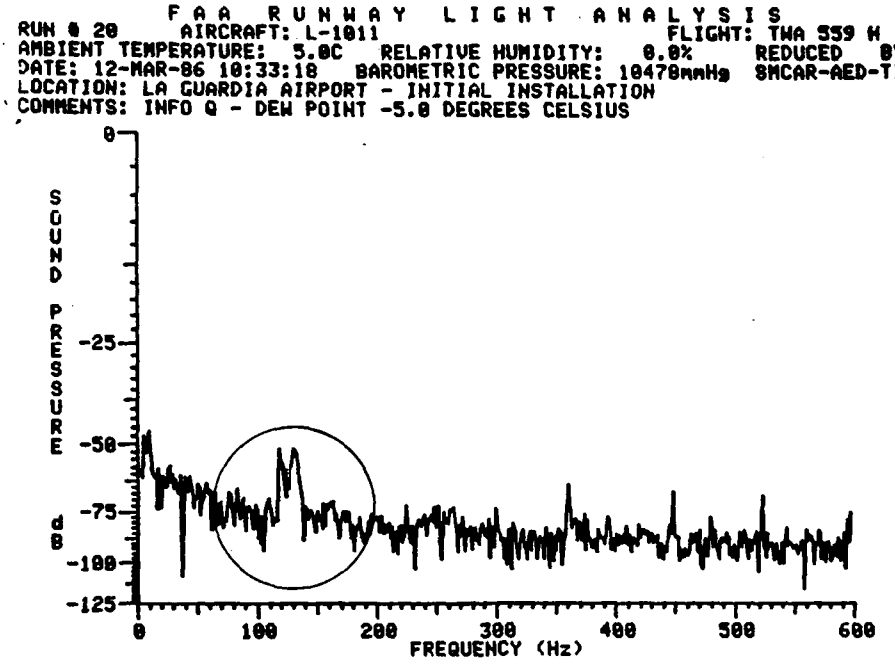

Figure 7A. Acoustic Power Spectral Density of Rolls-Royce Engine Showing Coherent Components

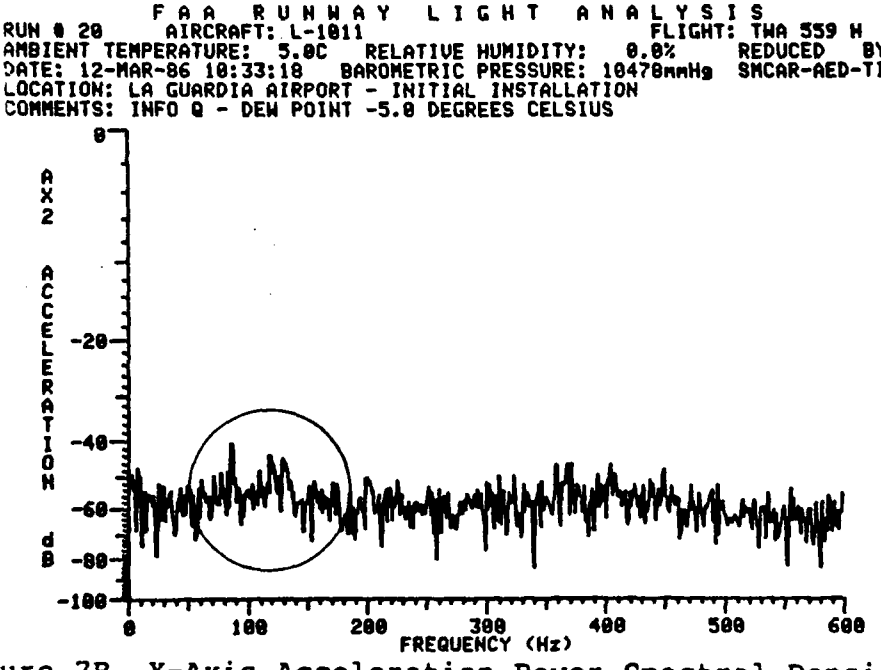

Figure 7B. X-Axis Acceleration Power Spectral Density showing same Coherent Components

FIGURE 7. ACOUSTIC ENERGY COUPLING OF COHERENT COMPONENTS

DATA DEPENDENCIES

AIRCRAFT EFFECTS

The larger, heavier aircraft, such as the L1011, 767 and A300 Airbus, produce higher accelerations, higher wind velocities, higher rates of change of temperature and higher sound pressure levels than the smaller aircraft. Some measurements were made on smaller commuter and business aircraft, such as the Lear, Mitsubishi, Beach 99, and Dash 7, 8 and almost negligible effects were recorded. The intermediate size aircraft produced effects somewhat less than the "heavies".

Before this project was begun, it was speculated that the newer high-bypass turbofan engines would have less of an effect than the older turbojet designs. It was thought that the significantly larger thrust cross-sectional area would reduce the intensity of the blast effect on a given area. This was definitely not observed in the measurements. In general, it can be stated that the larger the thrust and the heavier the aircraft, the higher its effect on the equipment at or near the threshold bar.

PILOT EFFECTS

The variability of pilot technique produced the highest variances in the measured data. The point at which engine runup was begun was a function of whether takeoff clearance was given on the taxiway or in takeoff position at the end of the runway. The point at which the aircraft started to roll varied also, each pilot appeared to have his own preferred starting point at the beginning of the runway. A variability of 50 to 150 feet from the threshold bar was noted in this starting point.

The way in which the engines were throttled up varied significantly from pilot to pilot, also. Some of these variabilities can be attributed to pilot "style". Some pilots increased power rapidly, so that full takeoff thrust was achieved very close (within 150-300 feet) to the threshold bar. In some cases, the engines were run up to full thrust while the aircraft was on its brakes. Other pilots seemed to prefer to gradually increase the power as the aircraft accelerated down the runway. In this case, full takeoff thrust might not be achieved until the sensors were out of range of the blast effects.

METEOROLOGICAL EFFECTS

The variabilities in the data produced by other effects made it difficult to detect any effects that were due solely to the weather conditions. The weather did have an effect on takeoff procedures and airport operations, but it did not appear to directly affect any of the parameters being measured.

AIRCRAFT/SENSOR DISPLACEMENT EFFECTS

The displacement of the aircraft, or more particularly, its engines from the sensor array, had a definite influence on the nature and the magnitude of the jet blast effects being measured. Displacement in this case is the vector sum of the horizontal distance between the engine and the sensor array and the engine height above the sensor array.

Typical contours of jet engine exhaust velocity and temperature are presented in Figure 8 and Figure 9. They are for the Boeing 727-100, 727-100C, and the 727-200 at breakaway thrust. Notice in each the horizontal displacement ("axial distance behind airplane") effect and also the effect of the vertical displacement component ("height above ground plane") on a sensor array mounted about one foot above the ground plane.

When the engines were very near the sensor array, so that the blast plume was directed above the array, the only effect noticed was a moderate acoustic coupling. That is, the strong acoustic energy radiating from the side and aft parts of the engine couples into the structures being monitored.

As the aircraft moves away, the blast plume begins to impinge on the structures being monitored, and the measured acceleration begins to significantly increase, as well as the measured velocity and the thermal effects. These effects reach a peak when the part of the blast plume having maximum velocities and temperature impinges on the structure. They then begin to gradually drop as the aircraft accelerates away. When the aircraft is beyond 8 to 10 aircraft lengths, almost no noticeable disturbance is noted.

MISCELLANEOUS EFFECTS

The loading of a particular aircraft had a significant effect on the data. If an aircraft was heavily laden, the pilot tended to throttle up under brakes and then release the brakes when full or near-full takeoff thrust was attained. This tended to expose the lamps and sensor array to higher levels of blast for longer time durations.

With a lightly loaded aircraft, the pilot tended to apply the throttles more gradually, with no brakes applied, and more likely than not, to increase throttle settings slowly as the aircraft accelerated away. This exposed the lamps and sensors to lower levels of jet blast for shorter durations.

Some seemingly dramatic effects were noted during the data acquisition phase of the project which were later characterized as erroneous. One effect noted was a marked drop in the surface temperature of one of the PAR-56 lamps. It was later discovered that a particularly vigorous takeoff on the part of a 727 pilot displaced several sandbags into Flushing Bay. These sandbags were securing the enclosure housing the conditioning amplifiers for the thermocouple temperature transducers. The jet blast ripped off the housing cover and the amplifiers blew backwards, detaching all three thermocouples

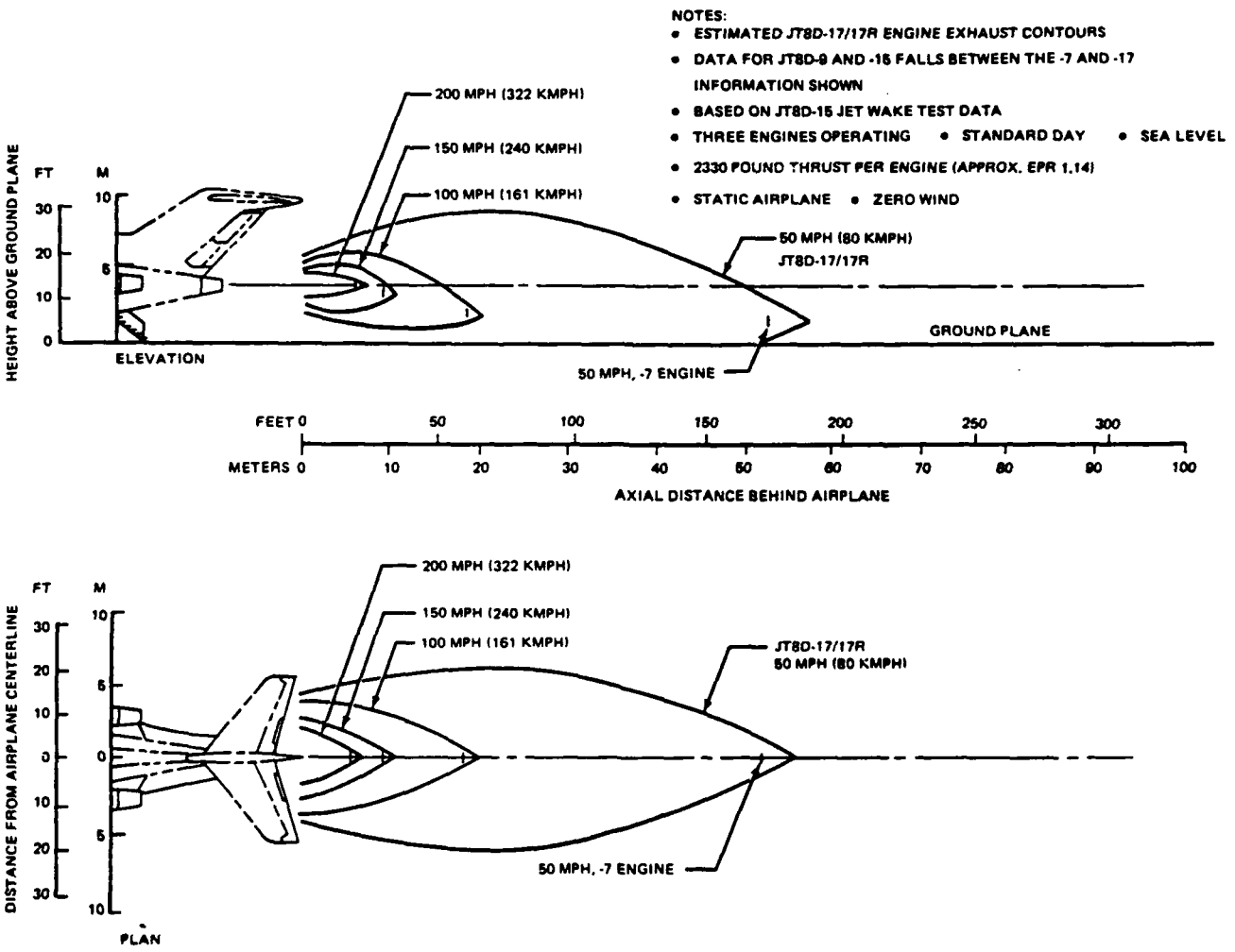

FIGURE 8. JET ENGINE EXHAUST VELOCITY CONTOURS: BREAKAWAY THRUST

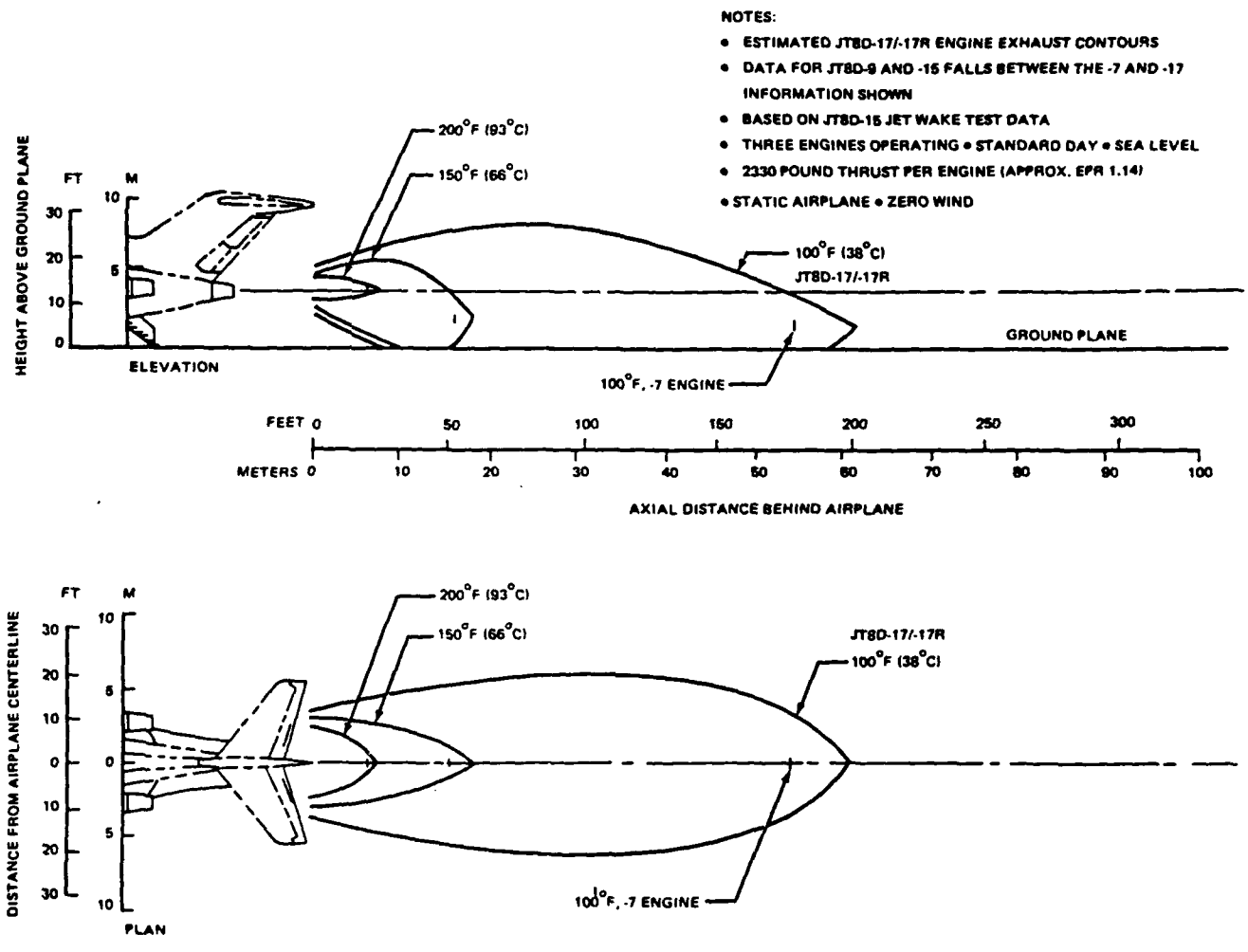

FIGURE 9. JET ENGINE EXHAUST TEMPERATURE CONTOURS: BREAKAWAY THRUST

from the bulb face. At several times during the data acquisition phase, the extreme magnitude of blast caused sensor cabling to be displaced or destroyed.

As was stated in the discussion, the thermal and moisture migration effects of the jet blast caused numerous anomalies and artifacts in the data which later had to be eliminated with digital signal processing techniques. The thermal effects were always present. The moisture migration effects were only present when the runway was very wet with precipitation. The jet blast lifted the moisture from the runway surface, atomizing it and then driving it into any small orifice in its path with great force.

EXTRAPOLATION OF DATA TO OTHER AIRCRAFT

The approach taken to determine whether a new type of aircraft or one which was not encountered during the data acquisition would have affected the worst case results found in the data acquired was as follows: In order to begin, it was necessary to obtain jet blast profile data from as many aircraft and jet engine manufacturers as possible. This information is given in terms of jet engine exhaust velocity and temperature contours as a function of displacement from the rear of the aircraft for both plan and elevation views. Typical exhaust contours for breakaway thrust are shown in Figures 8 and 9. This information was compiled for some 26 different types of aircraft from various domestic and foreign commercial transport manufacturers as well as some corporate and military aircraft manufacturers. Table 6 is a list of manufacturers whose published jet blast profile data were used in this worst case estimation analysis.

The next step was to amass the takeoff thrust blast profile data into a computer data base to allow its analysis. One powerful method of analysis is a scatter plot. Two scatter plots were produced from the data. These are plots in which all data points from all aircraft are plotted without lines being drawn between adjacent points. This type of data presentation allows one to easily determine any general trends in large amounts of data. Figure 10 is a scatter plot of published jet exhaust velocity at takeoff thrust versus displacement and figure 11 is a scatter plot of published jet exhaust temperature at takeoff thrust versus displacement. As can be seen in both of these plots, the exhaust velocity and its temperature follow definite trends due to the clustered nature of data points. For comparison purposes, the specific data for the Boeing 727 and the Grumman F-14 are highlighted in each plot in line form. These specific plots are very linear when presented on a log-log axis graph.

The production of the scatter plots and specific aircraft plots indicates that both the velocity and temperature of a jet engine exhaust blast have a definite relationship to the displacement from the rear of the aircraft. That is to say, that since the scatter plots show definite trends as to the nature of the relationship between displacement and velocity or temperature, a rough determination of the velocity or temperature of the jet exhaust of any other

TABLE 6

LIST OF MANUFACTURERS WHOSE PUBLISHED JET BLAST PROFILE DATA WERE USED IN WORST CASE ESTIMATION ANALYSIS

COMMERCIAL DOMESTIC TRANSPORT AIRCRAFT

Boeing, 707-120B, -320B, -320C
Engine Type(s): JT3D

Boeing, 720
Engine Type(s): JT3C

Boeing, 727-100, -100C, -200
Engine Type(s): JT8D-9, -15, -17, -17R

Boeing, 737-100, -200
Engine Type(s): JT8D-17

Boeing, 737-300
Engine Type(s): CFM56-3B1

Boeing, 747, 747SP
Engine Type(s): JT9D-3 BLOCK II, -7

Boeing, 747-400
Engine Type(s): Not Given

Boeing, 757-200
Engine Type(s): Not Given

Boeing, 767-200, -200ER, -300, -300ER
Engine Type(s): JT9D-7R4D/ -7R4E, CF6-80A/ -80A2, PW 4056/ CF6-80C2

Douglas, DC-8
Engine Type(s): JT3D or RCo 12

Douglas, DC-9
Engine Type(s): Not Given

Douglas, DC-10, Series 10, 10CF, 30, 30CF, 40, 40CF
Engine Type(s): JT9D-20/ -59A

Douglas, MD-80
Engine Type(s): Not Given

Lockheed, L-1011, -1, -100, -200
Engine Type(s): Not Given

COMMERCIAL FOREIGN TRANSPORT AIRCRAFT

Airbus, A 300 B2, B4, C4
Engine Type(s): JT9D, CF6-50C2

British Aerospace, BAC-111 400 Series
Engine Type(s): SPEY 511-14

British Aerospace, BAe-125-700/ -700
Engine Type(s): Garret TFE731-3

British Aerospace, Concorde
Engine Type(s): Not Given

Fokker, F-27, MK 200/500
Engine Type(s): Not Given

CORPORATE AIRCRAFT

Cessna, Citation II, III (Model 550, 650)
Engine Type(s): P&W JT15D-4, Garrett TFE731-3B

Falcon Jet, Falcon 50
Engine Type(s): Garrett TFE-731-3C (See data for Citation)

Gates Learjet, Models 23/24, 35/36, 35A/36A, 55/55B
Engine Type(s): Garrett TFE 731-2/3, General Electric CJ610

MILITARY AIRCRAFT

Lockheed, C130
Engine Type(s): Not Given

Grumman, F-14A, F-14A(PLUS), -14D
Engine Type(s): Pratt & Whitney TF-30, General Electric F110-400

Douglas, F-15
Engine Type(s): Pratt & Whitney F100-PW-100

Boeing, KC-135A/E/R
Engine Type(s): Pratt & Whitney J-57, JT3D-3B, CFMI CFM56-2B-1

TABLE 7

EXTRAPOLATION OF DATA TO OTHER AIRCRAFT NOT MEASURED

AIRCRAFT TYPE	PUBLISHED V_{100} MPH @ Takeoff	A_{RMS} g	A_{PEAK} g	$\lvert\Delta T_{max}\rvert$ DEGREES C
Boeing 747	170	5.0	17.6	5.2
Douglas DC-8	80	1.6	5.7	4.0
Grumman F-14	340	14.0	50.0	7.7
Concorde	220	7.5	26.0	6.0

It should be stressed again that the values listed in the above table should be used only as guidelines and not as hard numbers. They represent an attempt to predict physical phenomena which at best have a high degree of associated variability attached to them because of the many reasons listed in the section describing data dependencies. A more accurate algorithm could be derived only if a set of measurements were performed under tightly controlled laboratory conditions.

SUMMARY OF RESULTS

Acquiring data from 162 takeoff runs provided more than enough information for use in fulfilling the objectives of the project. The wealth of information contained in the raw data is highly distilled in the type of analysis done for the preparation of this report. The tables of key data parameters presented in previous sections give an overview of the more important parameters measured during the acquisition of data.

The absolute maximum parameter values encountered in this project are important design guidelines, when accompanied with the spectral and time plots. Table 8 lists these maximum values.

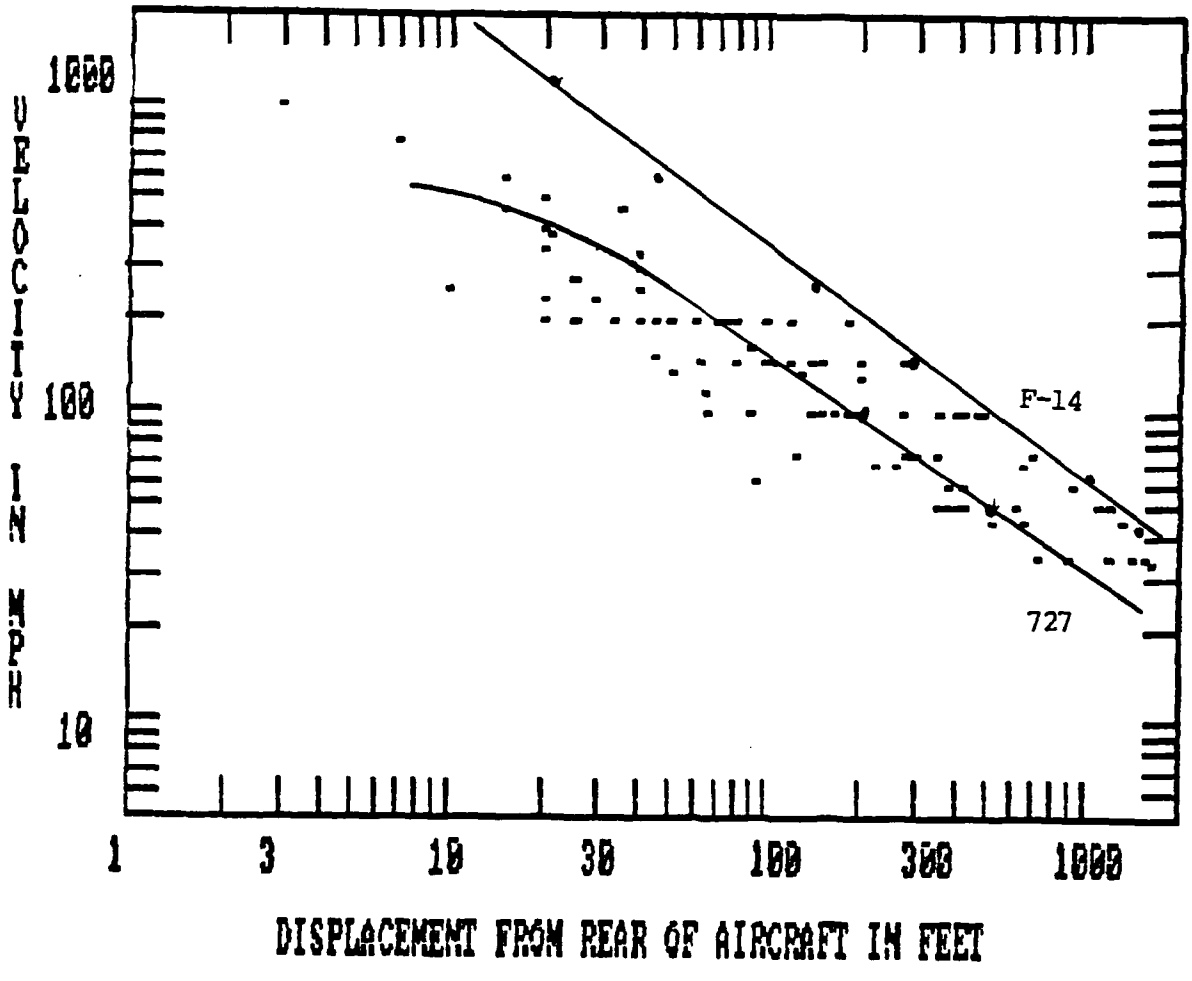

FIGURE 10. SCATTER PLOT OF PUBLISHED JET EXHAUST VELOCITY VS. DISPLACEMENT AT TAKEOFF THRUST

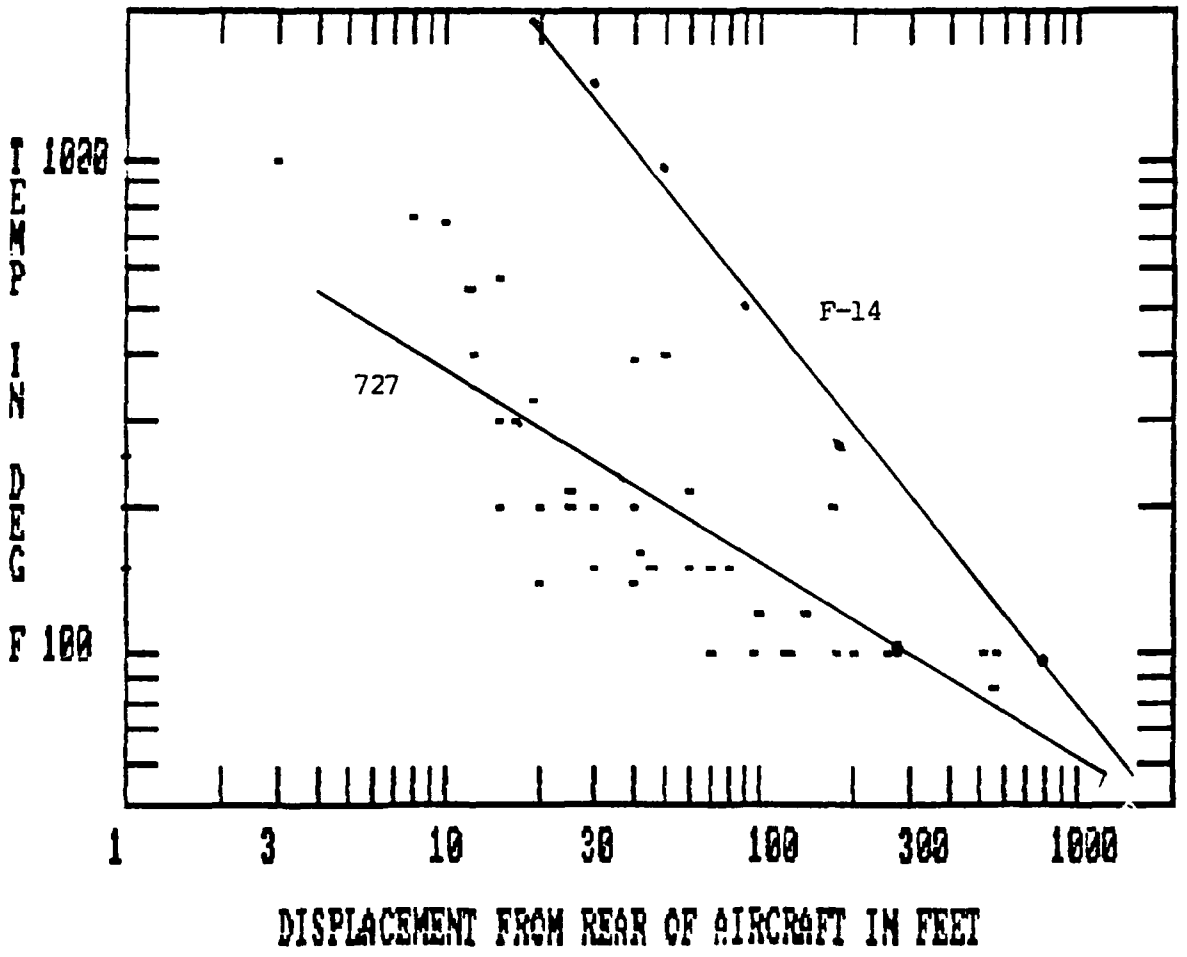

FIGURE 11. SCATTER PLOT OF PUBLISHED JET EXHAUST TEMPERATURE VS. DISPLACEMENT AT TAKEOFF THRUST

aircraft could be made by knowing only the velocity or temperature at any single point. This fact is important in trying to create an algorithm that allows the prediction of the effect of jet exhaust blast on equipment located in its vicinity.

The final step in the process is to take the jet exhaust velocity and temperature data for a specific aircraft and compare it to the worst case measurements acquired during this test for that aircraft and determine whether there exists a definite relationship between the exhaust blast characteristics of a specific type of aircraft/engine configuration and the worst case measurements acquired. If such a relationship exists, it is the final link between the published exhaust blast characteristics and what effect the blast will have on the equipment being exposed to it.

In the analysis of the exhaust velocity and temperature contours it was noted that the greatest variance or deviation from a mathematical model occurs near the rear of the aircraft. As one moves further away from the rear, the contours more closely adhere to a model. One immediate fact which probably contributes strongly to this variance is the position of the engine(s) with respect to the rear of the aircraft and the runway surface. It seems obvious that for the same engine, the exhaust velocity measured at the rear of the aircraft would be maximum when the engine is mounted at or very near the rear and low with respect to the runway surface Thus, as a starting point, an exhaust velocity measured 100 feet from the rear of an aircraft at takeoff thrust was chosen as a reasonable location which would be relatively insensitive to engine location. Then, the root-mean-square (RMS) acceleration measured at LaGuardia airport was compared to the published takeoff thrust exhaust velocity at 100 feet from the rear of each aircraft. A mathematical curve fit was attempted to the results of the above comparison and an equation relating RMS acceleration to the published exhaust velocity was developed.

This same process was repeated for the rate of change in temperature on the bulb face; relating it again to the published exhaust velocity at 100 feet from the rear of the aircraft at takeoff thrust. The resulting equations appear below:

RMS ACCELERATION

$$A_{RMS} = \frac{(V_{100})^{1.5}}{440} \qquad (3)$$

Where A_{RMS} is the RMS acceleration in g's and V_{100} is the manufacturer's published jet exhaust velocity in miles per hour at 100 feet from the rear of the aircraft at takeoff thrust.

PEAK ACCELERATION

$$A_{PEAK} = A_{RMS} * 3.5 \quad (4)$$

This is a rough approximation of the conversion of peak to RMS acceleration based on previous experience as well as on the data acquired in this test, but without knowing more about the concise statistical distribution of amplitude, it is reasonable to expect this ratio to apply.

RATE OF CHANGE OF TEMPERATURE AT THE BULB FACE

$$\left|\Delta T_{max}\right| = \frac{200 + V_{100}}{70} \quad (5)$$

Where $\left|\Delta T_{max}\right|$ is the absolute value of the maximum rate of change of bulb face temperature in degrees Celsius and V_{100} is the manufacturer's published exhaust velocity at 100 feet measured from the rear of the aircraft at takeoff thrust. The mixture of metric and english units was intentional, since most manufacturer's data is given in MPH versus feet from the rear.

It is important to note that the above formulae are at best approximations and should be used with consideration of the following guidelines: The equations should only be used for published takeoff thrust exhaust velocities in excess of 175-200 MPH, measured at 100 feet displacement, since at velocities less than 200 MPH, there would be no increase of any of the parameters given. The accuracy of the results given is no better than $\pm$ 50% due to the many variances in the measured data and also due to the accuracy with which a curve could be fit to the data. The above accuracy will hold for velocities up to 750-1000 MPH. It would be wise to perform actual measurements, either in a wind tunnel facility, or under actual conditions, similar to the type performed for this project, at higher velocities so that the extrapolation formulae would be verified and refined if necessary.

The formulae were used to extrapolate the data measured to several other key aircraft which were not measured during this project to see if any of them might cause the worst case environment values to increase above those observed in the data. Table 7 lists the results of the extrapolation:

TABLE 8

MAXIMUM PARAMETER VALUES ENCOUNTERED

Acceleration:	Single-shot peak	20 G/axis
	Vector sum/3 axes	34.6 G
	RMS	8 G/axis
	Vector sum/3 axes	13.8 G
Rate of change of temperature:	Bulb surface	10 oC/sec
	Blast plume	15 oC/sec
Blast Velocity:	To be determined from data	
Sound Pressure Level:		140 dBSPL

The above values are the maximum values encountered in the data which were acquired for this project. If absolute design limits were to be established, the extrapolated values listed in Table 7 should be used, with appropriate safety factors, since several key aircraft were not authorized to operate at LGA. Notable among the aircraft for which the runways at LGA are inappropriate are the 747, the 707, the DC-9, the re-engined DC-9 with CFM engines, and the Concorde; all of which can be expected to produce jet blast equal to or in excess of the blast produced by the aircraft which were measured. Thus, it is unlikely that the absolute worst-case conditions were encountered at LGA and the extrapolated values would more accurately characterize the worst-case environment than the values listed in Table 8.

Significant coupling of strong acoustic energy radiating from the jet engines into the lamp fixture when the jet blast plume was directed above the fixture was proven. This energy has coherent components in the spectral region below 200 Hertz, where it can be expected to produce accelerations in the mechanical parts of the lamp fixture which could excite incipient resonances which, in turn, could cause fatigue failure in those parts.

EXPERIMENTAL SHROUD ASSEMBLY TEST

An experimental PAR-56 lamp shroud (Figure 12) was designed, built and installed in a threshold light array near the conclusion of jet blast data collection at La Guardia International Airport. This was done because it was thought that a shielding effect could divert or reduce some of the blast effect and that a full-scale test of the shroud under actual conditions could be accomplished concurrently with the originally scheduled program without interference or additional costs. Further, if the test data would show that the use of a shroud will reduce the destructive effects of the jet blast, then a great cost benefit in time and money will have been achieved with a solution to the problem that much closer.

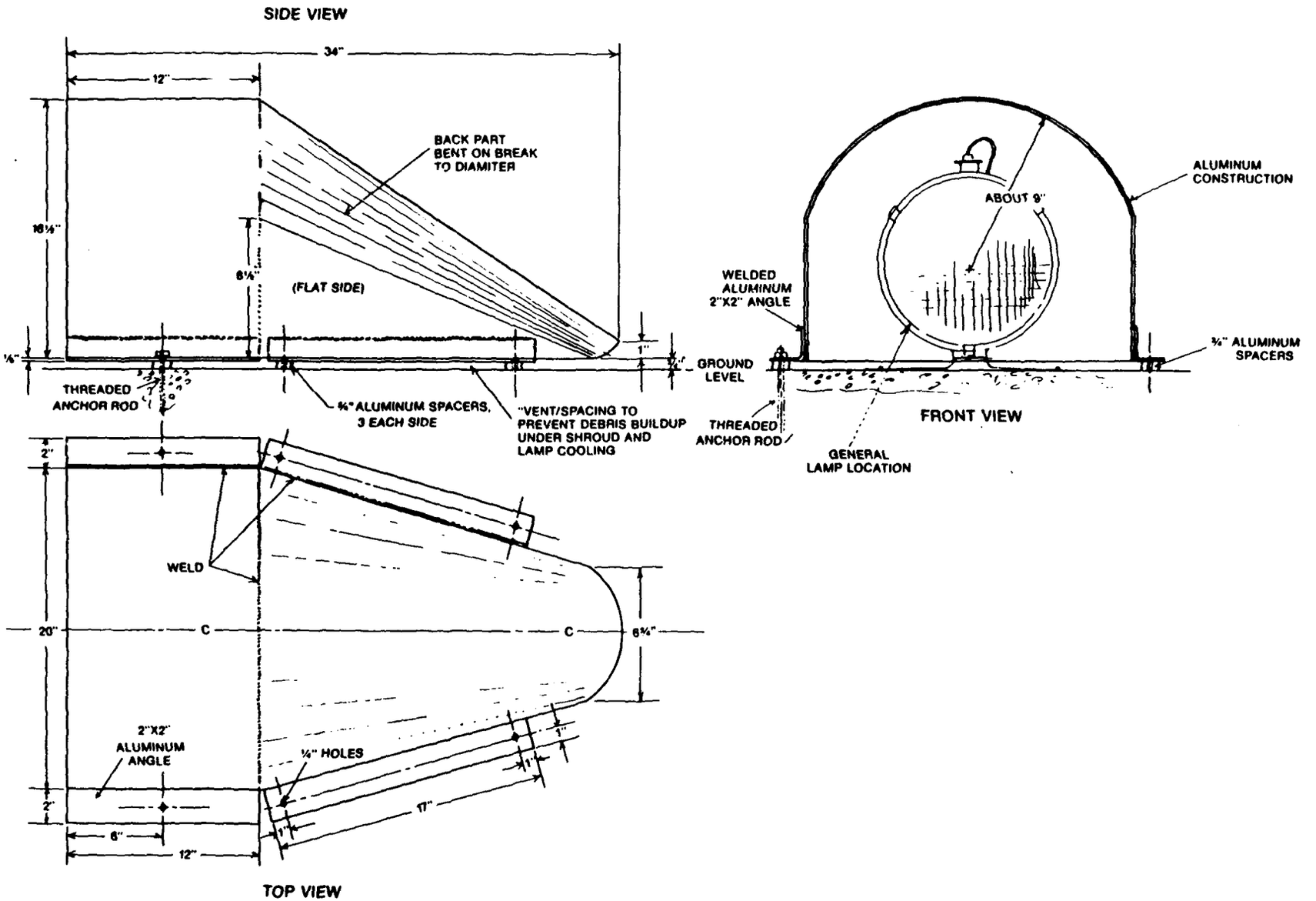

FIGURE 12. EXPERIMENTAL SHROUD ASSEMBLY

The data suggest that there is approximately a 50 percent reduction in the accelerations measured on the lamp fixture, and a similar decrease in the rate of temperature change to the lamp itself due to jet blast. Although lamp temperatures appeared to be 20 to 30 percent higher for the shrouded lamp, it is thought that this may not be detrimental after all because the rate of temperature change, which is much more deleterious, improved significantly.

These cursory test results suggest some modification to the basic shroud design. For example, improved venting could be accomplished by fabricating the shroud from expanded metal, wire cloth or perforated sheet metal. Although the shroud affords a measure of physical protection for the lamp assembly, the design of the shroud should be such that it would be lightweight, but strong and yet frangible enough to "give" if struck by an aircraft. It should be streamlined to act as a fairing for the lamp assembly to the runway with a low coefficient of drag that would divert the jet blast.

Attachment of the shroud, itself, must be directly to the runway to isolate it from the lamp assembly. This should be accomplished using shock mounts (rubber bushings that also provide a 1-inch vent spacing between the shroud and the runway).

CONCLUSIONS

The environment of the PAR-56 lamp fixtures mounted in the threshold bar is now well characterized:

- The expected accelerations in all axes due to jet blast plumes are known.
- The expected time rate-of-change of temperature due to jet blast plumes is known.
- The maximum wind velocities which can be expected are better taken from the published blast plume data rather than from the measured data.
- The maximum sound pressure level due to the jet turbines is known.
- The power spectral densities of accelerations and acoustic outputs are known.
- The coupling of strong acoustic engine output into accelerations has been proven.

The determination of these parameters was a primary objective of this project. Any equipment located near the threshold bar will be subjected to these environmental parameters. Thus, the parameters should be included in any new designs for such equipment.

Use of a protective shroud to reduce the hostile effects of the jet blast on the lamp assembiles could also reduce the premature failure rate to an acceptable level. In turn, this could permit continued use of existing lamp assembly installations and obviate any redsign.

APPENDIX A

DATA PLOTS FOR TWO SELECTED AIRCRAFT :

BOEING 767 (A-1 to A-15)

L-1011 (A-16 to A-30)

FAA PAR-56 RUNWAY LIGHT ANALYSIS

Aircraft Type: BOEING 767
Flight Number: AA 295 HEAVY
Date and Time: 18-MAR-86 07 43 52
Data Run Number: 102
Sensor Location: LA GUARDIA - THRESHOLD BAR RW 13 - 25,35,40,45 FT RIGHT OF CL
Comments: INFO J - DEW POINT 1 67 DEGREES CELSIUS - SUNNY

Ambient Temperature: 3.3 C
Relative Humidity: 88.8 %
Barometric Pressure: 769.1 mmHg
Data Channel Number: 2

BULB 1 TOP SURFACE TEMPERATURE

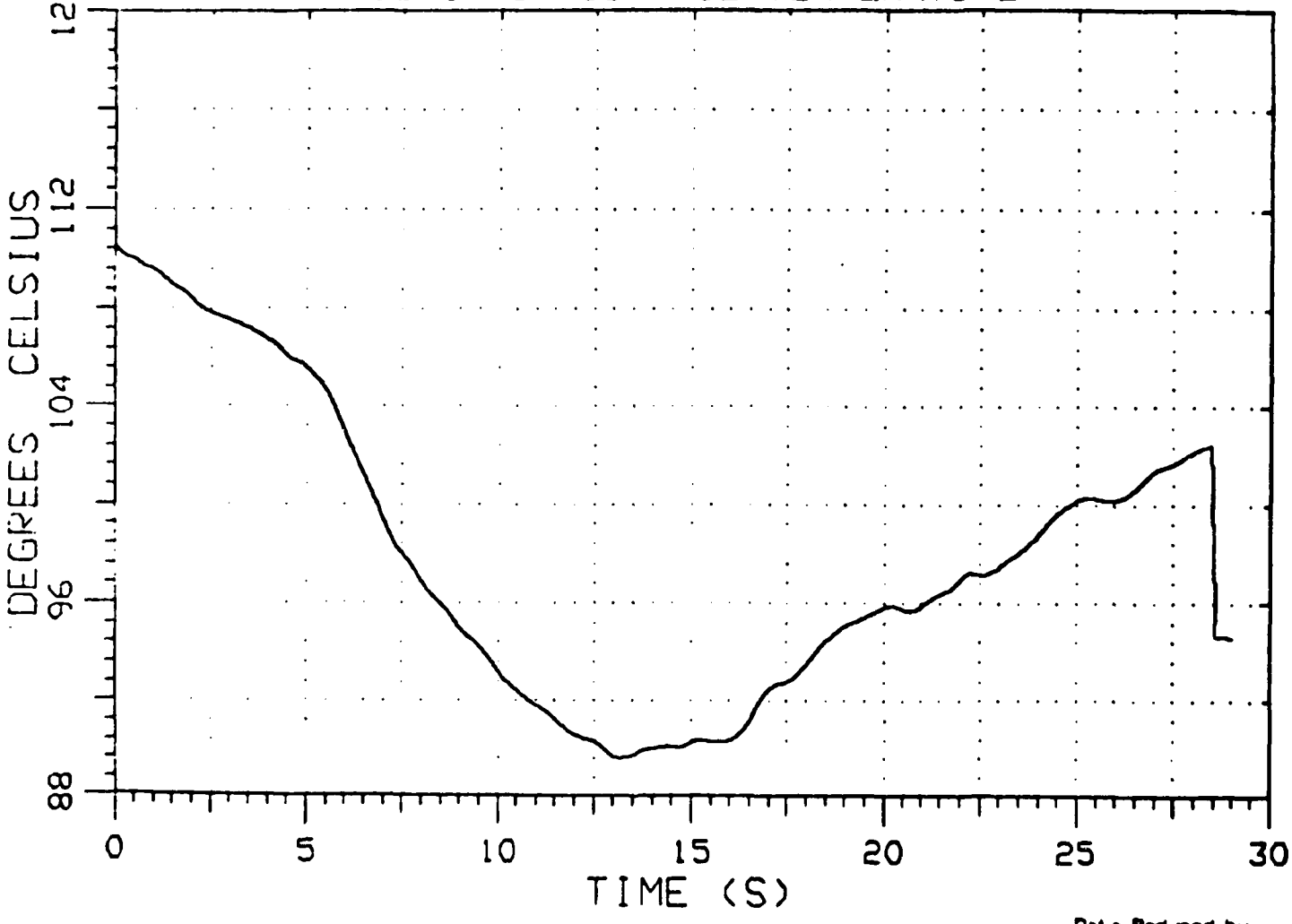

Data Reduced by:
SMCAR-AEC-TIL
DTFA03-84-A-40020

FAA PAR-56 RUNWAY LIGHT ANALYSIS

Aircraft Type: BOEING 767
Flight Number: AA 295 HEAVY
Date and Time: 18-MAR-86 07 43 52
Data Run Number: 102
Sensor Location: LA GUARDIA - THRESHOLD BAR RW 13 - 25,35,40,45 FT RIGHT OF CL
Comments: INFO J - DEW POINT 1 67 DEGREES CELSIUS - SUNNY

Ambient Temperature: 3.3 C
Relative Humidity: 88.8 %
Barometric Pressure: 769.1 mmHg
Data Channel Number: 4

BULB 1 LEFT SURFACE TEMPERATURE

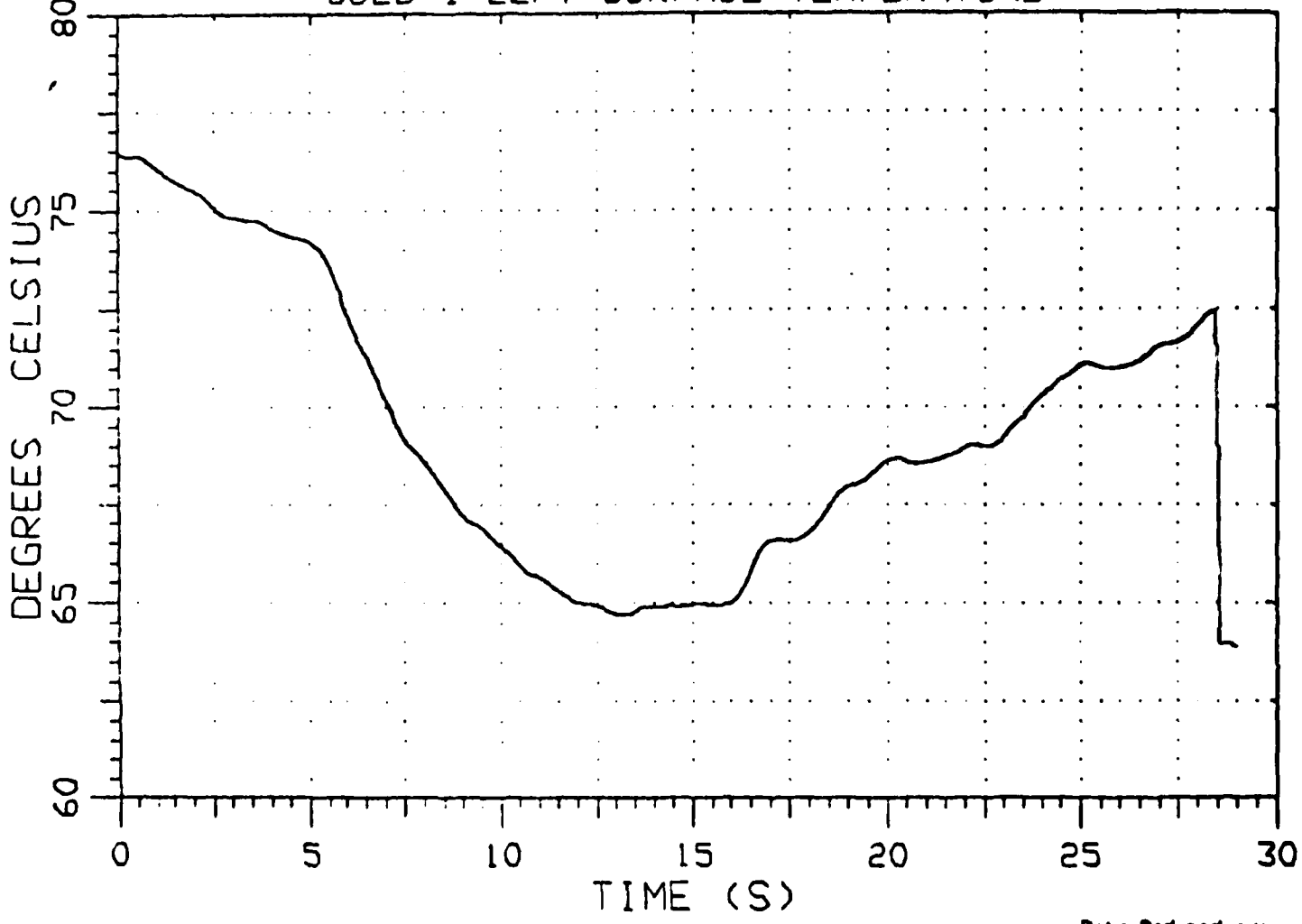

Data Reduced by:
SMCAR-AEC-TIL
DTFA03-84-A-40020

FAA PAR-56 RUNWAY LIGHT ANALYSIS

Aircraft Type: BOEING 767
Flight Number: AA 295 HEAVY
Date and Time: 18-MAR-86 07 43 52
Data Run Number: 102
Sensor Location: LA GUARDIA - THRESHOLD BAR RW 13 - 25,35,40,45 FT RIGHT OF CL
Comments: INFO J - DEW POINT 1 67 DEGREES CELSIUS - SUNNY

Ambient Temperature: 3.3 C
Relative Humidity: 88.8 %
Barometric Pressure: 769.1 mmHg
Data Channel Number: 4

BULB 1 RIGHT SURFACE TEMPERATURE

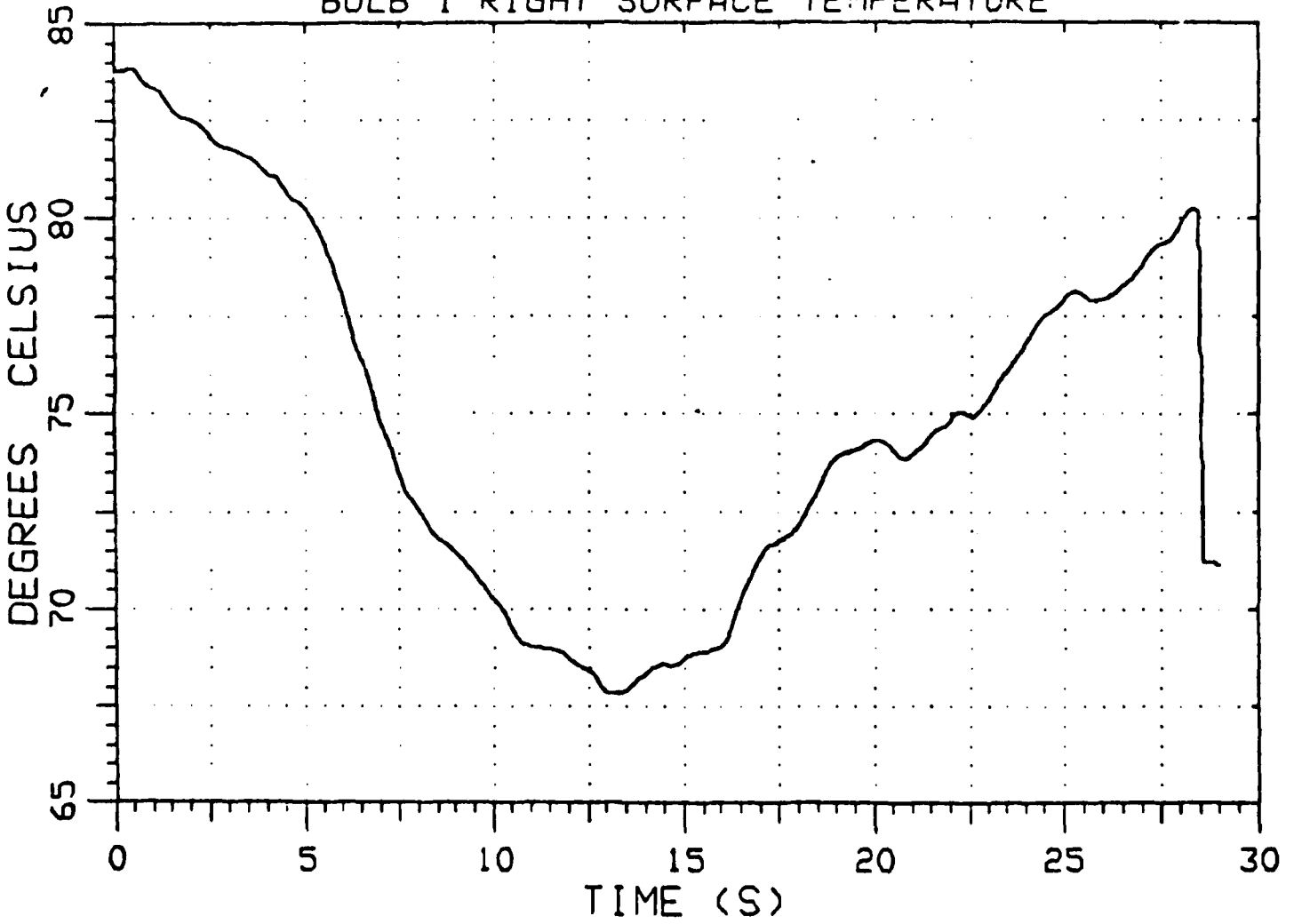

Data Reduced by:
SMCAR-AEC-TIL
DTFA03-84-A-40020

FAA PAR-56 RUNWAY LIGHT ANALYSIS

Aircraft Type: BOEING 767
Flight Number: AA 295 HEAVY
Date and Time: 18-MAR-86 07 43 52
Data Run Number: 102
Sensor Location: LA GUARDIA - THRESHOLD BAR RW 13 - 25,35,40,45 FT RIGHT OF CL
Comments: INFO J - DEW POINT 1 67 DEGREES CELSIUS - SUNNY

Ambient Temperature: 3.3 C
Relative Humidity: 88.8 %
Barometric Pressure: 769.1 mmHg
Data Channel Number: 4

BULB 2 ACCELEROMETER: X-AXIS

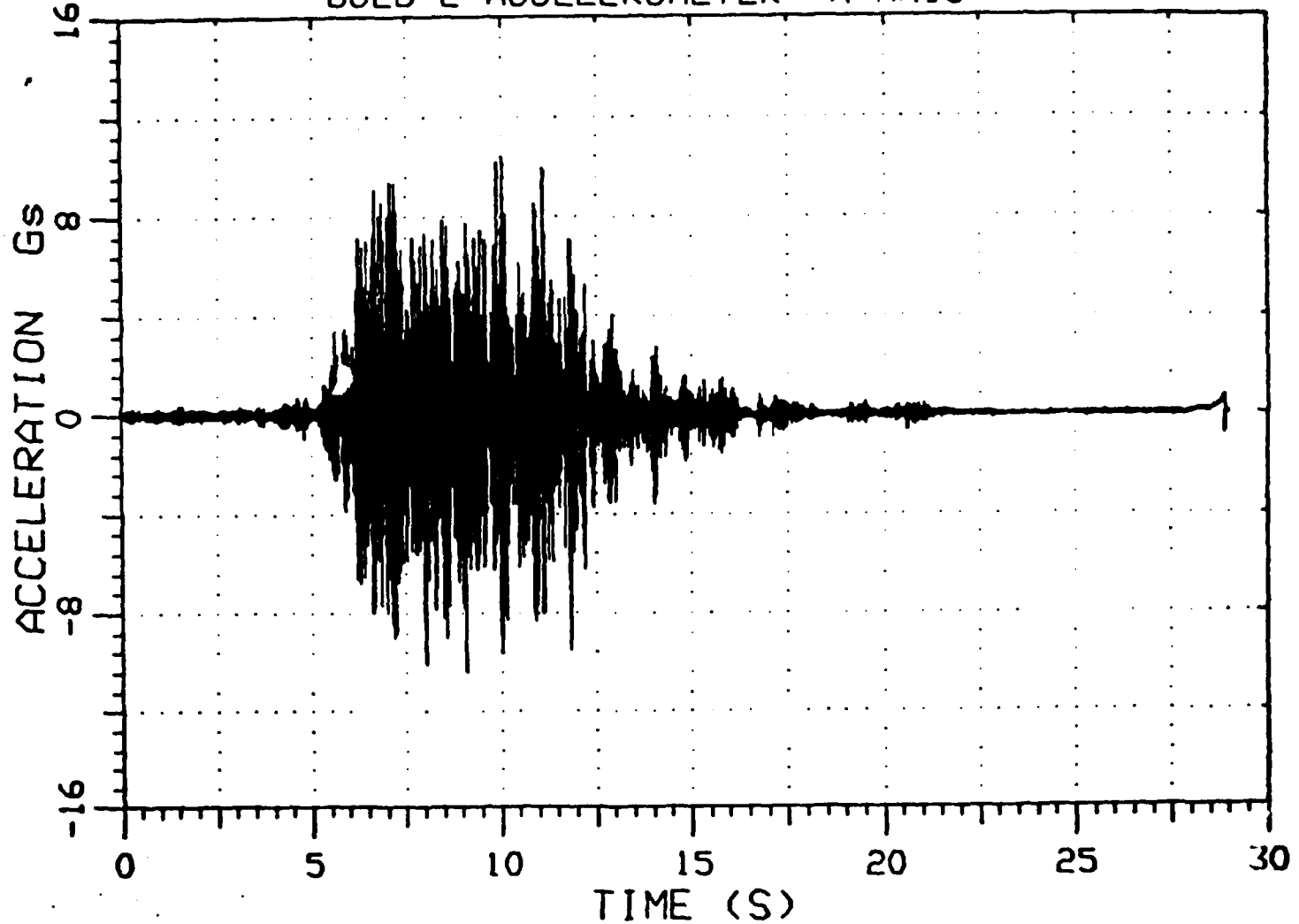

Data Reduced by:
SMEAR-AEC-TIL
DTFA03-84-A-40020

FAA PAR-56 RUNWAY LIGHT ANALYSIS

Aircraft Type: BOEING 767
Flight Number: AA 295 HEAVY
Date and Time: 18-MAR-86 07:43:52
Data Run Number: 102
Sensor Location: LA GUARDIA - THRESHOLD BAR RW 13 - 25,35,40,45 FT RIGHT OF CL
Comments: INFO J - DEW POINT 1 67 DEGREES CELSIUS - SUNNY

Ambient Temperature: 3.3 C
Relative Humidity: 88.8 %
Barometric Pressure: 769.1 mmHg
Data Channel Number: 3

BULB 2 ACCELEROMETER Y-AXIS

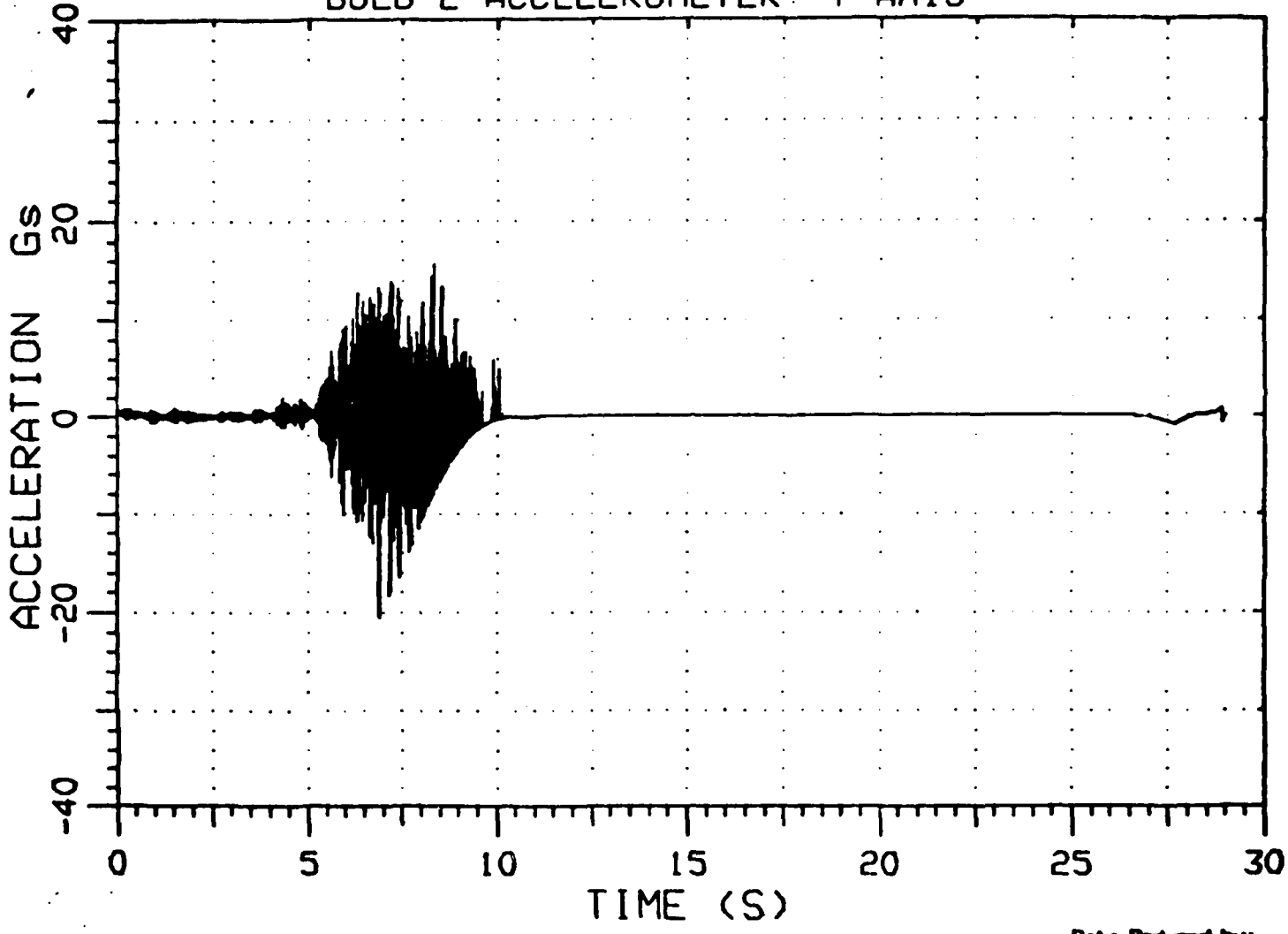

Data Reduced by:
SMCAR-AEC-TIL
DTFA03-84-A-40020

FAA PAR-56 RUNWAY LIGHT ANALYSIS

Aircraft Type:	BOEING 767	Ambient Temperature:	3.3 C
Flight Number:	AA 295 HEAVY	Relative Humidity:	88.8 %
Date and Time:	18-MAR-86 07 43 52	Barometric Pressure:	769.1 mmHg
Data Run Number:	102	Data Channel Number:	8
Sensor Location:	LA GUARDIA - THRESHOLD BAR RW 13 - 25,35,40,45 FT RIGHT OF CL		
Comments:	INFO J - DEW POINT 1.67 DEGREES CELSIUS - SUNNY		

BULB 2 ACCELEROMETER Z-AXIS

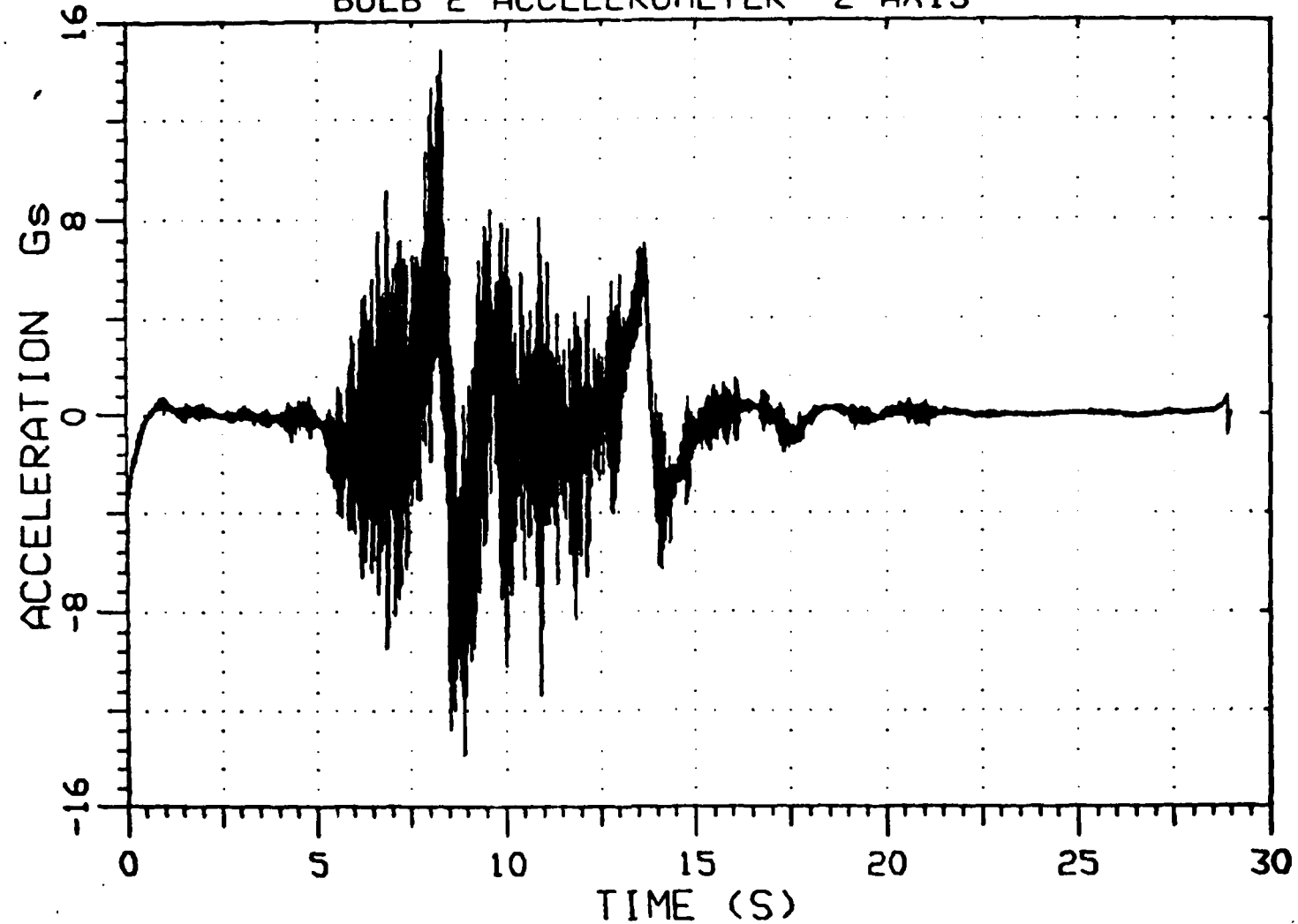

Data Reduced by:
SMEAR-AEC-TIL
DTFA03-84-A-40020

FAA PAR-56 RUNWAY LIGHT ANALYSIS

Aircraft Type: BOEING 767
Flight Number: AA 295 HEAVY
Date and Time: 18-MAR-86 07 43 52
Data Run Number: 102
Sensor Location: LA GUARDIA - THRESHOLD BAR RW 13 - 25,35,40,45 FT RIGHT OF CL
Comments: INFO J - DEW POINT 1 67 DEGREES CELSIUS - SUNNY

Ambient Temperature: 3.3 C
Relative Humidity: 88.8 %
Barometric Pressure: 769.1 mmHg
Data Channel Number: 4

BULB 2 TOP SURFACE TEMPERATURE

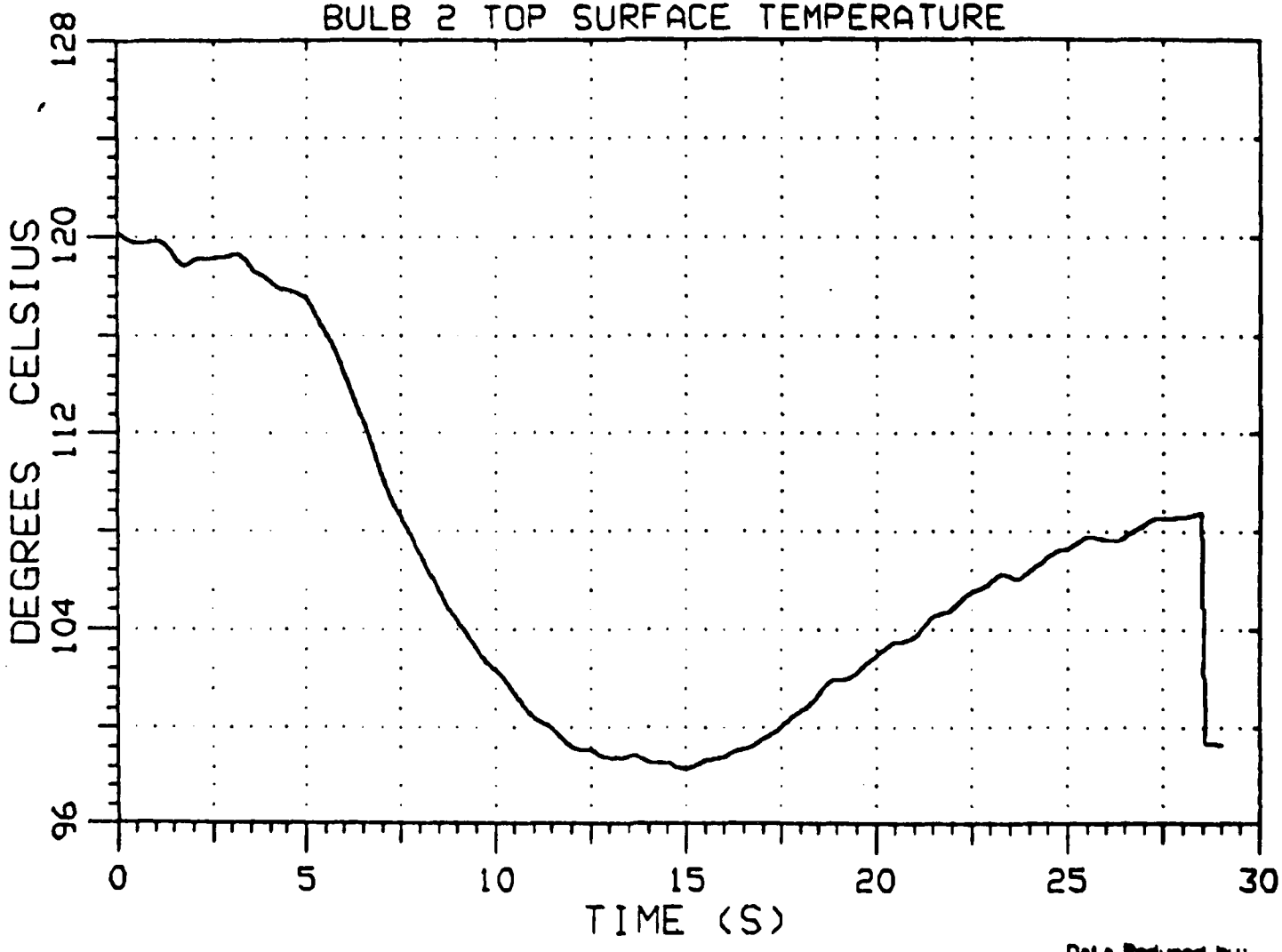

Data Reduced by:
SMCAR-AEC-TIL
DTFA03-84-A-40020

FAA PAR-56 RUNWAY LIGHT ANALYSIS

Aircraft Type:	BOEING 767	Ambient Temperature:	3.3 C
Flight Number:	AA 295 HEAVY	Relative Humidity:	88.8 %
Date and Time:	18-MAR-86 07 43 52	Barometric Pressure:	769.1 mmHg
Data Run Number:	102	Data Channel Number:	2
Sensor Location:	LA GUARDIA - THRESHOLD BAR RW 13 - 25,35,40,45 FT RIGHT OF CL		
Comments:	INFO J - DEW POINT 1 67 DEGREES CELSIUS - SUNNY		

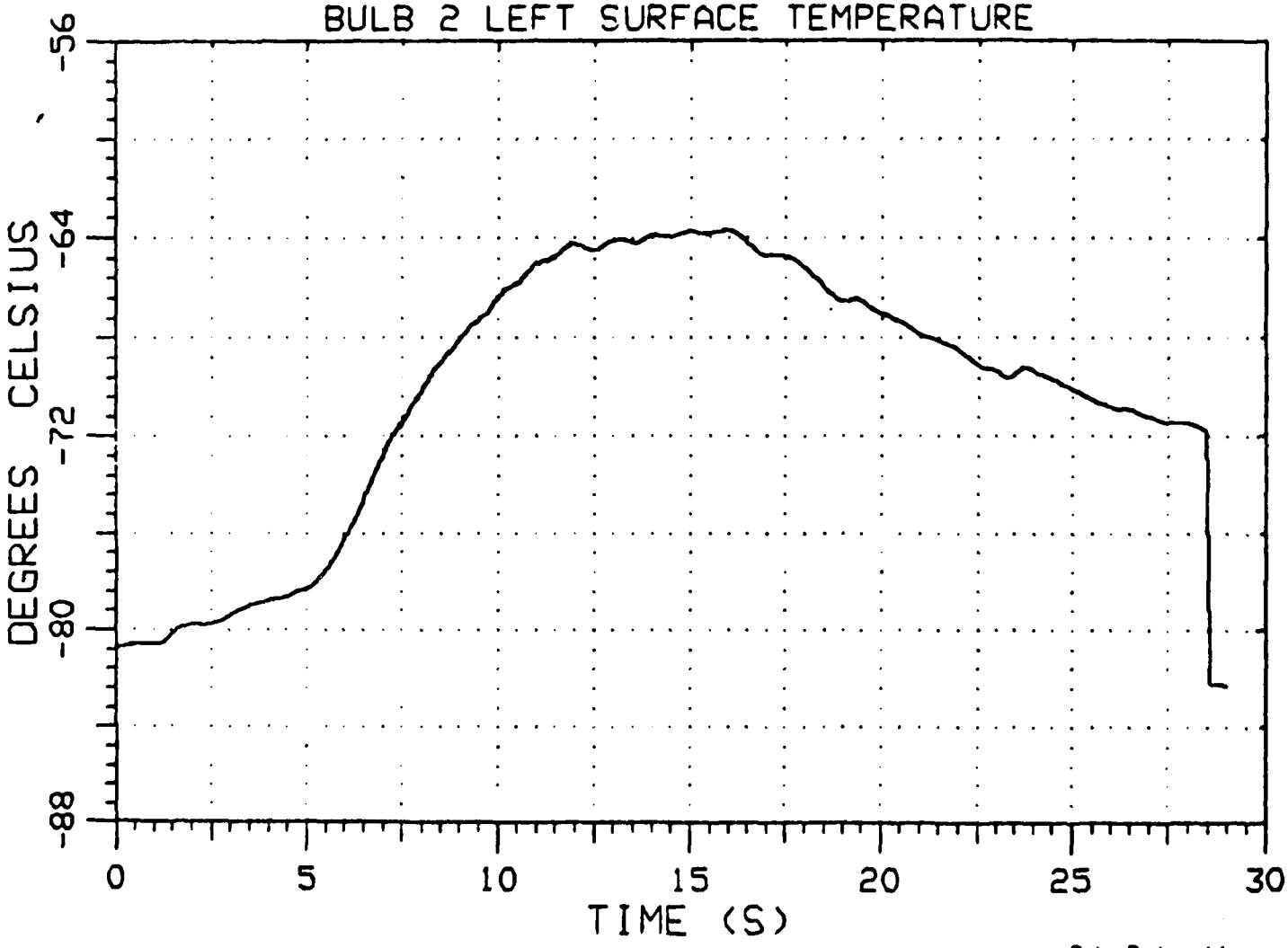

Data Reduced by:
SMCAR-AEC-TIL
DTFA03-84-A-40020

FAA PAR-56 RUNWAY LIGHT ANALYSIS

Aircraft Type: BOEING 767
Flight Number: AA 295 HEAVY
Date and Time: 18-MAR-86 07 43 52
Data Run Number: 102
Sensor Location: LA GUARDIA - THRESHOLD BAR RW 13 - 25,35,40,45 FT RIGHT OF CL
Comments: INFO J - DEW POINT 1 67 DEGREES CELSIUS - SUNNY

Ambient Temperature: 3.3 C
Relative Humidity: 88.8 %
Barometric Pressure: 769.1 mmHg
Data Channel Number: 2

BULB 2 RIGHT SURFACE TEMPERATURE

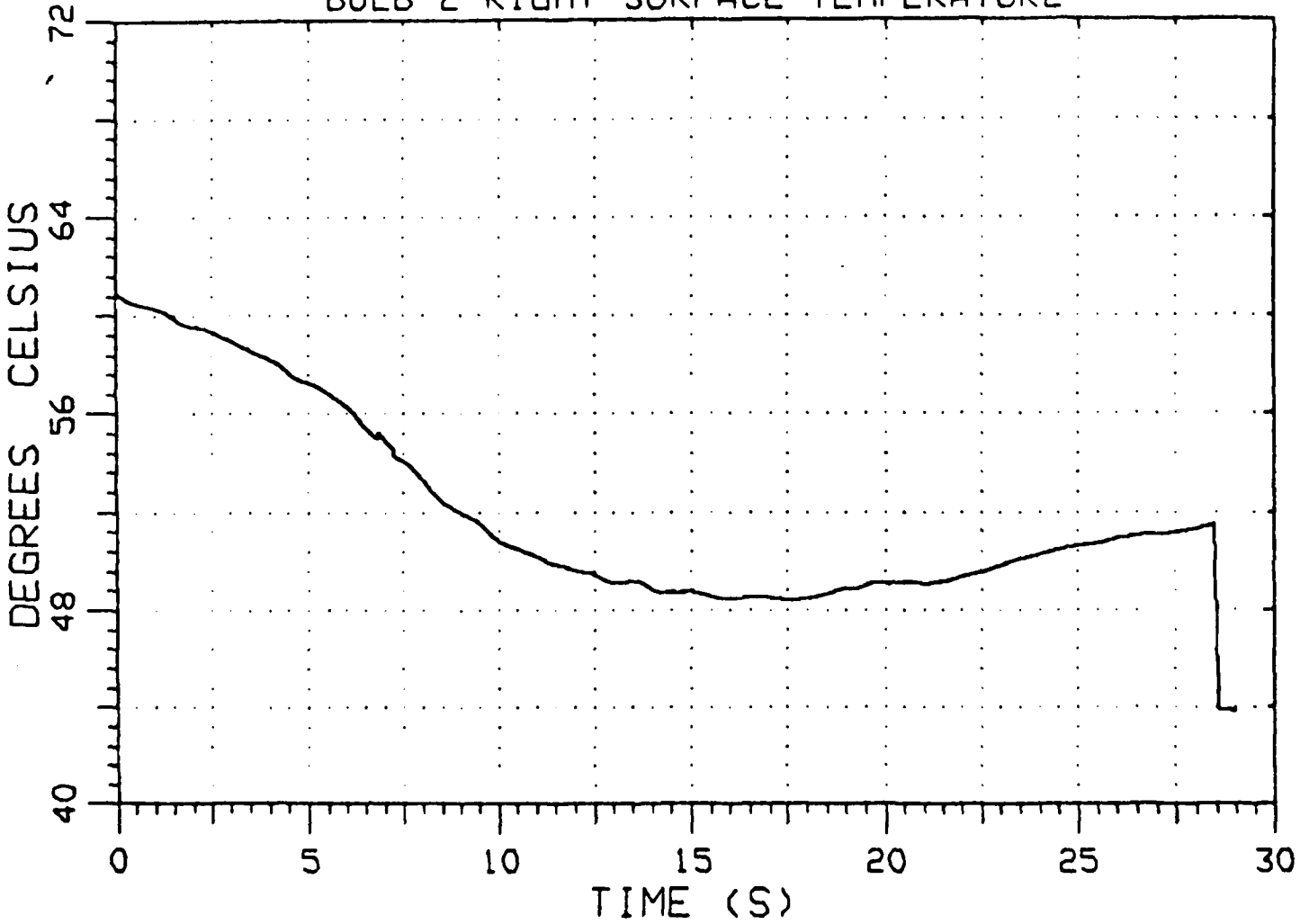

Data Reduced by
SMCAR-AEC-TIL
DTFA03-84-A-40020

FAA PAR-56 RUNWAY LIGHT ANALYSIS

Aircraft Type:	BOEING 767	Ambient Temperature:	3.3 C
Flight Number:	AA 295 HEAVY	Relative Humidity:	88.0 %
Date and Time:	18-MAR-96 07:43:52	Barometric Pressure:	769.1 mmHg
Data Run Number:	102	Data Channel Number:	10
Sensor Location:	LA GUARDIA - THRESHOLD BAR RW 13 - 25,35,40,45 FT RIGHT OF CL		
Comments:	INFO J - DEW POINT 1 67 DEGREES CELSIUS - SUNNY		

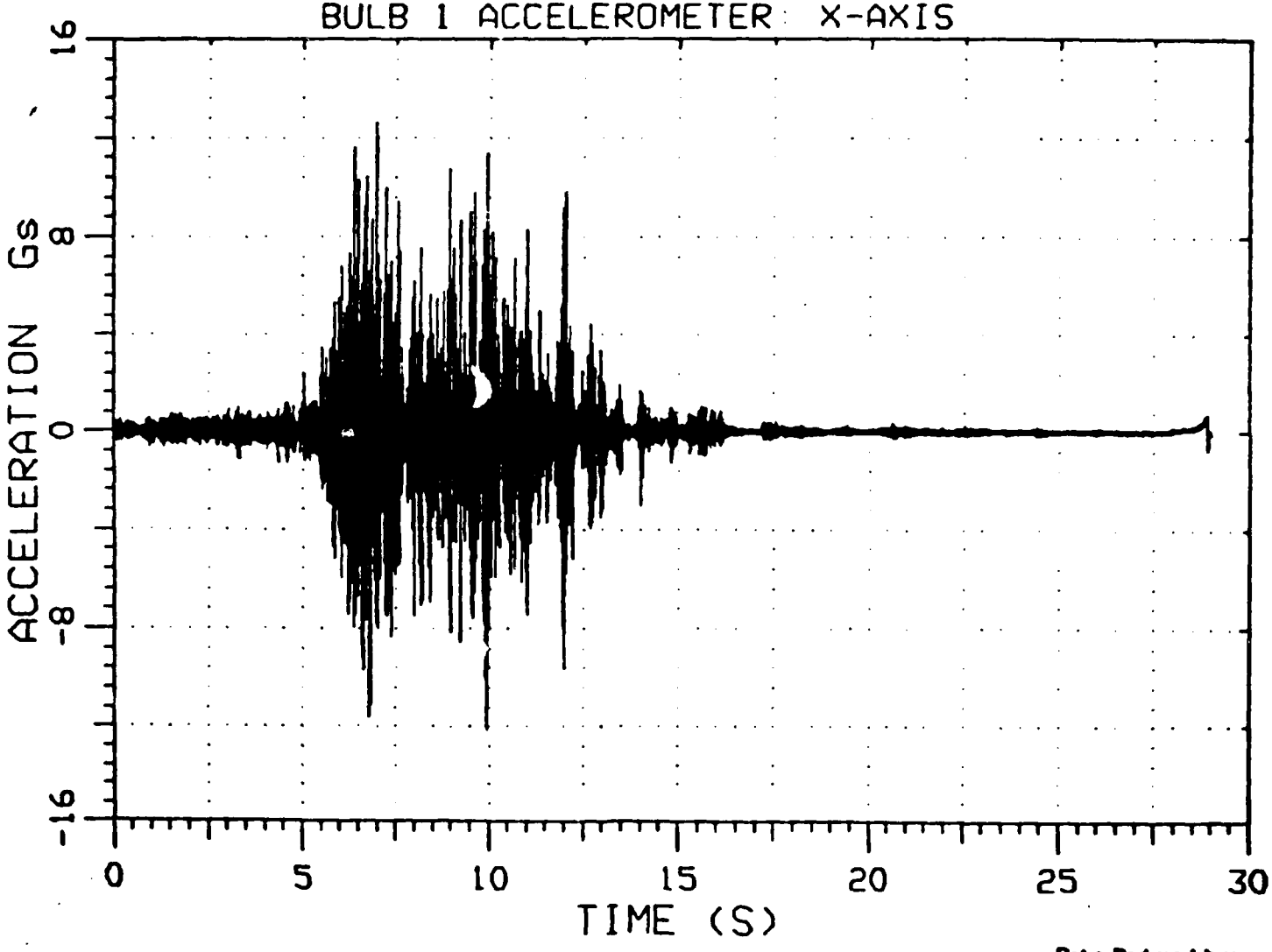

Data Reduced by:
SMCAR-AEC-TIL
DTFA03-94-A-40020

FAA PAR-56 RUNWAY LIGHT ANALYSIS

Aircraft Type:	BOEING 767	Ambient Temperature:	3 3 C
Flight Number:	AA 295 HEAVY	Relative Humidity:	88 8 %
Data and Time:	18-MAR-86 07.43 52	Barometric Pressure:	769.1 mmHg
Data Run Number:	102	Data Channel Number:	11
Sensor Location:	LA GUARDIA - THRESHOLD BAR RW 13 - 25,35,40,45 FT RIGHT OF CL		
Comments:	INFO J - DEW POINT 1 67 DEGREES CELSIUS - SUNNY		

BULB 1 ACCELEROMETER: Y-AXIS

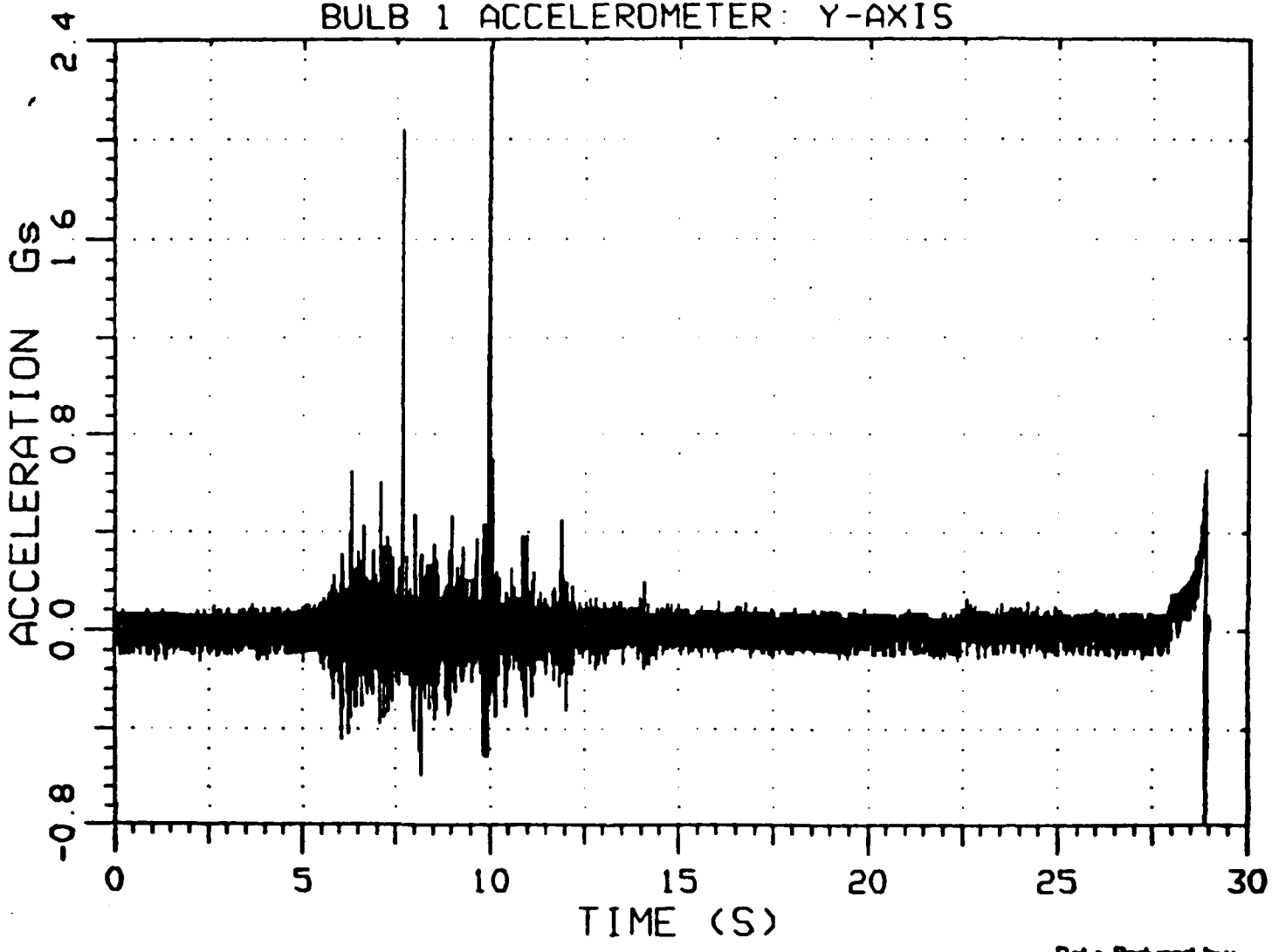

Data Reduced by:
SMCAR-AEC-TIL
DTFA03-84-A-40020

FAA PAR-56 RUNWAY LIGHT ANALYSIS

Aircraft Type: BOEING 767
Flight Number: AA 295 HEAVY
Date and Time: 18-MAR-86 07 43 52
Data Run Number: 102
Sensor Location: LA GUARDIA - THRESHOLD BAR RW 13 - 25,35,40,45 FT RIGHT OF CL
Comments: INFO J - DEW POINT 1 67 DEGREES CELSIUS - SUNNY

Ambient Temperature: 3 3 C
Relative Humidity: 88 8 %
Barometric Pressure: 769 1 mmHg
Data Channel Number: 12

BULB 1 ACCELEROMETER Z-AXIS

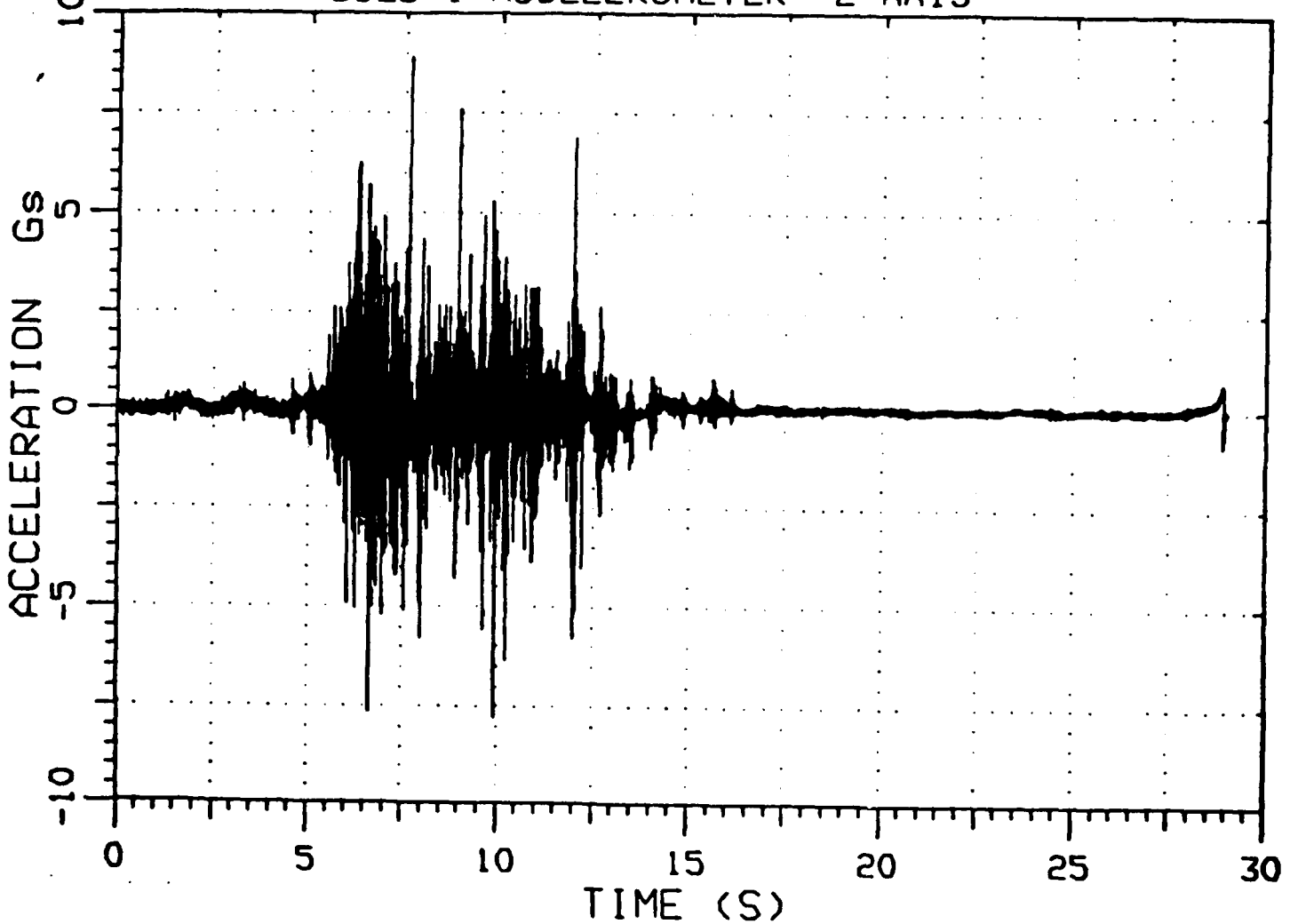

Data Reduced by:
SHEAR-AEC-TIL
DTFA03-84-A-40020

FAA PAR-56 RUNWAY LIGHT ANALYSIS

Aircraft Type: BOEING 767
Flight Number: AA 295 HEAVY
Date and Time: 18-MAR-86 07 43 52
Data Run Number: 102
Sensor Location: LA GUARDIA - THRESHOLD BAR RW 13 - 25,35,40,45 FT RIGHT OF CL
Comments: INFO J - DEW POINT 1 67 DEGREES CELSIUS - SUNNY

Ambient Temperature: 3.3 C
Relative Humidity: 88.8 %
Barometric Pressure: 769.1 mmHg
Data Channel Number: 4

FLUID TEMPERATURE: VELOCITY DATA

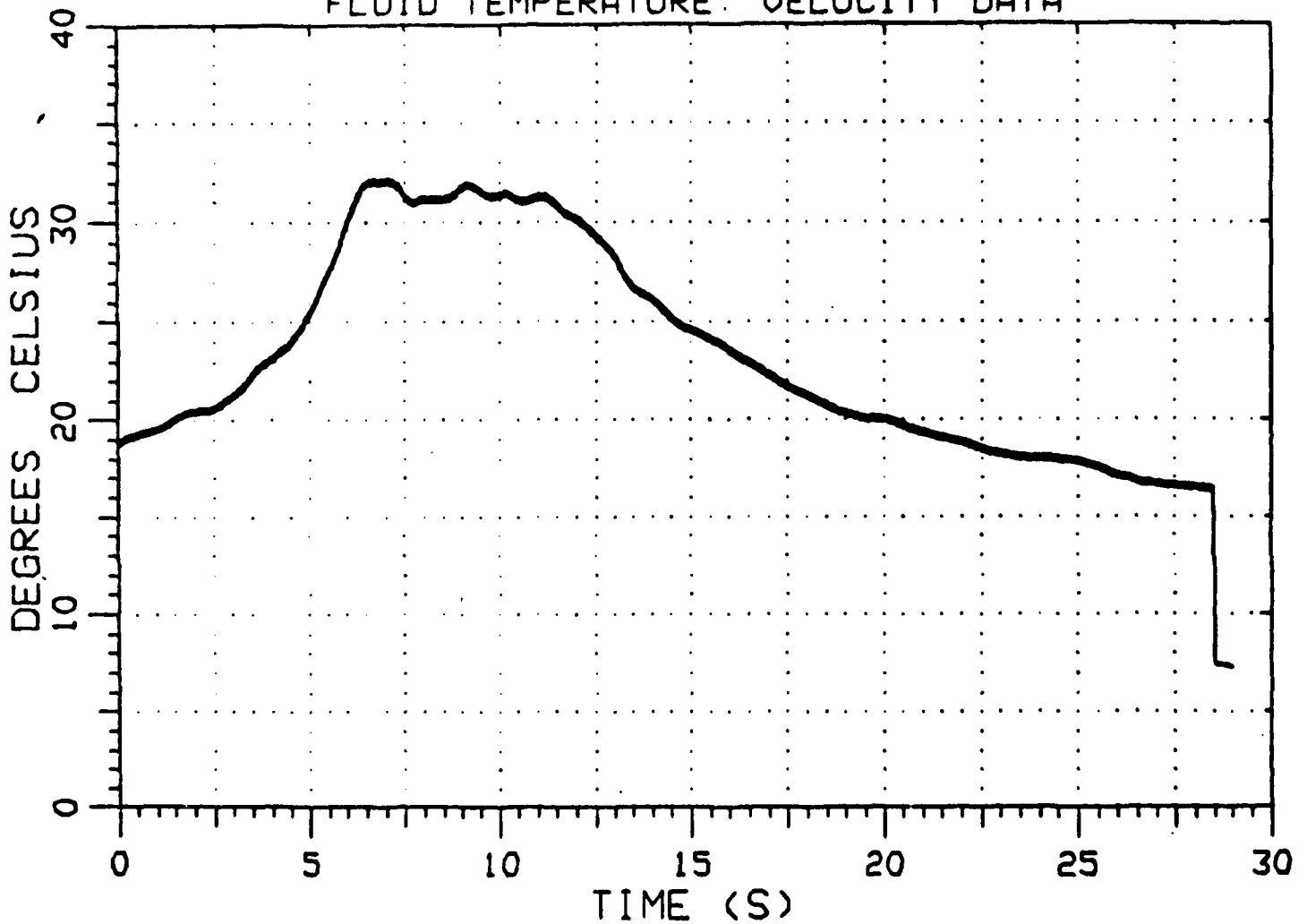

Data Reduced by:
SMCAR-AEC-TIL
DTFA03-84-A-40020

FAA PAR-56 RUNWAY LIGHT ANALYSIS

Aircraft Type	BOEING 767	Ambient Temperature	3 3 C
Flight Number	AA 295 HEAVY	Relative Humidity	88 8 %
Date and Time	18-MAR-86 07 43 52	Barometric Pressure	769 1 mmHg
Data Run Number	102	Data Channel Number	14
Sensor Location	LA GUARDIA - THRESHOLD BAR RW 13 - 25,35,40,45 FT RIGHT OF CL		PITOT A
Comments	INFO J - DEW POINT 1 67 DEGREES CELSIUS - SUNNY		

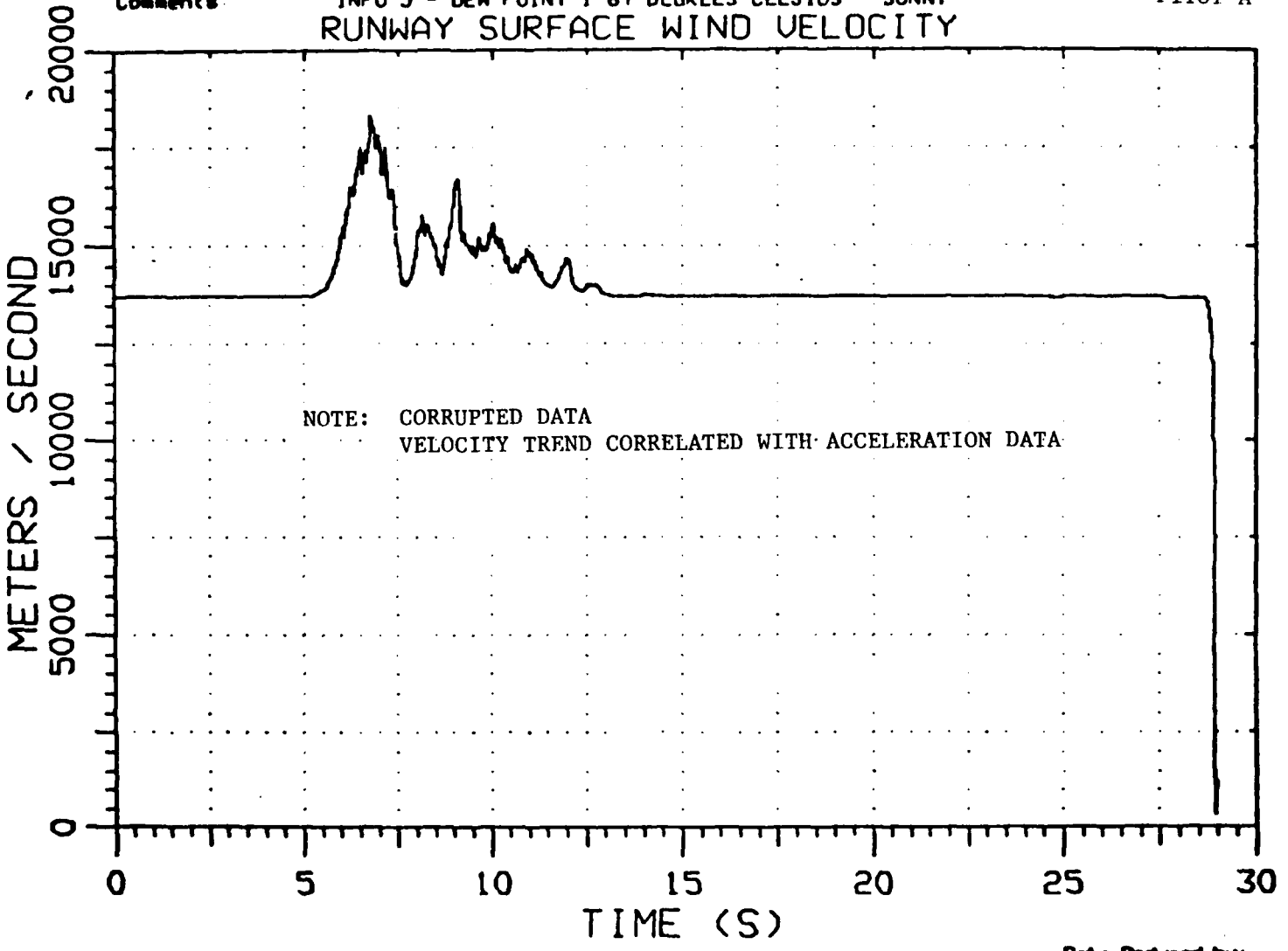

Data Reduced by:
SHCAR-AEC-TIL
DTFA03-84-A-40020

FAA PAR-56 RUNWAY LIGHT ANALYSIS

Aircraft Type:	BOEING 767	Ambient Temperature:	3 3 C
Flight Number:	AA 295 HEAVY	Relative Humidity	88 8 %
Date and Time:	18-MAR-86 07 43 52	Barometric Pressure:	769 1 mmHg
Data Run Number:	102	Data Channel Number	15
Sensor Location:	LA GUARDIA - THRESHOLD BAR RW 13 - 25,35,40,45 FT RIGHT OF CL		PITOT B
Comments:	INFO J - DEW POINT 1 67 DEGREES CELSIUS - SUNNY		

RUNWAY SURFACE WIND VELOCITY

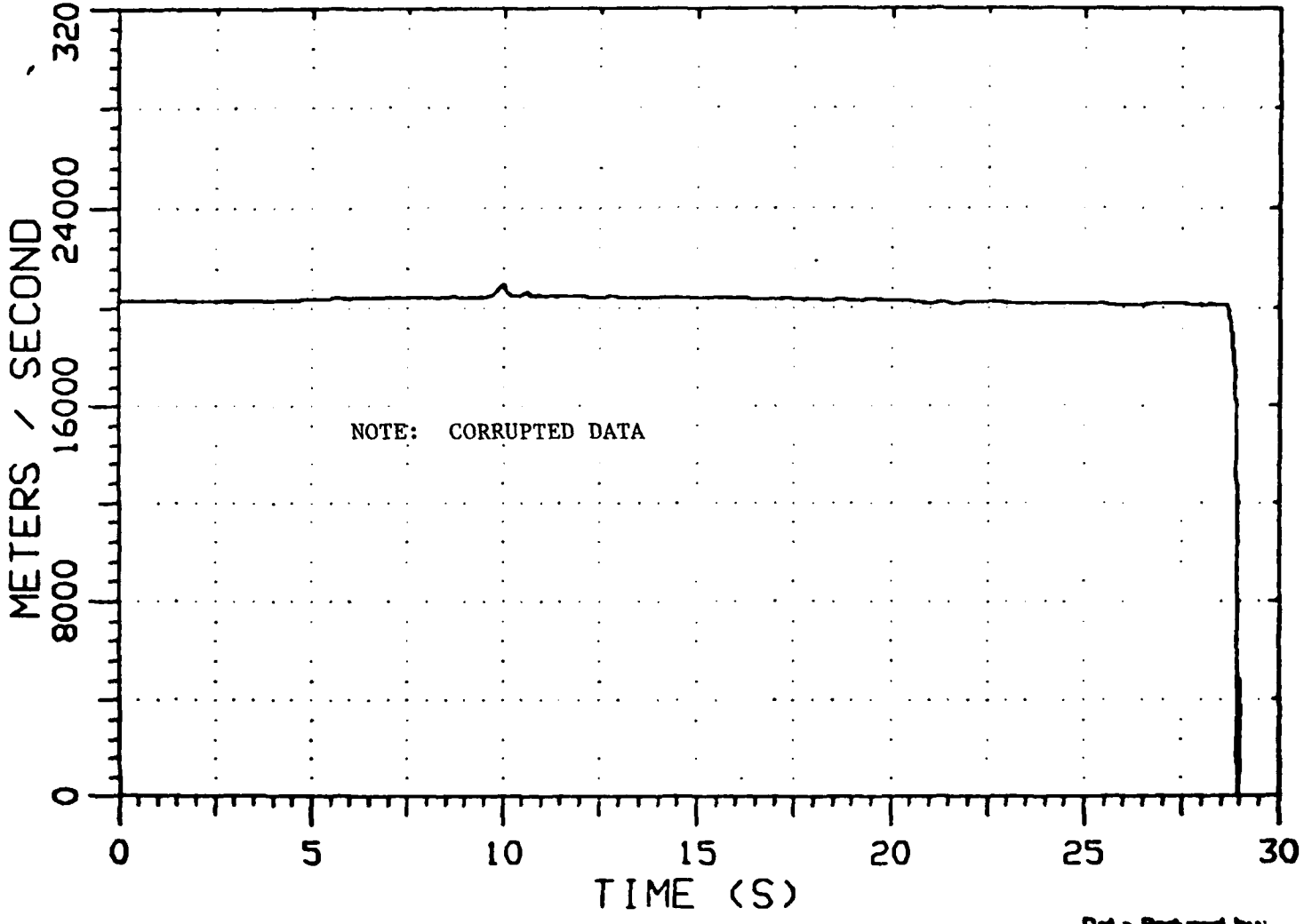

Data Reduced by:
SMCAR-AEC-TIL
DTFA03-84-A-40020

FAA PAR-56 RUNWAY LIGHT ANALYSIS

Aircraft Type: L-1011
Flight Number: TWA 559 H
Date and Time: 12-MAR-86 10 33 18
Data Run Number 020
Sensor Location: LA GUARDIA AIRPORT - INITIAL INSTALLATION
Comments: INFO Q - DEW POINT -5 0 DEGREES CELSIUS

Ambient Temperature: 5.0 C
Relative Humidity: 48.6 %
Barometric Pressure: 770.4 mmHg
Data Channel Number: 4

BULB 1 TOP SURFACE TEMPERATURE

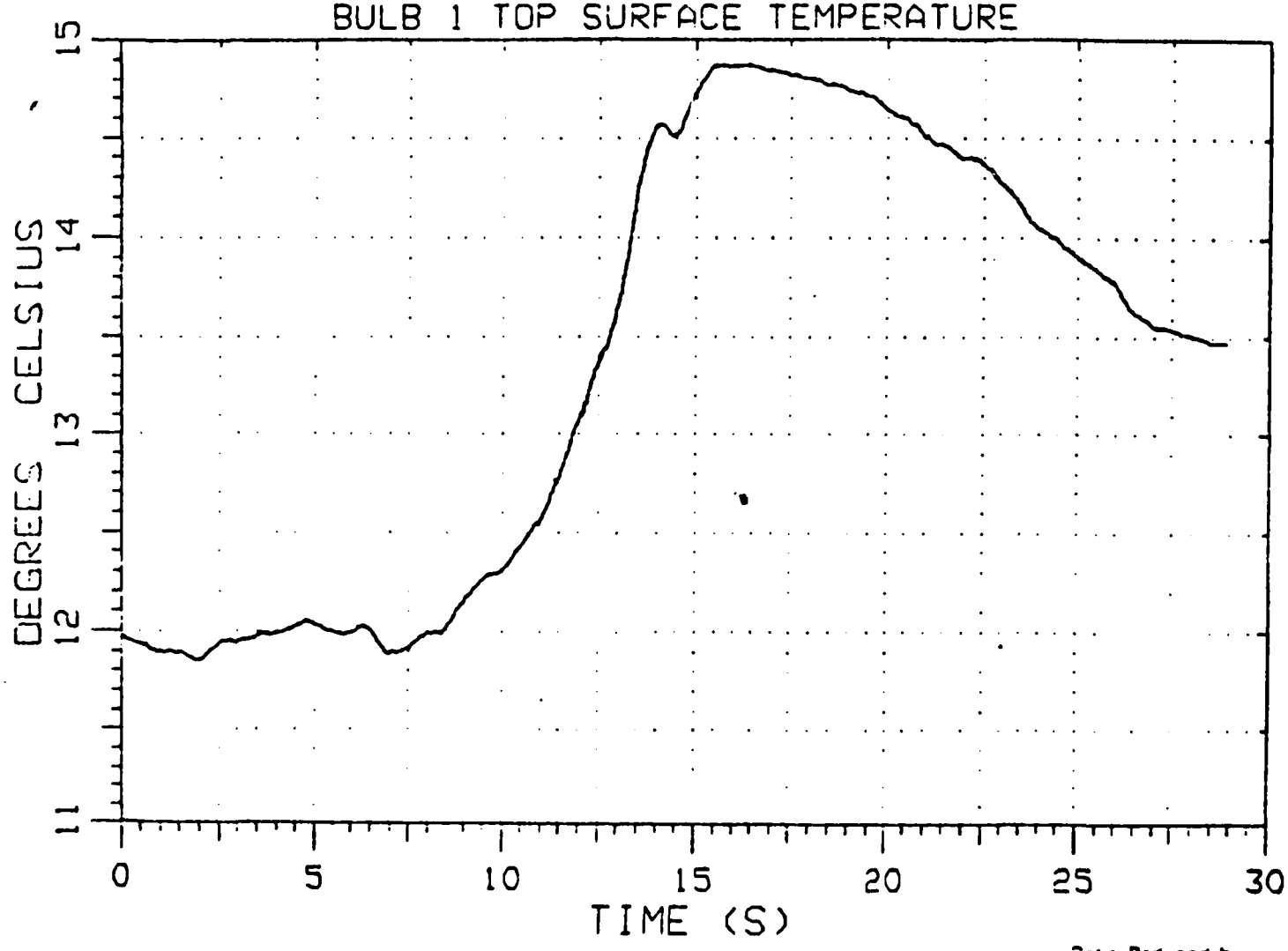

Data Reduced by
SMCAR-AEC-TIL
DTFA03-84-A-40029

FAA PAR-56 RUNWAY LIGHT ANALYSIS

Aircraft Type: L-1011
Flight Number: TWA 559 H
Date and Time: 12-MAR-86 10 33 18
Data Run Number 020
Sensor Location: LA GUARDIA AIRPORT - INITIAL INSTALLATION
Comments: INFO 0 - DEW POINT -5 0 DEGREES CELSIUS

Ambient Temperature: 5.0 C
Relative Humidity: 48.6 %
Barometric Pressure: 770.4 mmHg
Data Channel Number: 4

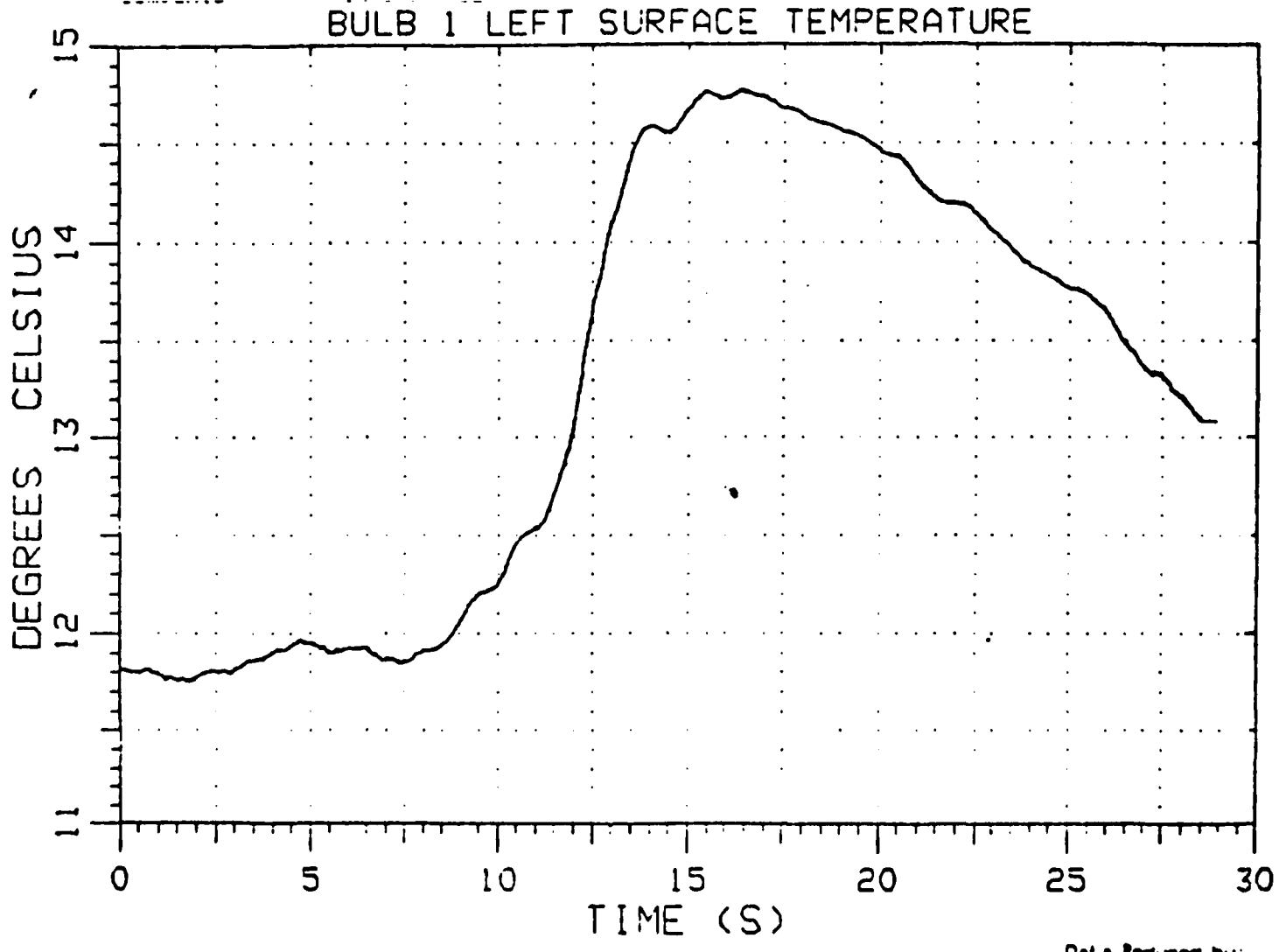

Data Reduced by:
SYCAR-AEC-T:_
DTFAC3-84-A-40020

FAA PAR-56 RUNWAY LIGHT ANALYSIS

Aircraft Type: L-1011
Flight Number: TWA 559 H
Date and Time: 12-MAR-86 10 33 18
Data Run Number 020
Sensor Location: LA GUARDIA AIRPORT - INITIAL INSTALLATION
Comments: INFO 0 - DEW POINT -5 0 DEGREES CELSIUS

Ambient Temperature: 5.0 C
Relative Humidity: 48.6 %
Barometric Pressure: 770.4 mmHg
Data Channel Number: 4

BULB 1 RIGHT SURFACE TEMPERATURE

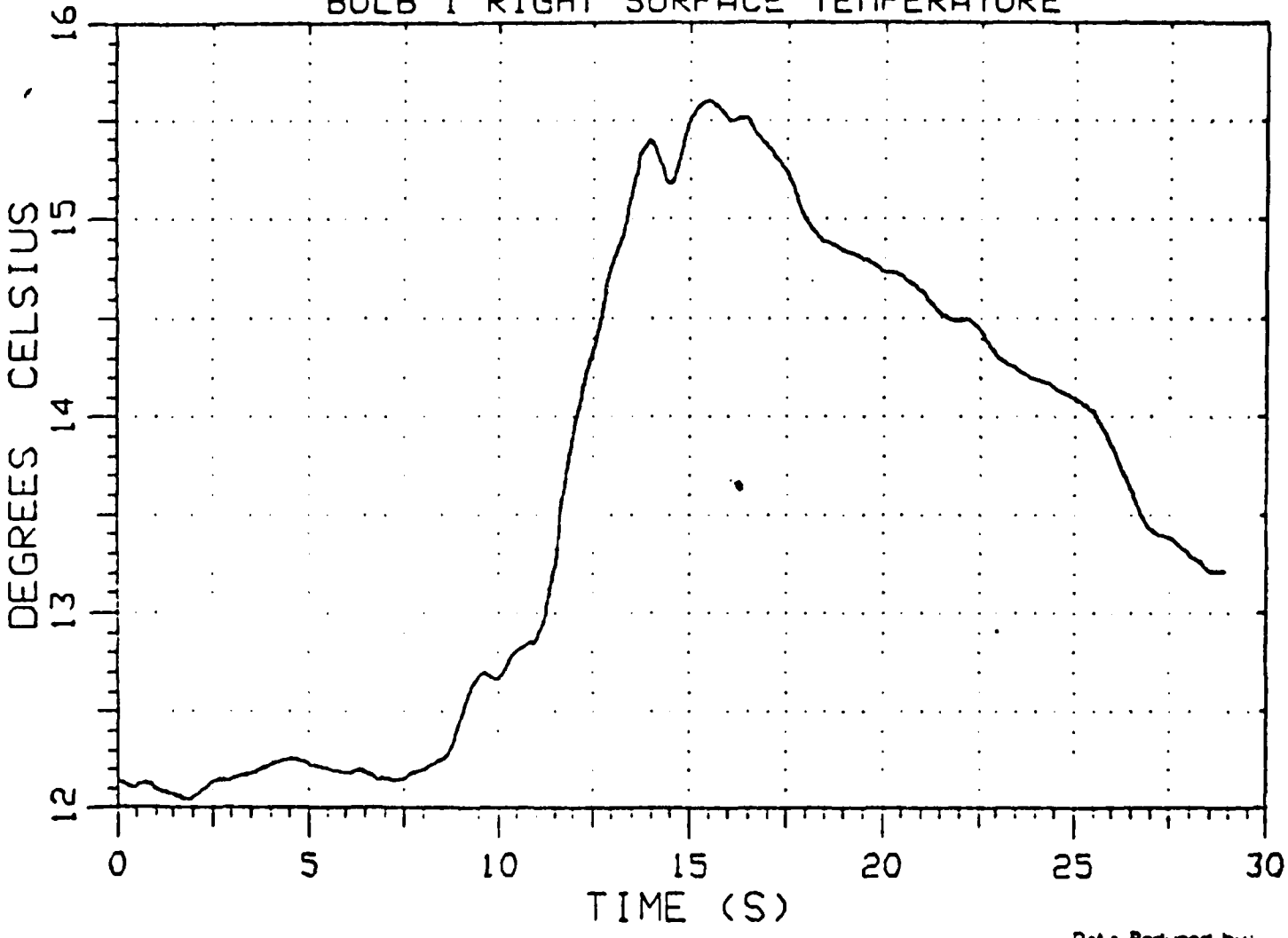

Data Reduced by
SMSAR-AEC-TIL
DTFA03-84-A-40020

FAA PAR-56 RUNWAY LIGHT ANALYSIS

Aircraft Type: L-1011
Flight Number: TWA 559 H
Date and Time: 12-MAR-86 10 33 18
Data Run Number 020
Sensor Location: LA GUARDIA AIRPORT - INITIAL INSTALLATION
Comments: INFO Q - DEW POINT -5 0 DEGREES CELSIUS

Ambient Temperature: 5.0 C
Relative Humidity: 48.6 %
Barometric Pressure: 770.4 mmHg
Data Channel Number: 4

BULB 2 ACCELEROMETER X-AXIS

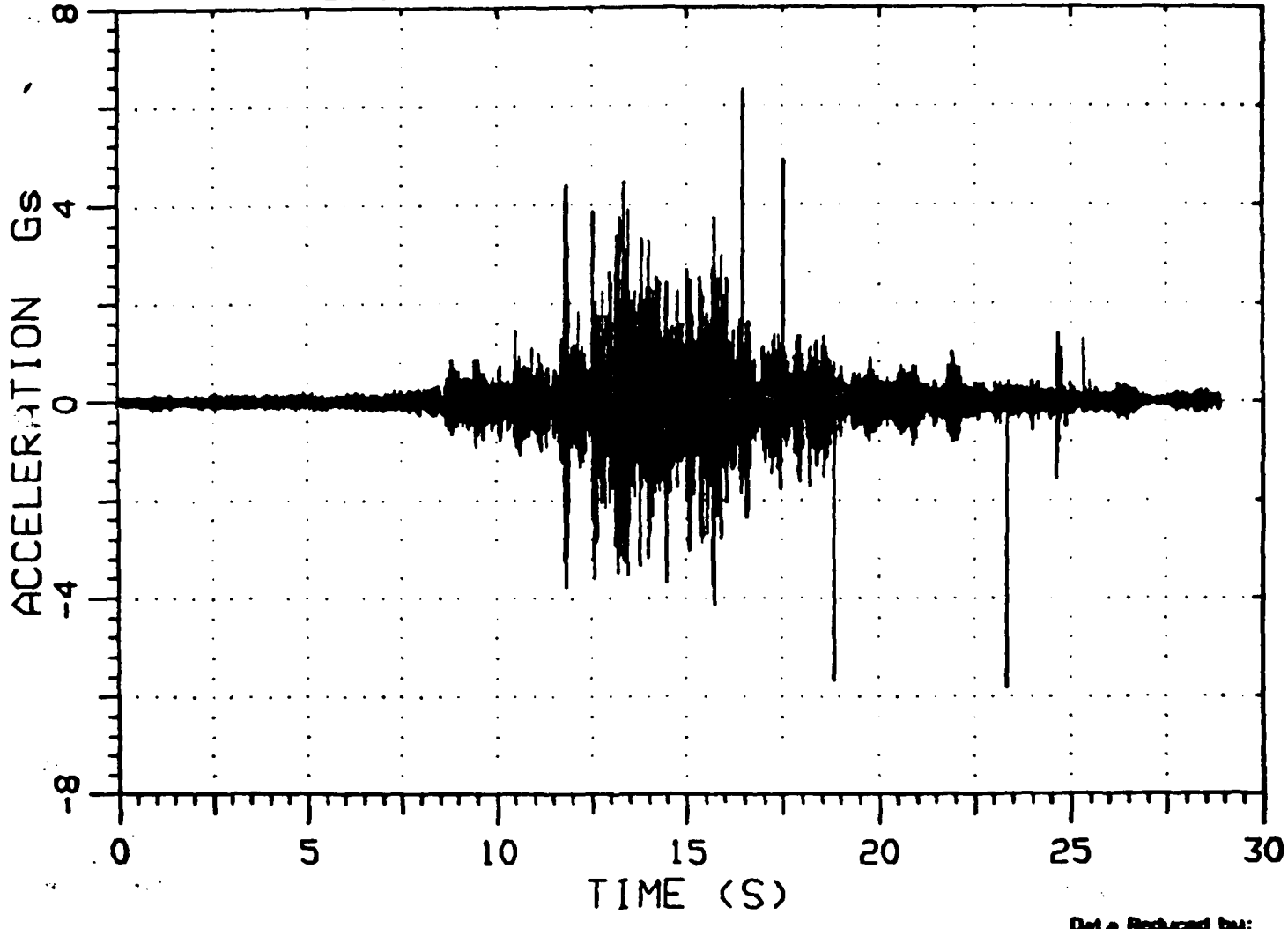

Data Reduced by:
SMEAR-AEC-TIL
DTFA03-84-A-40020

FAA PAR-56 RUNWAY LIGHT ANALYSIS

Aircraft Type: L-1011
Flight Number: TWA 559 H
Date and Time: 12-MAR-86 10:33 18
Data Run Number: 020
Sensor Location: LA GUARDIA AIRPORT - INITIAL INSTALLATION
Comments: INFO 0 - DEW POINT -5 0 DEGREES CELSIUS

Ambient Temperature: 5.0 C
Relative Humidity: 48.6 %
Barometric Pressure: 770.4 mmHg
Data Channel Number: 3

BULB 2 ACCELEROMETER Y-AXIS

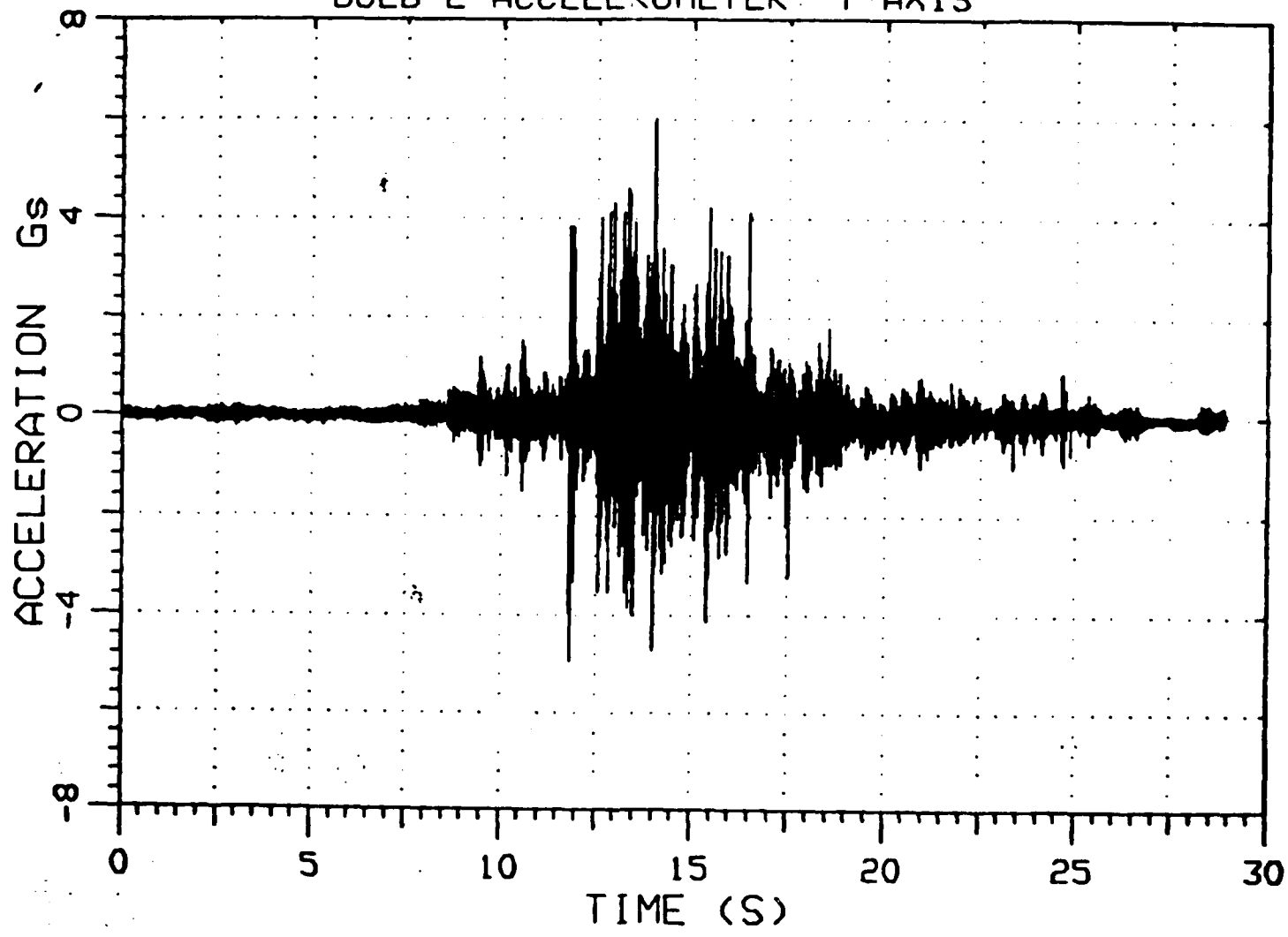

Data Reduced by:
SHCAR-AEC-TIL
DTFA03-84-A-40020

FAA PAR-56 RUNWAY LIGHT ANALYSIS

Aircraft Type: L-1011
Flight Number: TWA 559 H
Date and Time: 12-MAR-86 10 33 18
Data Run Number 020
Sensor Location: LA GUARDIA AIRPORT - INITIAL INSTALLATION
Comments: INFO 0 - DEW POINT -5.0 DEGREES CELSIUS

Ambient Temperature: 5 0 C
Relative Humidity: 48 6 %
Barometric Pressure: 770 4 mmHg
Data Channel Number: 8

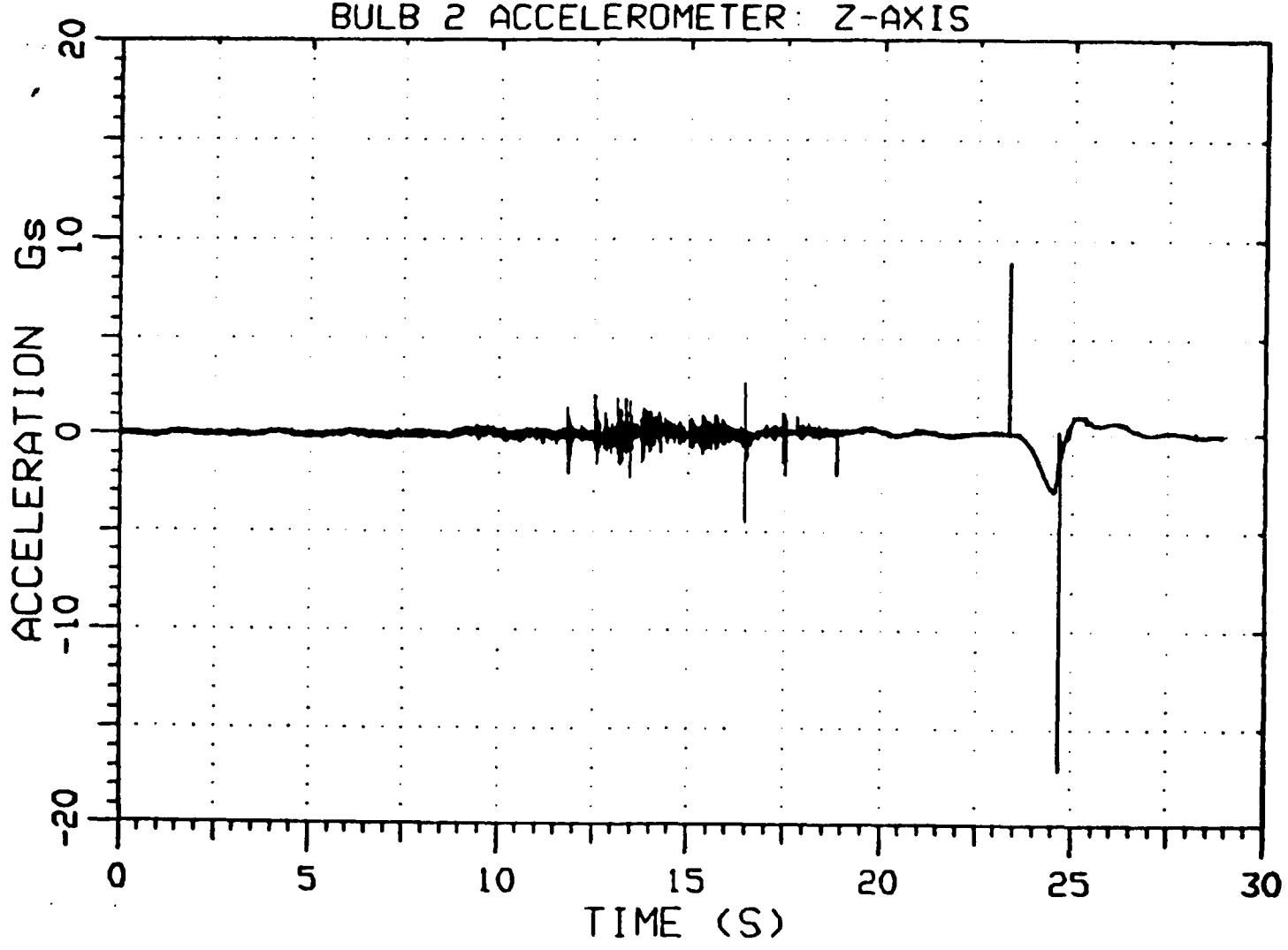

Data Reduced by:
SHCAR-AEC-TIL
DTFA03-84-A-40020

FAA PAR-56 RUNWAY LIGHT ANALYSIS

Aircraft Type: L-1011
Flight Number: TWA 559 H
Date and Time: 12-MAR-86 10 33 18
Data Run Number 020
Sensor Location: LA GUARDIA AIRPORT - INITIAL INSTALLATION
Comments: INFO 0 - DEW POINT -5 0 DEGREES CELSIUS

Ambient Temperature: 5.0 C
Relative Humidity: 48.6 %
Barometric Pressure: 770.4 mmHg
Data Channel Number: 4

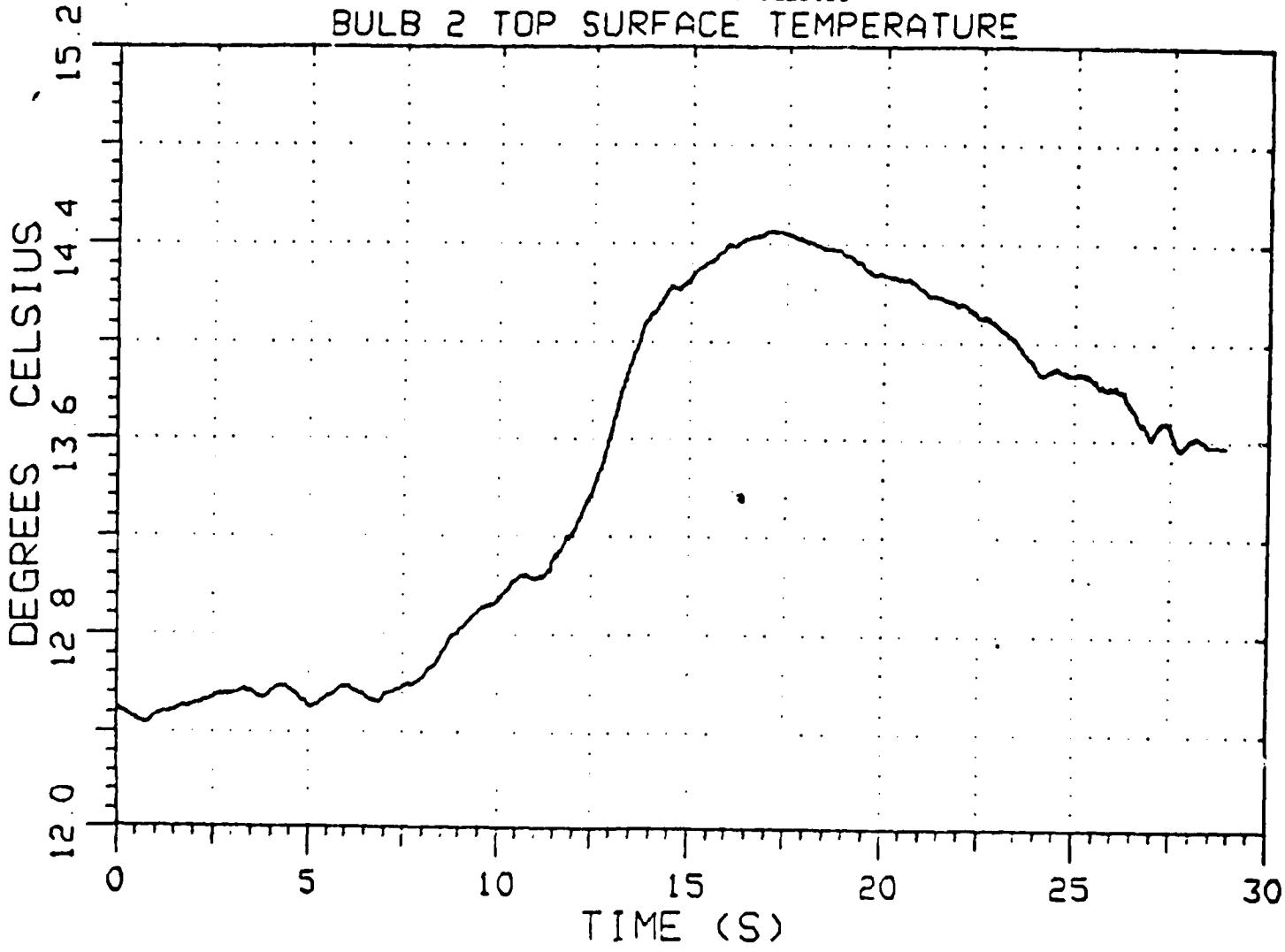

Data Reduced by
SYCOR-AEC-TIL
DTFA03-84-A-40020

FAA PAR-56 RUNWAY LIGHT ANALYSIS

Aircraft Type: L-1011
Flight Number: TWA 559 H
Date and Time: 12-MAR-86 10 33 18
Data Run Number 020
Sensor Location: LA GUARDIA AIRPORT - INITIAL INSTALLATION
Comments: INFO Q - DEW POINT -5 0 DEGREES CELSIUS

Ambient Temperature: 5.0 C
Relative Humidity: 48.6 %
Barometric Pressure: 770.4 mmHg
Data Channel Number: 4

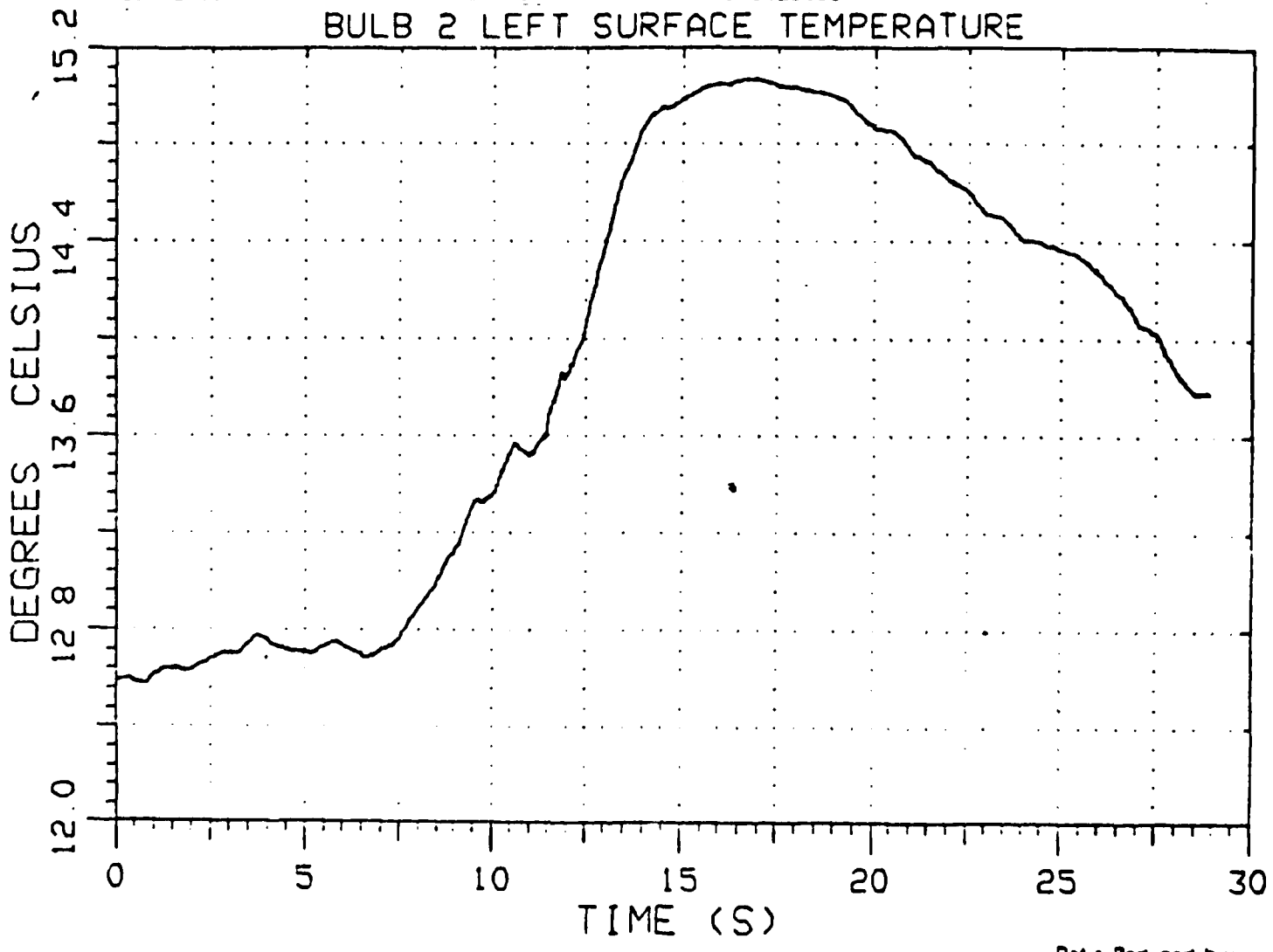

Data Reduced by:
SMCAR-AEC-TIL
DTFA03-84-A-40020

FAA PAR-56 RUNWAY LIGHT ANALYSIS

Aircraft Type: L-1011
Flight Number: TWA 559 H
Date and Time: 12-MAR-86 10 33 18
Data Run Number 020
Sensor Location: LA GUARDIA AIRPORT - INITIAL INSTALLATION
Comments: INFO 0 - DEW POINT -5 0 DEGREES CELSIUS

Ambient Temperature: 5.0 C
Relative Humidity: 48.6 %
Barometric Pressure: 770.4 mmHg
Data Channel Number: 4

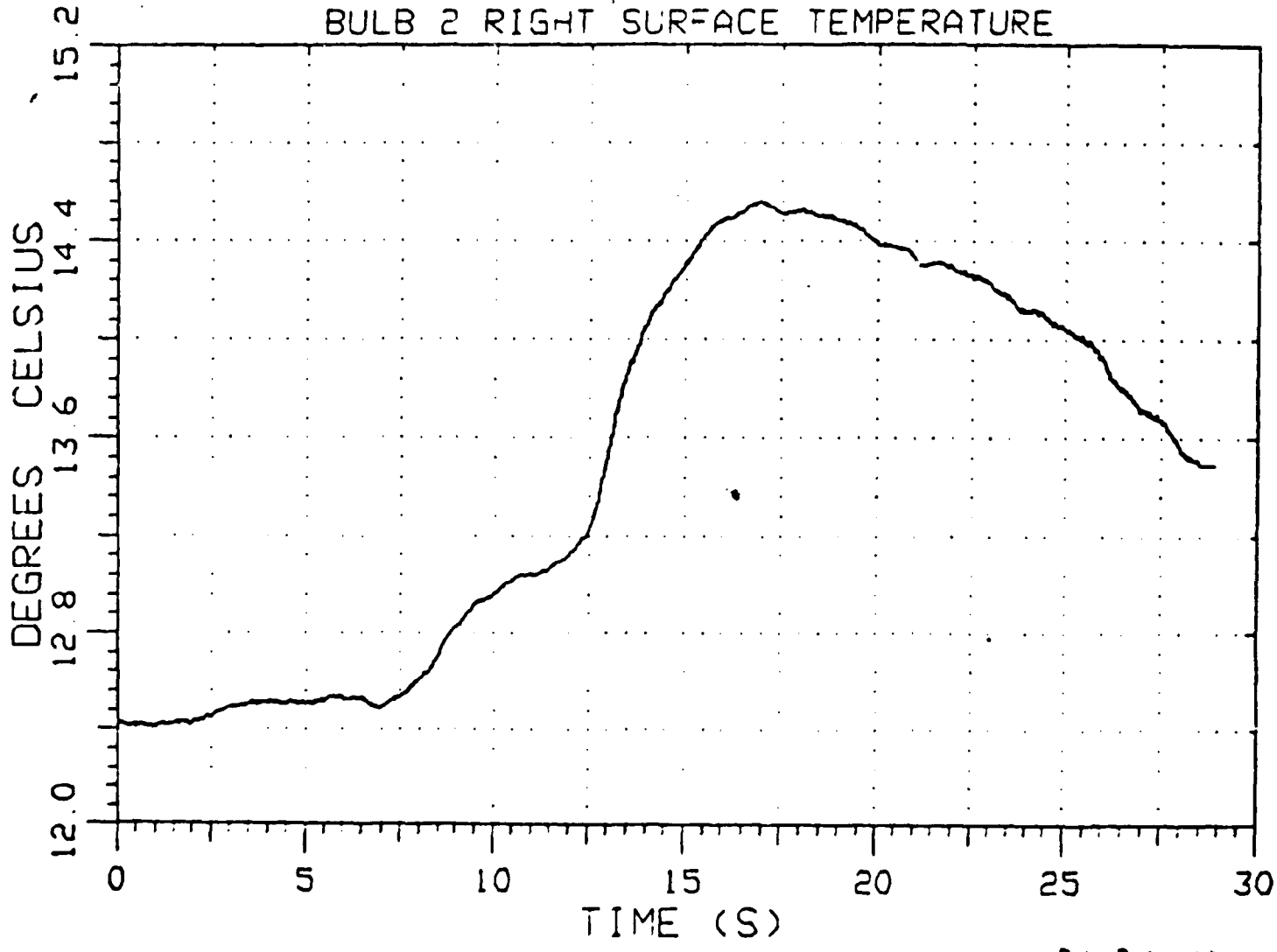

Data Reduced by
SYCOR-GEC-TIL
CONTRACT-DOT-FA83-84-A-40020

FAA PAR-56 RUNWAY LIGHT ANALYSIS

Aircraft Type: L-1011
Flight Number: THA 559 H
Date and Time: 12-MAR-86 10:33:18
Data Run Number: 020
Sensor Location: LA GUARDIA AIRPORT - INITIAL INSTALLATION
Comments: INFO 0 - DEW POINT -5 0 DEGREES CELSIUS

Ambient Temperature: 5.0 C
Relative Humidity: 48.6 %
Barometric Pressure: 770 4 mmHg
Data Channel Number: 10

BULB 1 ACCELEROMETER X-AXIS

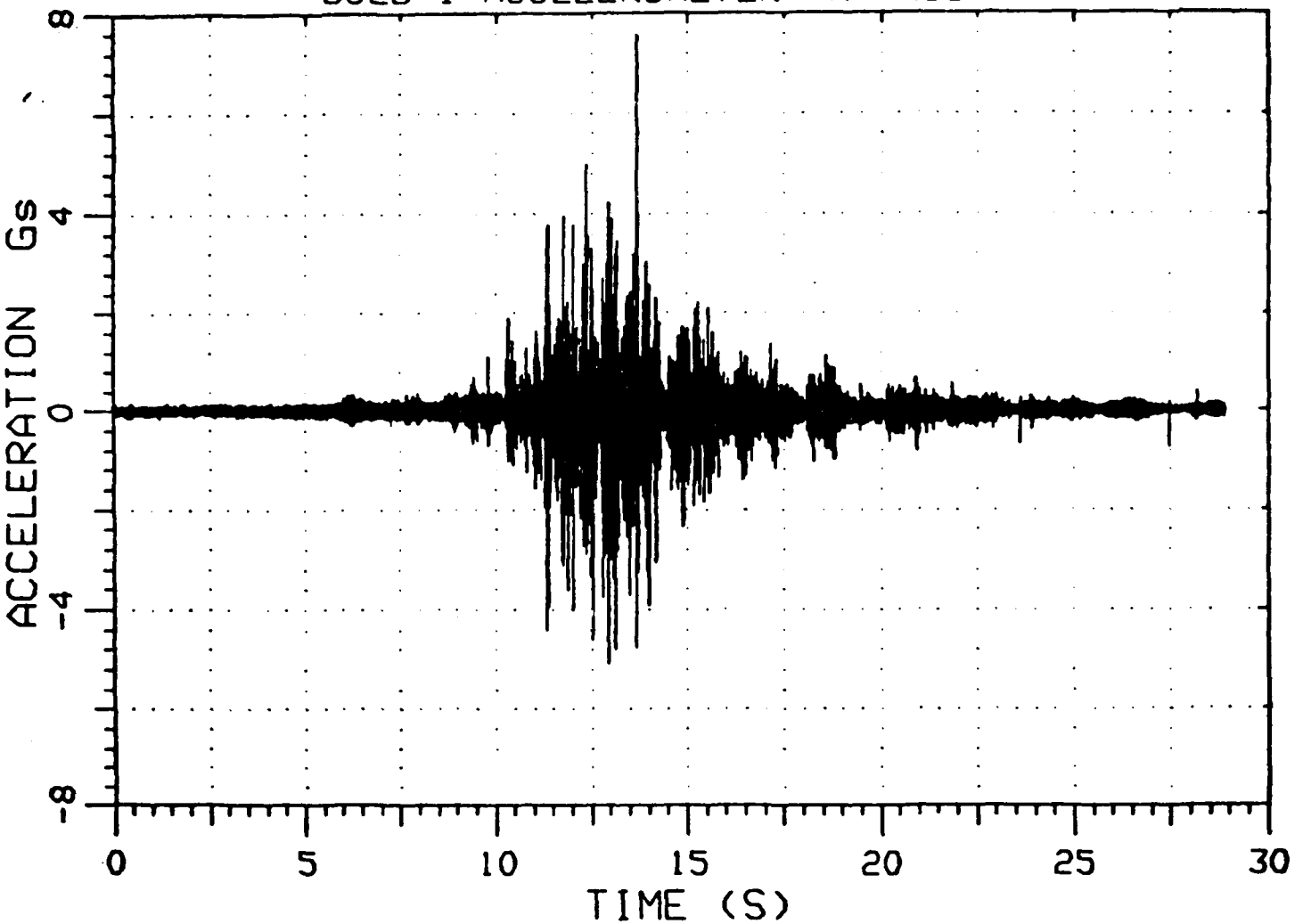

Data Reduced by:
SHCAR-AEC-TIL
DTFA03-84-A-40020

FAA PAR-56 RUNWAY LIGHT ANALYSIS

Aircraft Type: L-1011
Flight Number: TWA 559 H
Date and Time: 12-MAR-86 10:33:18
Data Run Number: 020
Sensor Location: LA GUARDIA AIRPORT - INITIAL INSTALLATION
Comments: INFO 0 - DEW POINT -5.0 DEGREES CELSIUS

Ambient Temperature: 5.0 C
Relative Humidity: 48.6 %
Barometric Pressure: 770.4 mmHg
Data Channel Number: 17

BULB 1 ACCELEROMETER Y-AXIS

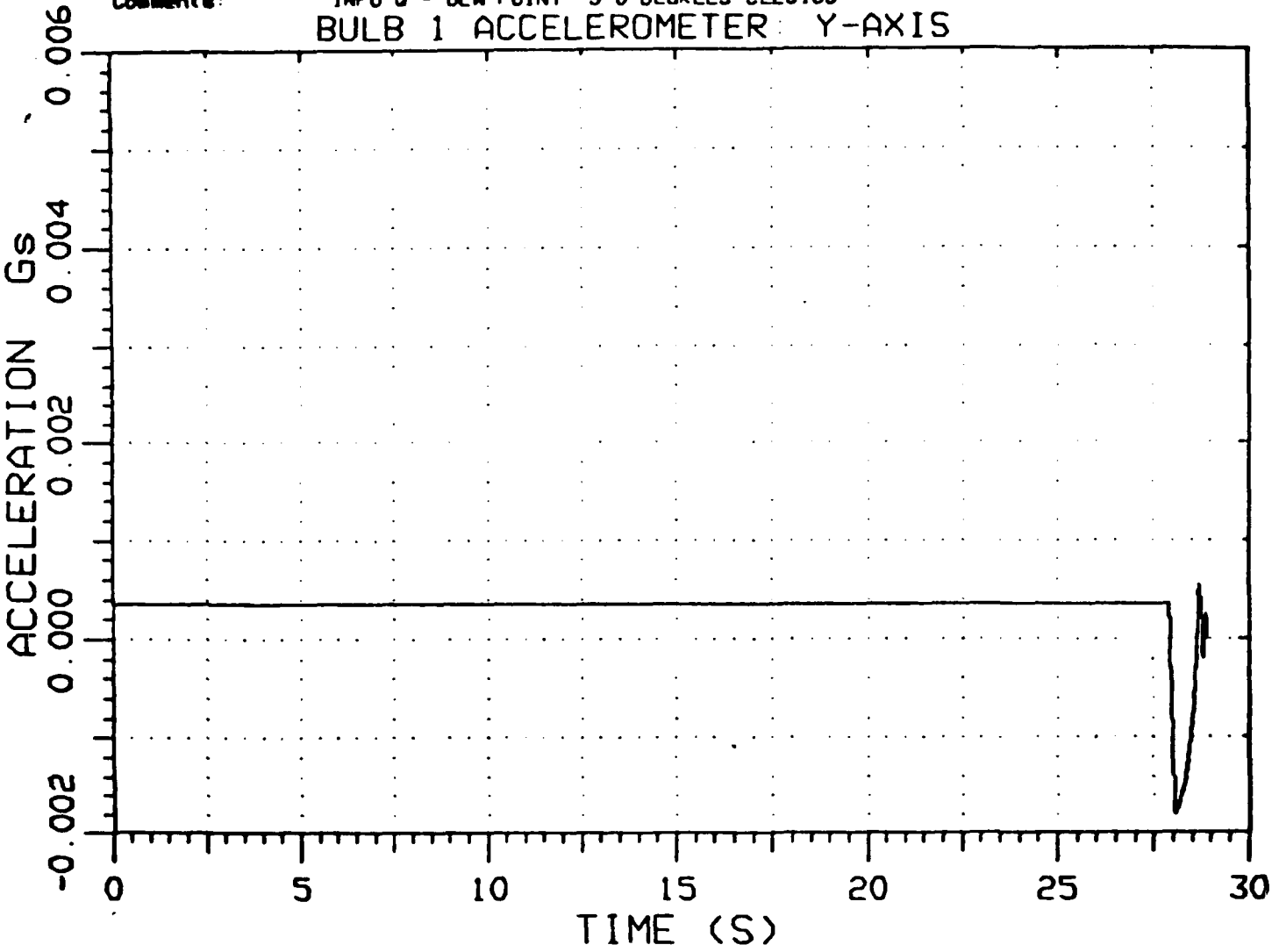

Data Reduced by:
SMCAR-AEC-TIL
DTFA03-84-A-40020

FAA PAR-56 RUNWAY LIGHT ANALYSIS

Aircraft Type: L-1011
Flight Number: THA 559 M
Date and Time: 12-MAR-86 10 33 18
Data Run Number: 020
Sensor Location: LA GUARDIA AIRPORT - INITIAL INSTALLATION
Comments: INFO 0 - DEW POINT -5 0 DEGREES CELSIUS

Ambient Temperature: 5 0 C
Relative Humidity: 48 6 %
Barometric Pressure: 770 4 mmHg
Data Channel Number: 12

BULB 1 ACCELEROMETER Z-AXIS

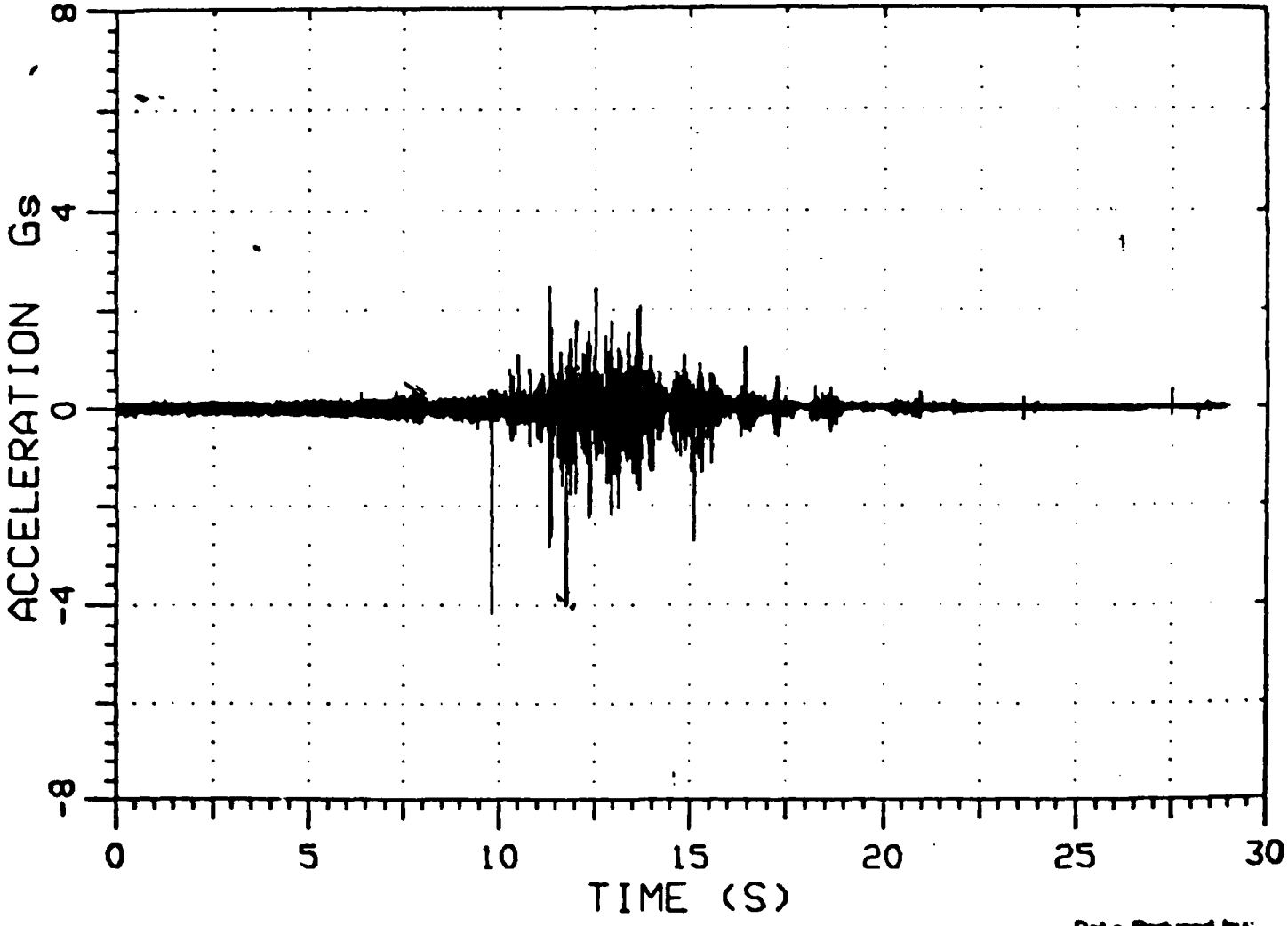

Data Reduced by:
SHCAR-REC-TIL
DTFA03-84-A-40021

FAA PAR-56 RUNWAY LIGHT ANALYSIS

Aircraft Type: L-1011
Flight Number: TWA 559 H
Date and Time: 12-MAR-86 10 33 18
Data Run Number 020
Sensor Location: LA GUARDIA AIRPORT - INITIAL INSTALLATION
Comments: INFO 0 - DEW POINT -5 0 DEGREES CELSIUS

Ambient Temperature: 5.0 C
Relative Humidity: 48.6 %
Barometric Pressure: 770.4 mmHg
Data Channel Number: 4

FLUID TEMPERATURE: VELOCITY DATA

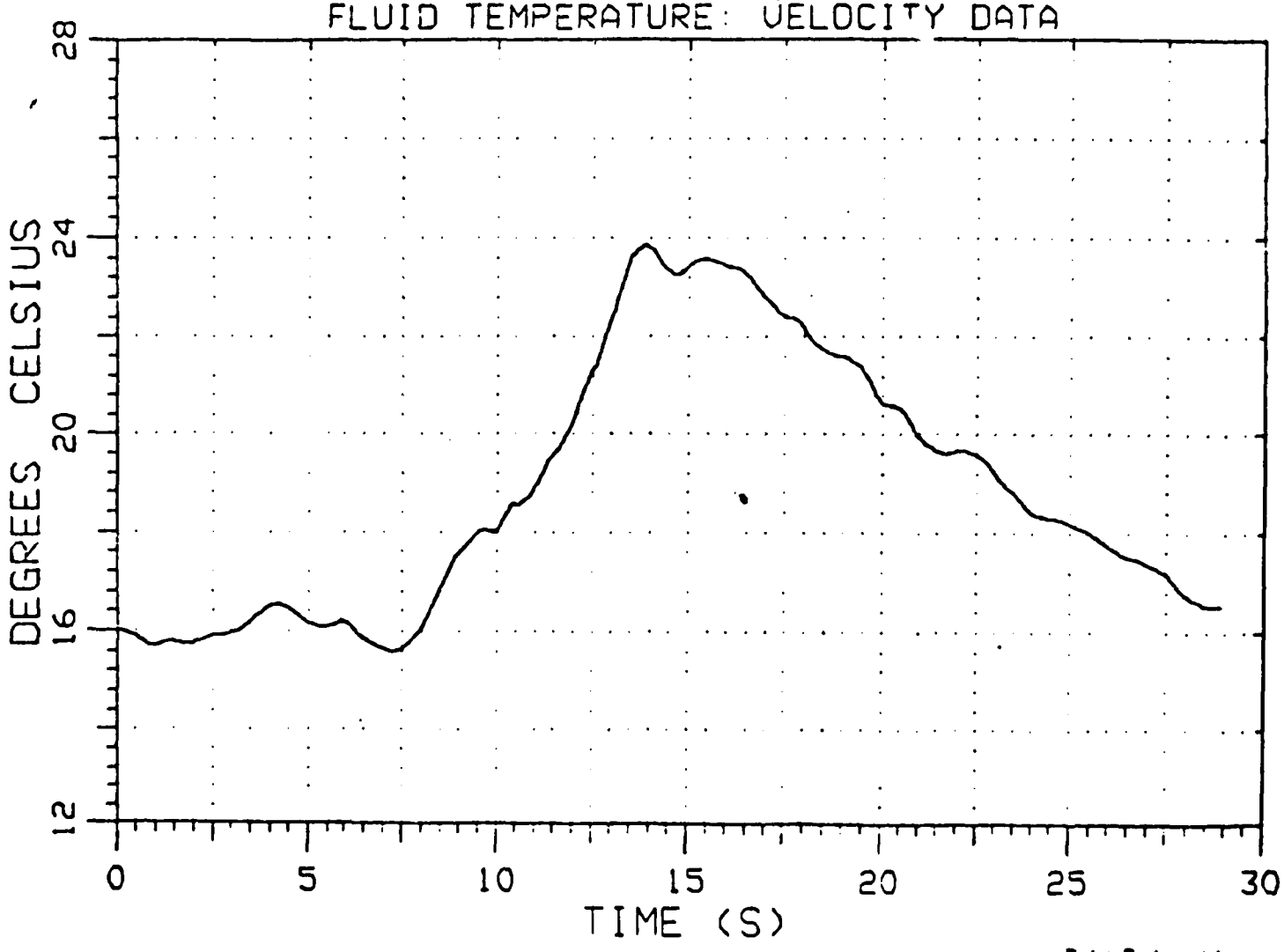

Data Reduced by:
SMCAR-AEC-TIL
DTFA03-84-A-40020

FAA PAR-56 RUNWAY LIGHT ANALYSIS

Aircraft Type: L-1011
Flight Number: TWA 559 H
Date and Time: 12-MAR-86 10:33:18
Data Run Number: 020
Sensor Location: LA GUARDIA AIRPORT - INITIAL INSTALLATION
Comments: INFO 0 - DEW POINT -5.0 DEGREES CELSIUS

Ambient Temperature: 5.0 C
Relative Humidity: 48.6 %
Barometric Pressure: 770.4 mmHg
Data Channel Number: 14
PITOT A

RUNWAY SURFACE WIND VELOCITY

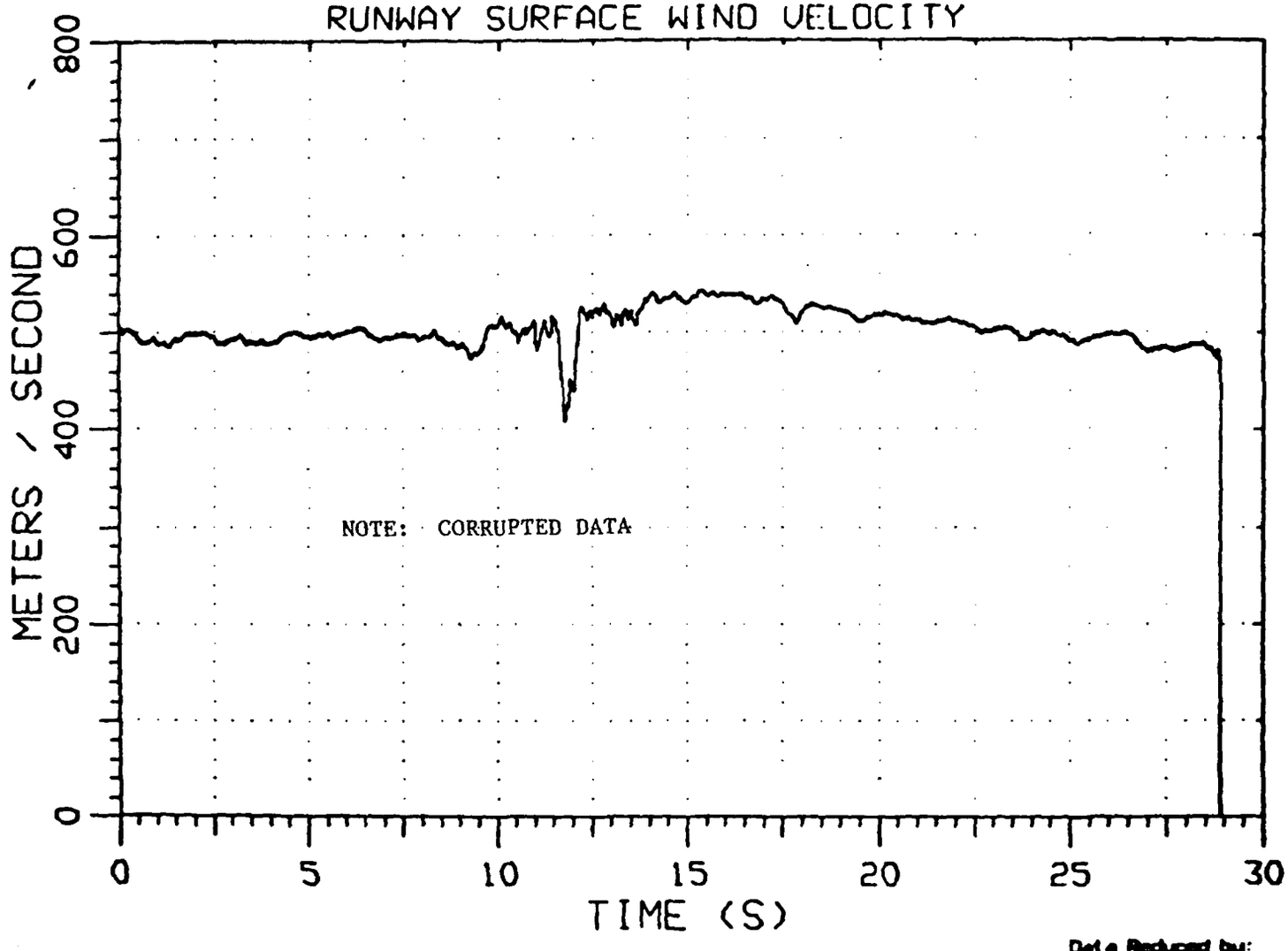

Data Reduced by:
SMEAR-AEC-TIL
DTFA03-84-A-40020

FAA PAR-56 RUNWAY LIGHT ANALYSIS

Aircraft Type: L-1011
Flight Number: TWA 559 H
Date and Time: 12-MAR-86 10 33 18
Data Run Number: 020
Sensor Location: LA GUARDIA AIRPORT - INITIAL INSTALLATION
Comments: INFO 0 - DEW POINT -5 0 DEGREES CELSIUS

Ambient Temperature: 5 0 C
Relative Humidity: 48 6 %
Barometric Pressure: 770 4 mmHg
Data Channel Number: 15
PITOT B

RUNWAY SURFACE WIND VELOCITY

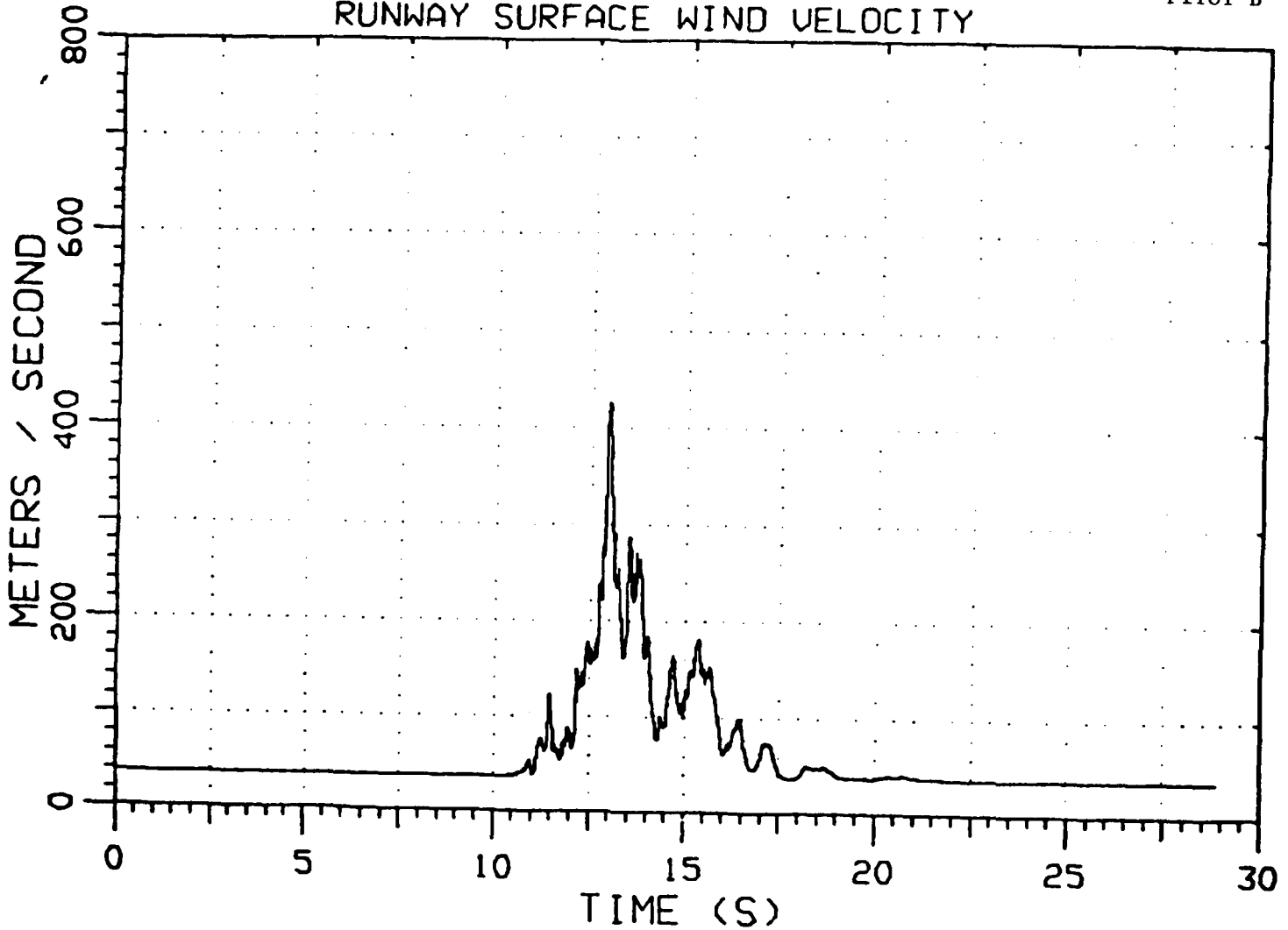

Data Reduced by:
SHCAR-AEC-TIL
DTFA03-84-A-40020

APPENDIX B

ACQUIRED DATA RUN LIST

This list is a computer printout of all data runs acquired at La Guardia Airport. The tape number at the top of the list refers to the digital magnetic tapes containing all the data. The run number is the data run number, number 1 being the first data run acquired during this test, with consecutive numbering up to number 162, which was the last data run acquired for this test. The acquisition date, aircraft type and the flight number are self-explanatory. The run numbers are used as reference numbers on the video tapes also.

TAPE 1

FILE	RUN #	ACQUISITION DATE	AIRCRAFT TYPE	FLIGHT #
1	1	06-MAR-86 06:48:02	UNKNOWN	UNKNOWN
2	2	06-MAR-86 08:09:02	BOEING 727	EA 119
3	3	11-MAR-86 03:57:02	NONE	NONE
4	4	11-MAR-86 06:26:35	BUSINESS JET	N210M
5	5	11-MAR-86 07:02:02	BOEING 737-300	NY AIR 143
6	6	11-MAR-86 07:22:36	AIR BUS 300	EA 1160 HEAV
7	9	11-MAR-86 07:37:36	BOEING 727	EA 583
8	11	11-MAR-86 08:00:06	DC 9	REPUBLIC 17
9	12	11-MAR-86 08:07:43	MD-80	NY AIR 1
10	13	11-MAR-86 08:15:21	BOEING 727	EA 1411
11	14	12-MAR-86 07:16:58	<NONE>	<NONE>
12	15	12-MAR-86 07:37:33	<NONE>	<NONE>
13	18	12-MAR-86 10:21:22	BOEING 727	UNITED 167
14	19	12-MAR-86 10:26:44	AIRBUS A300	PAN AM 41 H
15	20	12-MAR-86 10:33:18	L-1011	TWA 559 H
16	21	12-MAR-86 11:07:20	JET PROPELLER	N234RP
17	22	12-MAR-86 11:12:22	DC-9	US AIR 191
18	23	12-MAR-86 11:17:22	AIRBUS A300	EA 1040 H
19	24	12-MAR-86 11:27:03	BOEING 767	NW ORIENT 20
20	25	12-MAR-86 11:42:55	DC-9	METROLINK 19
21	26	12-MAR-86 11:48:51	BOEING 737	PIEDMONT 439
22	27	12-MAR-86 11:58:36	BOEING 727	AA 502

TAPE 2

FILE	RUN #	ACQUISITION DATE	AIRCRAFT TYPE	FLIGHT #
1	28	12-MAR-86 12:07:35	BAC 310	EMPIRE 919
2	29	12-MAR-86 12:23:18	BOEING 727	UNITED 911
3	30	12-MAR-86 12:35:51	CESSNA CITATION	N22FK
4	31	12-MAR-86 12:47:04	DC-10	AA 491 HEAVY
5	32	12-MAR-86 12:52:47	BOEING 737	UNITED 1007
6	33	12-MAR-86 13:16:09	AIRBUS A300	EA 1060 HEAV
7	34	12-MAR-86 13:23:34	BOEING 757	EA 1461 HEAV
8	35	12-MAR-86 13:40:44	BOEING 727	AA 543
9	36	12-MAR-86 13:53:07	AIRBUS A300	PAN AM 245 H
10	37	12-MAR-86 13:58:29	BOEING 737-300	NY AIR 147
11	38	12-MAR-86 14:02:54	BOEING 767	DELTA 707 HE
12	39	12-MAR-86 14:10:31	DC-9	EA 651
13	40	12-MAR-86 14:21:50	BOEING 737	PEIDMONT 340
14	41	12-MAR-86 14:38:00	AIRBUS A300	EA 21 HEAVY
15	42	12-MAR-86 14:44:33	BOEING 727	EA 1470
16	44	13-MAR-86 07:05:57	FALCON TRI-ENGINE BZ JET	N65B
17	45	13-MAR-86 07:20:01	BOEING 767	DELTA 809 HE
18	46	13-MAR-86 07:27:55	BOEING 737	UNITED 1001
19	47	13-MAR-86 07:37:47	HAWKER BUSINESS JET	N700NY
20	48	13-MAR-86 07:58:46	BOEING 767	AA 295 HEAVY
21	49	13-MAR-86 08:04:49	BOEING 737	PEIDMONT 467
22	50	13-MAR-86 08:20:03	MD-80	NY AIR 1

TAPE 3

FILE	RUN #	ACQUISITION DATE	AIRCRAFT TYPE	FLIGHT #
1	51	13-MAR-86 08:32:12	BOEING 757	UNITED 903 H
2	52	13-MAR-86 08:45:30	L-1011	DELTA 494 HE
3	53	13-MAR-86 08:51:02	BOEING 757	EA 207 HEAVY
4	54	13-MAR-86 09:04:24	BOEING 767	DELTA 803 HE
5	55	13-MAR-86 09:18:12	BOEING 727	NW ORIENT 20
6	56	13-MAR-86 09:33:53	L-1011	DELTA 93 H
7	57	13-MAR-86 09:40:36	L-1011	TWA 419 H
8	58	13-MAR-86 09:48:15	DC-10	AA 85 HEAVY
9	59	13-MAR-86 10:06:24	BOEING 737-300	PEIDMONT 525
10	60	13-MAR-86 11:22:25	BOEING 727	AA 141
11	61	13-MAR-86 11:30:53	FALCON TRI-ENGINE	CFSCL
12	62	13-MAR-86 11:36:09	BOEING 737	PEIDMONT 337
13	63	13-MAR-86 11:41:39	BOEING 727	EA 545
14	64	13-MAR-86 11:50:56	AIRBUS A300	EA 1030 HEAV
15	65	13-MAR-86 11:59:2[illegible]	DC-9	NY AIR 7
16	66	14-MAR-86 06:36:4[illegible]	HAWKER BUSINESS JET	N540R
17	68	14-MAR-86 07:44:56	BOEING 767	AA 285 HEAVY
18	69	14-MAR-86 07:56:09	MD-80	CONT 127
19	70	14-MAR-86 08:45:58	AIRBUS A300	EA 1010 H
20	72	14-MAR-86 08:51:13	L-1011	EA 11 H
21	73	14-MAR-86 08:55:51	BOEING 737	PEIDMONT 477
22	74	14-MAR-86 09:43:44	DC-10	AA 85 HEAVY

TAPE 4

FILE	RUN #	ACQUISITION DATE	AIRCRAFT TYPE	FLIGHT #
1	75	14-MAR-86 10:04:59	L-1011	TWA 419 H
2	76	14-MAR-86 10:31:02	L-1011	TWA 559 H
3	77	14-MAR-86 10:39:06	BOEING 727	TWA 5051
4	78	14-MAR-86 10:45:20	BOEING 757	EA 207 HEAVY
5	79	14-MAR-86 10:52:05	DC-9	EA 377
6	80	14-MAR-86 10:56:28	FOKKER F-28	EMPIRE 943
7	82	14-MAR-86 11:13:28	DC-9	US AIR 176
8	83	17-MAR-86 06:31:53	<NONE>	<NONE>
9	84	17-MAR-86 06:38:27	<NONE>	<NONE>
10	85	17-MAR-86 06:45:01	<NONE>	<NONE>
11	86	17-MAR-86 06:55:01	<NONE>	<NONE>
12	87	17-MAR-86 07:01:36	<NONE>	<NONE>
13	88	17-MAR-86 13:11:45	BOEING 767	TWA 129 HEAV
14	89	17-MAR-86 13:18:02	DC-9	REPUBLIC 633
15	90	17-MAR-86 13:22:38	BOEING 737	PIEDMONT 159
16	91	17-MAR-86 13:31:06	BOEING 727	EA 1461
17	92	17-MAR-86 13:35:43	AIRBUS A300	EA 1060 HEAV
18	93	17-MAR-86 13:41:41	FALCON TRI-ENGINE	N297W
19	94	17-MAR-86 13:55:10	BOEING 757	EA 107
20	95	17-MAR-86 14:02:57	BOEING 767	DELTA 707 H
21	96	17-MAR-86 14:29:12	AIRBUS A300	EA 1070 HEAV
22	97	18-MAR-86 07:02:21	BOEING 727	EA 1401

TAPE 5

FILE	RUN #	ACQUISITION DATE	AIRCRAFT TYPE	FLIGHT #
1	98	18-MAR-86 07:14:56	BOEING 767	AA 511 HEAVY
2	99	18-MAR-86 07:22:27	BOEING 727	NW ORIENT 28
3	100	18-MAR-86 07:26:54	AIRBUS A300	EA 1160 HEAV
4	101	18-MAR-86 07:37:12	DC-9	US AIR 245
5	102	18-MAR-86 07:43:52	BOEING 767	AA 295 HEAVY
6	103	18-MAR-86 07:49:43	BOEING 727	AA 297
7	104	18-MAR-86 07:57:03	BOEING 737	UNITED 1003
8	105	18-MAR-86 08:02:46	DASH 7	RANDSOME 180
9	106	18-MAR-86 08:06:49	MD-80	CONT 127
10	107	18-MAR-86 08:23:28	BOEING 767	UNITED 903 H
11	108	18-MAR-86 08:29:56	F-28	PIEDMONT 829
12	109	18-MAR-86 08:39:54	DC-9	US AIR 127
13	110	18-MAR-86 08:43:58	FALCON TRI-ENGINE	N65B
14	111	18-MAR-86 08:51:27	BOEING 737	UNITED 1065
15	112	18-MAR-86 09:03:35	L-1011	EA 11 HEAVY
16	113	18-MAR-86 09:09:03	BOEING 757	EA 207
17	114	18-MAR-86 09:13:41	DC-9	US AIR 239
18	115	18-MAR-86 09:25:30	AIRBUS A300	EA 1020 HEAV
19	116	18-MAR-86 09:33:14	L-1011	DELTA 407 H
20	117	18-MAR-86 09:54:18	DC-10	AA 85 HEAVY
21	118	18-MAR-86 10:00:48	DC-9	EA 585
22	119	18-MAR-86 10:30:20	L-1011	TWA 559 HEAV

TAPE 6

FILE	RUN #	ACQUISITION DATE	AIRCRAFT TYPE	FLIGHT #
1	120	18-MAR-86 10:41:16	BOEING 727	DELTA 419
2	121	18-MAR-86 10:53:20	AR-42 TWO ENGINE PROPELL	COMMAND 2640
3	122	18-MAR-86 11:09:18	BOEING 727	EA 1441
4	123	18-MAR-86 11:13:02	BOEING 767	UNITED 909 H
5	124	18-MAR-86 11:20:49	HAWKER BUSINESS JET	N700NY
6	125	18-MAR-86 11:54:39	BOEING 727	AIR CAN 707
7	126	18-MAR-86 12:04:39	BAC 111	US AIR 469
8	127	18-MAR-86 12:09:28	F-28	EMPIRE 919
9	128	18-MAR-86 12:15:27	AIRBUS A300	EA 1050 HEAV
10	129	18-MAR-86 12:20:55	BOEING 727	EA 659
11	130	18-MAR-86 12:26:30	BOEING 757	DELTA 135
12	131	18-MAR-86 12:37:37	DC-10	AA 491 HEAVY
13	132	18-MAR-86 12:47:25	AIRBUS A300	EA 17 HEAVY
14	133	18-MAR-86 13:00:37	BOEING 767	TWA 129 H
15	134	18-MAR-86 13:03:44	GRUMMAN GULFSTREAM	N343K
16	135	18-MAR-86 13:12:46	BOEING 737	PIEDMONT 259
17	136	18-MAR-86 13:20:35	BOEING 757	EA 107
18	137	18-MAR-86 13:25:49	BOEING 727	AA 321
19	138	19-MAR-86 06:46:34	CITATION BUSINESS JET	N797CW
20	139	19-MAR-86 06:57:33	BOEING 727	FED EXP 286
21	140	19-MAR-86 07:07:32	BOEING 737	UNITED 1001
22	141	19-MAR-86 07:15:32	BOEING 727	AA 171

TAPE 7

FILE	RUN #	ACQUISITION DATE	AIRCRAFT TYPE	FLIGHT #
1	142	19-MAR-86 07:21:48	BOEING 767	AA 511 HEAVY
2	143	19-MAR-86 07:31:13	BOEING 767	DELTA 809 H
3	144	19-MAR-86 07:39:47	DC-9	US AIR 285
4	145	19-MAR-86 07:54:55	DC-9	REPUBLIC 359
5	146	19-MAR-86 08:02:17	BOEING 767	AA 295 HEAVY
6	147	19-MAR-86 08:16:55	DC-9	OZARK 781
7	148	19-MAR-86 08:24:17	BOEING 767	UNITED 903 H
8	149	19-MAR-86 08:36:21	AIRBUS A300	EA 1010 H
9	150	19-MAR-86 08:45:51	BOEING 757	EA 207
10	151	19-MAR-86 08:53:09	BOEING 757	EA 410
11	152	19-MAR-86 09:08:21	L-1011	DELTA 407 H
12	153	19-MAR-86 09:20:13	DASH 7 4-ENGINE PROP	N2655P
13	154	19-MAR-86 09:26:50	BAC 111	US AIR 231
14	155	19-MAR-86 09:30:06	L-1011	DELTA 494 H
15	156	19-MAR-86 09:40:55	AIRBUS A300	EA 1021 H
16	157	19-MAR-86 09:46:13	L-1011	TWA 419 H
17	158	19-MAR-86 09:54:55	F-28	EMPIRE 943
18	159	19-MAR-86 10:15:08	DC-10	AA 85 HEAVY
19	160	19-MAR-86 10:22:15	AIRBUS A300	EA 1030 HEAV
20	161	19-MAR-86 11:13:24	BOEING 727	EA 1040
21	162	19-MAR-86 11:24:15	BOEING 767	UNITED 909 H